M 2014

U.PORTO
INSTITUTO DE CIÊNCIAS BIOMÉDICAS ABEL SALAZAR
UNIVERSIDADE DO PORTO

Bioassay-guided isolation of cyanobacterial metabolites with anticancer activity

TIAGO ANDRÉ BARROS AFONSO

DISSERTAÇÃO DE MESTRADO APRESENTADA

AO INSTITUTO DE CIÊNCIAS BIOMÉDICAS ABEL SALAZAR

DA UNIVERSIDADE DO PORTO EM

TOXICOLOGIA E CONTAMINAÇÃO AMBIENTAIS

Tiago André Barros Afonso

Bioassay-guided isolation of cyanobacterial metabolites with anticancer activity.

Dissertation for the Master Degree in Environmental Toxicology and Contamination submitted to the Institute of Biomedical Sciences of Abel Salazar from the University of Porto.

Supervisor – Doctor Pedro Leão.
Category – Postdoctoral fellow.
Affiliation – Interdisciplinary Center of Marine and Environmental Research.

Co-supervisor – Doctor Maria Rosário Martins.
Category – Associate Professor.
Affiliation – School of Allied Health Sciences, Polytechnic Institute of Porto.

Acknowledgements

For the realization of this Master's thesis I relied on the support and assistance of many people to whom I would like to give my thank you.

First of all, I would like to thank my supervisor Pedro Leão, for the help and knowledge transmitted throughout the work as well as the availability to respond to my questions even from a few thousand miles away. To my co-supervisor Rosário Martins for the help and shared knowledge along the realization of several thesis steps. I give my big thank you to all for allowing me the opportunity to work in this field of study and to share this work with the scientific community.

To the Interdisciplinary Centre of Marine and Environmental Research (CIIMAR), Institute of Biomedical Sciences of Abel Salazar from the University of Porto (ICBAS) and Faculty of Sciences from the University of Porto (FCUP).

To the Portuguese Foundation for Science and Technology (FCT) for financial support with the projects PTDC/MAR-BIO/2818/2012, PTDC/MAR/102638/2008 and PEst-C/MAR/LA0015/2013. To Programa Operacional Regional do Norte (ON.2—O Novo Norte) through the project MARBIOTECH (reference NORTE-07-0124-FEDER-000047) within the SR&TD Integrated Program MARVALOR—Building research and innovation capacity for improved management and valorisation of marine resources, and to the European Regional Development Fund through the project NOVOMAR (reference 0687-NOVOMAR-1-P).

To all the members of LEGE's (Laboratory of Ecotoxicology, Genomics and Evolution) team for providing a relaxing and friendly work environment and helping with some of my questions and doubts when necessary. Special thanks to Sofia Costa, Ângela Pinheiro and Marco Preto for always helping me when necessary and for always being available to answer all my doubts and questions. Also, a special thanks to Margarida Costa for providing me with the biomass of *Synechocystis salina* LEGE 06099.

To professor doctor Vitor Vasconcelos for accepting me in the laboratory to perform my master's thesis.

To my master colleagues Miguel, João, Catarina Caetano, Joana, Rita, Catarina Santos, Susana and Ana for the sharing experiences and good times, for always being ready to help in any circumstance, a huge thank you.

To my friends and family back home for always supporting and making me work through the hard times, specially my parents and sister to whom I dedicate all this work.

To all the people here mentioned I give my most appreciated thank you!

Abstract

The extremely high diversity of organisms present in our oceans has led researchers to give great importance to the marine environment as a source of natural products. Marine cyanobacteria, in particular, are known for their ability to synthesize secondary metabolites with potential for novel drug discovery in the treatment of several human diseases. A large number of studies already performed in these organisms have been mainly focused on the filamentous and colonial forms. They revealed a high variety of compounds with anticancer activity while many cyanobacterial genera, namely unicellular free-living forms, have been largely overlooked. Studies on the bioactivity of these less studied genera have recently been performed at the Laboratory of Ecotoxicology Genomics and Evolution, LEGE – CIIMAR, revealing promising results. In this work, we aimed to isolate and characterize novel compounds from unicellular free-living species using a bioassay-guided isolation approach. Cytotoxicity of strains/fractions was studied on the RKO, MG63 and T47D cancer cell lines and the isolation of the compounds was guided by the bioactivity in these cancer cells. To complement bioactivity search, enzyme inhibition and antimicrobial assays were also performed. Partial characterization of the isolated compounds was achieved by Nuclear Magnetic Resonance spectroscopy and Liquid Chromatography – Mass Spectrometry.

Cyanobacterial cultures were performed and extracts were obtained from lyophilized biomass. *In vitro* cultures of the human cell lines were also established. The 3-(4,5-dimethylthiazol-2-yl)-2,5-diphenyltetrazolium bromide (MTT) assay was used to evaluate the cellular viability of cancer cells exposed to the different fractions obtained. IC50 values of the compounds were calculated by testing a range of concentrations in the same cancer cell lines. Isolation of the compounds was performed by wet chemistry extraction techniques and HPLC.

The MTT results revealed several sub-fractions which induced a decrease in cells viability for the *Synechocystis salina* LEGE 06099 strain. The enzymatic and antimicrobial assays revealed no activity from each fraction of this strain. Thus, following only MTT activity we were able to isolate several different compounds and to partially characterize their structure. Compounds F-5.4 and F-6.2.1 revealed moderate toxicity to these tested cell lines, being the T47D the most sensitive.

Another strain was used, uncultured Chroococcales LEGE 10410 strain, and molecular identification through the 16S rRNA gene revealed that this strain belonged to the genus *Chroococcidiopsis.* The MTT results revealed no significant bioactivity, while the enzymatic and antimicrobial assays showed interesting results for some fractions. However, further fractionation and isolation of these fractions is necessary.

Here, we discovered a family of novel compounds obtained from the cyanobacterial strain *Synechocystis salina* LEGE 06099 with moderate anticancer activity, although further analysis on their structure is necessary.

Resumo

A elevada diversidade de espécies marinhas presente nos nossos oceanos levou os investigadores a dar grande importância ao ambiente marinho como fonte de novos produtos naturais. Em particular, as cianobactérias marinhas são conhecidas pela sua capacidade de sintetizar metabolitos secundários com potencial para a descoberta de novas drogas no tratamento de diversas doenças humanas, incluindo o cancro. O elevado número de estudos já feitos para estes organismos têm dado principal destaque às espécies filamentosas e coloniais. Estas revelaram uma grande variedade de compostos com actividade anti-cancerígena, enquanto vários géneros de cianobactérias, nomeadamente os géneros unicelulares de vida livre, têm sido amplamente negligenciados. Estudos sobre a actividade biológica destas espécies menos estudadas têm sido realizados no Laboratório de Ecotoxicologia, Genómica e Evolução LEGE – CIIMAR e revelaram resultados interessantes. Neste trabalho, os principais objectivos foram isolar e caracterizar novos compostos de espécies unicelulares de vida livre usando uma abordagem de isolamento guiada por bioensaios. A citotoxicidade das fracções foi examinada nas linhagens cancerígenas humanas RKO, MG63 e T47D e o isolamento dos compostos seguiu a actividade observada nestas células. Para complementar a procura por bioactividade, foram também utilizados ensaios enzimáticos e antimicrobianos. A caracterização estrutural parcial dos compostos isolados foi realizada por Ressonância Magnética Nuclear e Cromatografia Líquida – Espectrometria de Massa.

Realizaram-se culturas de cianobactérias e os seus extractos brutos foram obtidos a partir da biomassa liofilizada. As linhagens tumorais foram mantidas em culturas *in vitro.* O teste de brometo 3-(4.5-dimetiltiaziol-2-il)-2.5-difeniltetrazolio (MTT) foi usado para avaliar a viabilidade celular das células cancerígenas expostas às diferentes fracções obtidas. O IC50 dos compostos foi calculado para as mesmas linhagens celulares usando um intervalo de concentrações conhecidas. O isolamento dos compostos foi realizado por técnicas aquosas de extracção química e HPLC.

Os resultados do ensaio MTT revelaram várias sub-fracções que induziram um decréscimo na viabilidade celular para a estirpe *Synechocystis salina* LEGE 06099. Os ensaios enzimáticos e antimicrobianos não revelaram bioactividade para nenhuma das fracções. Seguindo a actividade biológica registada pelo ensaio MTT conseguiram-se isolar diferentes compostos e caracterizar parcialmente as suas estruturas. Os compostos F-5.4 e F-6.2.1 revelaram toxicidade moderada nas diferentes linhas celulares, sendo que a linha T47D revelou ser a mais sensível.

Para além da estirpe LEGE 06099, foi também usada a estirpe desconhecida Chroococcales LEGE 10410 e através da análise molecular do gene 16S rRNA identificou-se como pertencendo ao género *Chroococcidiopsis.* Os resultados do ensaio MTT não revelaram actividade significativa para nenhuma das fracções testadas enquanto os ensaios enzimáticos e antimicrobianos revelaram algumas fracções interessantes. Contudo, é necessário continuar o fraccionamento e possível isolamento de compostos desta estirpe.

Aqui, descobrimos uma família de novos compostos com actividade anti-cancerígena obtidos a partir de *S. salina* LEGE 06099, embora análise mais detalhada sobre as suas estruturas seja necessária.

Table of contents

1. Introduction 1

1.1. Cyanobacteria 2
1.2 Bioactive compounds from marine cyanobacteria 3
1.3 Methodology used to detect and isolate new compounds 9
1.3.1 Nuclear Magnetic Resonance Spectroscopy 10
1.3.2 Liquid Chromatography - Mass Spectrometry 11

2. Objectives 12
3. Materials and Methods 13

3.1 Cyanobacterial strains 13
3.2 DNA extraction, PCR, cloning and sequencing of LEGE 10410 13
3.3 Extraction and bioassay-guided fractionation of *S. salina* LEGE 06099 biomass 14
3.4 Semi-preparative HPLC conditions 18

3.4.1. Sub-fraction F-5 19
3.4.2. Sub-fraction F-6 19
3.4.3. Sub-fraction F-6.2 20
3.4.4 Sub-fraction F-6.3 20
3.4.5 Sub-fraction F-7 20

3.5 Extraction and fractionation of Uncultured Chroococcales strain LEGE 10410 21
3.6 LC-HR-ESI-MS analysis 21
3.7 NMR analysis 22
3.8 Cell lines and cytoxicity assays 22
3.9 Enzymatic assays 23

3.9.1 HDAC assay 23
3.9.2 Proteasome assay 24

3.10 Antimicrobial screening susceptibility assay 24

4. Results and Discussion 25

4.1 Extraction and bioassay-guided fractionation of *S. salina* biomass 25
4.2 LC-HR-ESI-MS and NMR of the Fractions obtained. 31

4.2.1 Compound F-5.4 31

4.2.2 Compound F-6.2.1 35
4.2.3. Compound F-7.4 38
4.2.4 Compounds F-6.3.2, F-6.3.3 and F-6.3.8 41
4.5 IC50 of the compounds 43
4.6 MarinLit search of the obtained compounds. 45
4.7 Extraction and fractionation of Uncultured Chroococcales strain LEGE 10410 46
4.8 Molecular identification of Uncultured Chroococcales strain LEGE 10410……..... 48
5. Conclusion 50
6. References 51
7. Appendix 62
7.1 Appendix I – MTT viability assays (96 well plates; 3.3 x 10^4 cells per well; 4 hours exposure to MTT). 62
7.2 Appendix II – 2D NMR data of compounds F-5.4, F-6.2.1 and F-7.4. 68
7.3 Appendix III – UV-Vis data for each compound. 74

Figure index

Figure 1 – 20 Marine-derived drugs and clinical trial agents divided by their subsequently shown or predicted source organisms (20 total) (Adapted from Gerwick and Moore, 2012)……..…….…….…….…….…….……..……..…..2

Figure 2 – Biological activity of 128 isolated compounds from marine cyanobacteria (Tan, 2007)…….…….…….…….…….…….……..……4

Figure 3 – Marine cyanobacteria from the order Oscillatoriales indicating the major species that produce secondary bioactive compounds (Gerwick *et al.,* 2008)……..6

Figure 4 – System assemblage for the extraction of the crude extract……..……..…15

Figure 5 – Apparatus for the vacuum liquid chromatography (VLC)……16

Figure 6 – System assemblage for the normal phase column chromatography of fraction F…….…….……...…….…….…….…….…….……..…..17

Figure 7 – Cell viability (% of negative control) from E13010 crude extract and VLC fractions (A – I) with the concentration of 100 μg mL^{-1}(*) and 10 μg mL^{-1} on the RKO (a), MG63 (b) and T47D (c) cancer cell lines, with two exposure times, 24H and 48H at 3.3 x 10^4 cells per well. Negative control corresponded to 1% DMSO and positive control to 20% DMSO……..25/26

Figure 8 – Chromatogram of E13010 F-5 showing highlighted sub-fraction F-5.4. Conditions of the injection were as followed: 100 μL at a concentration of ~19 mg mL^{-1}…….…….…….…….…….…….…….…….…….……27

Figure 9 – Chromatogram of E13010 F-6 showing highlighted sub-fraction F-6.2 (1); F-6.3 (2) and F-6.4 (3). Conditions of the injection were as followed: 200 μL at a concentration of ~8 mg mL^{-1}…….…….…….…….…….…….…….…….……..28

Figure 10 – Chromatogram of E13010 F-6.2 showing highlighted sub-fraction F-6.2.1. Conditions of the injection were as followed: 40 μL at a concentration of ~1 mg mL^{-1}…...28

Figure 11 – Chromatogram of E13010 F-6.3 showing highlighted sub-fractions F-6.3.2 (1), F-6.3.3 (2) and F-6.3.8 (3). Conditions of the injection were as followed: 40 μL at a concentration of ~1 mg mL^{-1}…….…….…….…….…….…….…29

Figure 12 – Chromatogram of E13010 F-7 showing highlighted sub-fraction F-7.4. Conditions of the injection were as followed: 200 μL at a concentration of ~4 mg mL^{-1}.....30

Figure 13 – LC-MS analysis of all fractions obtained. Panel A) Liquid Chromatography of all individual fractions and a pool of all fractions. Panel B) Mass spectrum for each of the main chromatographic peaks of each fraction.....32/33

Figure 14 – ^{1}H-NMR (A) and ^{13}C-NMR (B) spectra of compound F-5.4/F-6.4 in $CDCl_3$ (recorded at 400 MHz).....34

Figure 15 – ^{1}H-NMR (A) and ^{13}C-NMR (B) spectra of compound F-6.2.1 in DMSO-d_6 (recorded at 600 MHz).....36

Figure 16 – ^{1}H-NMR (A) and ^{13}C-NMR (B) spectra of compound F-7.4 in DMSO-d_6 (recorded at 600 MHz).....38

Figure 17 – ^{1}H-NMR spectra of compound F-6.3.3 (A) and F-6.3.8 (B) in DMSO-d_6 (recorded at 600 MHz).....42

Figure 18 – ^{1}H-NMR spectra of compound F-6.3.8 in DMSO-d_6 (recorded at 600 MHz).....43

Figure 19 – Dose-response curves obtained for compound E13010 F-5.4 in MG63 osteosarcoma cancer cell line (a), RKO colon carcinoma cancer cell line (b) and T47D breast carcinoma cancer cell line (a).....44

Figure 20 – Chymotrypsin-like proteasome activity when tested with E14010 VLC fractions (A-I). Fractions tested at a final concentration of 3 μg mL^{-1}. The proteasome inhibitor epoxomicin was used for the positive control.....47

Figure 21 – Caspase-like proteasome activity when tested with E14010 VLC fractions (A-I). Fractions tested at a final concentration of 3μg mL^{-1}. The proteasome inhibitor epoxomicin was used for the positive control (the used concentration was not sufficient to cause inhibition).....47

Figure 22 – Antibiogram of *C. albicans* exposed to E14027 VLC fractions (A-I). Each blank disk was impregnated with 15 μL of a 1 mg mL^{-1} solution (DMSO). DMSO was used as the negative control.....48

Figure 23 – Amplicon obtained from the 16S rRNA gene for the strain LEGE 10410.....49

Table index

Table 1 – Five marine natural products that are FDA-Approved agents. Adapted from Gerwick and Moore, 2012.……..……..……..……...1

Table 2 - Marine cyanobacterial compounds with potential anticancer properties. Adapted from Costa *et al.,* 2012……..……..……..……..……..……..6/9

Table 3 - Gradient used for the VLC fractionation……..…….…..15

Table 4 – Gradient used for the normal phase gravity column chromatography of fraction F……..……..……..……...……..……..……..……..…..17

Table 5 – Fraction pooling after TLC……..……..……..……..……...18

Table 6 – Mobile phase gradient used for the semi-preparative HPLC on sub-fraction F-5……..……..……..……..……...19

Table 7 – Mobile phase gradient used for the semi-preparative HPLC on sub-fraction F-6……..……..……..……..……..19

Table 8 – Mobile phase gradient used for the analytical-scale HPLC on sub-fraction F-6.2……..……..……..……..……20

Table 9 - Mobile phase gradient used for the chromatographic separation of all tested samples……..……..……..……..……..……..……..……..22

Table 10 – Compendium of all isolated fractions with interest for further chemical analysis and their respective obtained mass……..……..……..……..……..……..……30

Table 11 - NMR spectroscopy data for F-5.4 in $CDCl_3$ at 600 MHz……..……35

Table 12 - NMR spectroscopy data for F-6.2.1 in DMSO-d_6 at 400 MHz……37

Table 13 - NMR spectroscopy data for F-7.4 in DMSO-d_6 at 400 MHz……...40

Table 14 – IC_{50} of compounds F-5.4 and F-6.2.1 in the MG63, RKO and T47D cancer cell lines……..……..……..……..……..……..……..……..43

Table 15 – MarinLit search for each compounds mass……..……..……..……...45

Appendixes

Appendix I - MTT viability assays (96 well plates; 3.3 x 10^4 cells per well; 4 hours exposure to MTT)……63

Figure 1 – Cell viability (% of negative control) from E13010 Fraction F sub-fractions (F-2 – F-12) with the concentration of 30 μg mL^{-1}(*) and 3 μg mL^{-1} on the RKO (a), MG63 (b) and T47D (c) cancer cell lines, with two exposure times, 24H and 48H at 3.3 x 10^4 cells per well. Negative control corresponded to 1% DMSO and positive control to 20% DMSO.

Figure 2 – Cell viability (% of negative control) from E13010 Fraction F-5 sub-fractions (F-5.1 – F-5.10) with the concentration of 30 μg mL^{-1}(*) and 3 μg mL^{-1} on the RKO (a), MG63 (b) and T47D (c) cancer cell lines, with two exposure times, 24H and 48H at 3.3 x 10^4 cells per well. Negative control corresponded to 1% DMSO and positive control to 20% DMSO.

Figure 3 – Cell viability (% of negative control) from E13010 Fraction F-6 sub-fractions (F-6.1 – F-6.12) with the concentration of 30 μg mL^{-1}(*) and 3 μg mL^{-1} on the RKO (a), MG63 (b) and T47D (c) cancer cell lines, with two exposure times, 24H and 48H at 3.3 x 10^4 cells per well. Negative control corresponded to 1% DMSO and positive control to 20% DMSO.

Figure 4 – Cell viability (% of negative control) from E13010 Fraction F-6.2; F-6.3 and F-7 sub-fractions with the concentration of 30 μg mL^{-1}(*) and 3 μg mL^{-1} on the RKO (a), MG63 (b) and HT29 (c) cancer cell lines, with two exposure times, 24H and 48H at 3.3 x 10^4 cells per well. Negative control corresponded to 1% DMSO and positive control to 20% DMSO.

Figure 5 – Cell viability (% of negative control) from E14027 VLC Fractions (A-I) with the concentration of 30 μg mL^{-1}(*) and 3 μg mL^{-1} on the RKO (a) and MG63 (b) cancer cell lines, with two exposure times, 24H and 48H at 3.3 x 10^4 cells per well. Negative control corresponded to 1% DMSO and positive control to 20% DMSO (T47D cell line had growing problems*).

Figure 6 – Dose-response curves obtained for compound E13010 F-6.2.1 in MG63 osteosarcoma cancer cell line (a), RKO colon carcinoma cancer cell line (b) and T47D breast carcinoma cancer cell line (a).

Appendix II - 2D NMR data of compounds F-5.4, F-6.2.1 and F-7.4……69

Figure 1 – HSQC (A) and HMBC (B) spectra of compound F-5.4/F-6.4 in $CDCl_3$ (recorded at 400 MHz).

Figure 2 – COSY (A) and NOESY (B) spectra of compound F-5.4/F-6.4 in $CDCl_3$ (recorded at 400 MHz).

Figure 3 – HSQC (A) and HMBC (B) spectra of compound F-6.2.1 in DMSO-d_6 (recorded at 600 MHz).

Figure 4 – COSY spectra of compound F-6.2.1 in DMSO-d_6 (recorded at 600 MHz).

Figure 5 – HSQC (A) and HMBC (B) spectra of compound F-7.4 in DMSO-d_6 (recorded at 600 MHz).

Figure 6 – COSY spectra of compound F-7.4 in DMSO-d_6 (recorded at 600 MHz).

Appendix III - UV-Vis data for each compound……..……..75

Figure 1 – UV-Vis spectra of compound F-5.4 in MeOH (Absorption maxima was registered at 281 nm with an OD of 0.180).

Figure 2 – UV-Vis spectra of compound F-6.2.1 in MeOH (Absorption maxima was registered at 282 nm with an OD of 0.099).

Figure 3 – UV-Vis spectra of compound F-6.3.2 in MeOH (Absorption maxima was registered at 285 nm with an OD of 0.041).

Figure 4 – UV-Vis spectra of compound F-6.3.3 in MeOH (Absorption maxima was registered at 282 nm with an OD of 0.040).

Figure 5 – UV-Vis spectra of compound F-6.3.8 in MeOH (Absorption maxima was registered at 282 nm with an OD of 0.042).

Figure 6 – UV-Vis spectra of compound F-7.4 in MeOH (Absorption maxima was registered at 281 nm with an OD of 0.201).

List of Abbreviations

BLASTn - Basic local alignment and search tool for nucleotide

CEMUP – Centro de Materiais da Universidade do Porto

CIIMAR – Interdisciplinary Centre of Marine and Environmental Research

COSY – Correlation spectroscopy

DMEM – Dulbecco's Modified Eagle Medium

DMSO – Dimethyl sulfoxide

DNA – Deoxyribonucleic acid

ESI – Electrospray ionization

FDA – US Food and Drug Administration

HDAC – Histone deacetylase

HMBC – Heteronuclear multiple bond correlation

HPLC – High performance liquid chromatography

HR – High resolution

HSQC – Heteronuclear single quantum coherence

IC_{50} – Half maximum inhibitory concentration

LC – Liquid chromatography

LEGE – Laboratory of Ecotoxicology, Genomics and Evolution

LPS – Lipopolysaccharides

MH – Mueller-Hinton agar

MS – Mass spectrometry

MTT – 3-(4.5-dimethylthiazol-2-yl)-2.5-diphenyl tetrazolium bromide

NMR – Nuclear Magnetic Resonance

NOESY – Nuclear Overhauser effect spectroscopy

NRPs – Non-ribosomal peptides

NRPS – Non-ribosomal peptide synthetases

PCR – Polymerase chain reaction

PDA – Photodiode array

PKS – Polyketides synthases

PSI – Photosystem I

PSII - Photosystem II

RB flasks – Round bottom flasks

rRNA – Ribosomal ribonucleic acid

RP – Reverse phase

RT – Retention time

TLC – Thin layer chromatography

TMS – Tetrametil-silano

VLC – Vacuum liquid chromatography

1. Introduction

Over the last century, natural products have been an extremely rich source of drugs and structural templates for starting materials with exceptional importance for drug discovery for the treatment of infectious, neurological, cardiovascular, immunological, inflammatory and oncological human diseases (Butler, 2008; Newman and Cragg, 2012). The importance of such natural products is also remarkable as they can give rise to synthetic analogues with improved pharmacological and pharmacokinetic properties (Newman and Cragg, 2012). Natural products usually show pharmacological or biological activity and are produced by a large variety of living organisms, such as plants, invertebrates, fungi and bacteria (Mishra and Tiwari, 2011). The extremely high diversity of organisms present in our oceans has led researchers to consider the marine environment as a very rich source of natural products (Gerwick and Moore, 2012).

Marine organisms such as mollusks, sponges, tunicates, cnidarians, red, brown and green macroalgae, phytoplankton and bacteria (including cyanobacteria) have been the most studied in the research area of bioactive compounds (Blunt *et al*., 2013). From some of these groups, several success cases of natural compounds that were developed into therapeutics have been described (Table 1). Besides already FDA-Approved agents, other marine natural products inspired compounds are currently undergoing phase I, II and III clinical trials (Mayer *et al*., 2010).

Table 1 – Five marine natural products that are FDA-Approved Agents. Adapted from Gerwick and Moore, 2012.

Compound name	Collected source organism	Predicted biosynthetic source	Disease area
Cytarabine (Ara-C)	Sponge	Bacterium	Cancer
Viadarabine (Ara-A)	Sponge	Bacterium	Antiviral
Ziconotide	Cone snails	Mollusks	Pain
Trabectedin (ET-743)	Tunicate	Bacterium	Cancer
Brentuximab vedotin (SGN-35)	Mollusk	Cyanobacterium	Cancer

Although many of the marine natural compounds have been collected from sponges, tunicates or mollusks, it has been shown, or there is a strong suspicion that the

actual producers of these bioactive compounds are some of the microorganism species that they harbor, or of which they feed on (Gerwick and Moore, 2012).

Among microorganisms, bacteria are the most prolific species, thus being called the jewels of the world's ocean and accounting for the highest part of clinical trial and approved pharmaceutical drugs (Figure 1) (Gerwick and Moore, 2012).

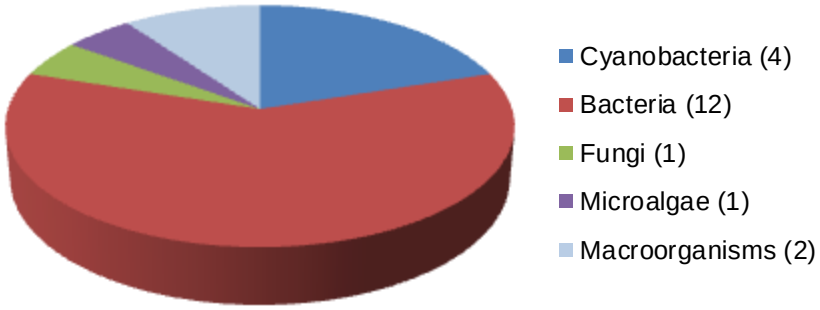

Figure 1 – 20 Marine-derived drugs and clinical trial agents divided by their subsequently shown or predicted source organisms (20 total) (Adapted from Gerwick and Moore, 2012).

From the microbial world, cyanobacteria were found to be an exceptionally prolific source of secondary metabolites, and continue to be a main biological source for the discovery of lead compounds for drug discovery (Dixit and Suseela, 2013).

1.1. Cyanobacteria

Cyanobacteria are prokaryotic gram-negative organisms that have the ability to perform photosynthesis. As gram-negatives, cyanobacteria have a layered and complex cell wall constituted by a thin peptidoglycan layer and periplasmic space between the inner cytoplasmic membrane and the outer cell membrane. This peptidoglycan layer is, however, thicker in cyanobacteria than in other gram-negative bacteria (Hoiczyk & Hansel, 2000). The outer membrane is chemically characterized by the presence of lipopolysaccharides (LPS), phospholipids and proteins while the periplasmic space is gel-like in consistency due to its composition of a high concentration of proteins and enzymes for nutrient acquisition, peptidoglycan synthesis and modification of toxic compounds (Madigan *et al*., 2003).

Regarding morphology, cyanobacteria can be unicellular (free living), colonial or filamentous. Photosynthetic reactions take place in the internal thylakoids, which are a membrane system with photosynthetic pigments. Cyanobacteria reproduce asexually by fission, fragmentation, hormogonia or akinete germination (Ferreira and Sousa, 1998).

Cyanobacteria are the only oxygenic photosynthetic bacteria, with photosystems (PSI and PSII), using H_2O as a photoreductant in the electron transport chain and consuming CO_2 as a carbon source (Castenholz and Boone, 2001). Furthermore, cyanobacteria can also be anaerobic photoautotrophs using H_2S, thiosulfate, or H_2 as alternative electron donors and can also perform nitrogen fixation (Whitton & Potts, 2002; Cohen & Gurevitz, 2006).

Organisms of this prokaryotic group have been found in most of the natural illuminated environments known so far, including terrestrial, freshwater and marine ecosystems. This wide distribution across the world reflects a large variety of species capable to adapt to numerous environmental conditions, much of them extreme, such as ice fields, deserts or hot springs, where they can survive and thrive (Biondi *et al.,* 2008; Vasconcelos, 2006). For certain genera, this adaptation to adverse conditions can be explained by the presence of specialized cyanobacterial cells such as heterocysts, which are used for nitrogen fixation in nitrogen depleted environments and/or akinetes, which have the capacity to store reserve substances and protect the organism during periods of darkness, dessication or cold (Ferreira & Sousa, 1998; Madigan *et al*., 2003).

The aquatic environment is where the cyanobacteria are more prevalent. These organisms are common in freshwater, brackish and marine environments around the globe where they can exist in either benthic or planktonic communities. For many years, cyanobacteria have been the subject of innumerous studies due to their negative impacts on freshwater ecosystems, where they can form harmful blooms causing severe changes in water quality and because they have the ability to release toxins (Vasconcelos, 2006; Martins *et al*., 2005). However, in more recent years, the study of marine cyanobacteria has come into focus, mainly due to their potential to produce very interesting natural compounds with biological activity and with high potential as pharmacological agents (Nunnery *et al*., 2010).

1.2 Bioactive compounds from marine cyanobacteria

Overall, cyanobacteria have been recognized as harmful to a large variety of organisms due to the potential production of toxic compounds, such as hepatotoxins, neurotoxins, cytotoxins, among others (Bláha *et al*., 2009). However, an increased

number of studies regarding marine cyanobacteria capability to produce bioactive compounds that are pharmacologically interesting for the treatment of human diseases, have been performed (Nunnery *et al*., 2010; Uzair *et al.,* 2012; Dixit and Suseela, 2013). For this reason, several bioactive compounds from these organisms were described where activity as antibacterial, anti-inflammatory, antiviral, antifungal, algaecides and in the particular case of this work, anticancer agents have been found (Figure 2) (Schlegel *et al.,* 1999; Martins *et al.,* 2008; Mayer *et al.,* 2011; Costa *et al.,* 2012; Rath & Priyadarshani, 2013).

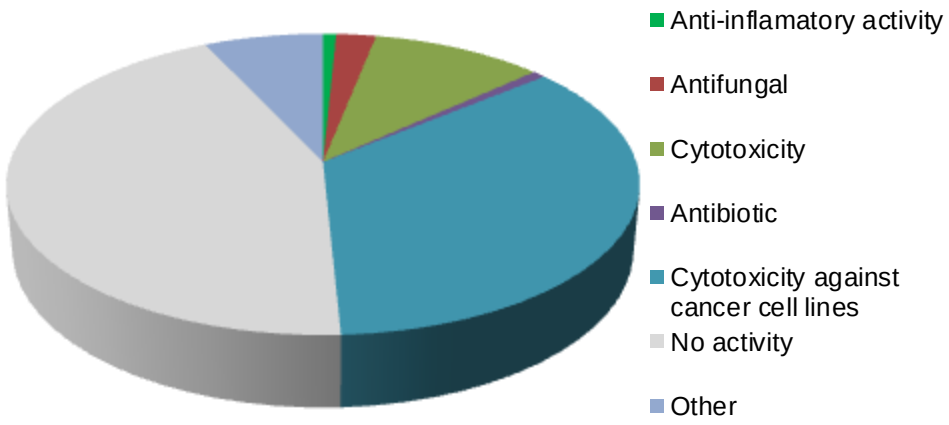

Figure 2 – Biological activity of 128 isolated compounds from marine cyanobacteria (Tan, 2007).

To date, most compounds have been isolated from the orders Oscillatoriales and Nostocales, followed by Chroococcales and Stigonematales, while only few compounds from the order Pleurocapsales were described (Tidgewell *et al.,* 2010). Of the nearly 800 compounds reported from marine cyanobacteria, almost half correspond to the order Oscillatoriales where the genus *Moorea* (formerly Lyngbya, Engene *et al*., 2012) is the most prolific, followed by the genera *Oscillatoria* and *Symploca* (Figure 3) (Gerwick *et al.,* 2008). Studies of this subject have been mainly focused on the more complex species such as the filamentous forms that grow in high densities in the tropical and subtropical regions, thus being easily collected and cultured in large quantities, yielding enough biomass for chemical investigations (Schlegel *et al.,* 1999). On the other hand, many marine cyanobacterial genera, namely unicellular free-living forms have been largely overlooked. Their existence in lower densities in the environment turns their collection and isolation processes more difficult, making it necessary to culture large amounts of

biomass in the laboratory to proceed to the chemical investigations (Leão *et al.,* 2013). The fact that filamentous and colonial forms appear to have larger genomes than the unicellular free-living ones, thus better accommodating polyketide (PKS) and non-ribosomal peptide (NPKS) pathways, is another reason as why these complex species have been the major source of a variety of bioactive compounds (Shih et al., 2013).

The biosynthetic pathways for these compounds are a widely studied topic. So far the majority of these compounds appear to be synthesized by NRPS or NRPS/PKS hybrid pathways (Welker & Dohren, 2006), pathways that lead to the production of a wide diversity of metabolites (Nunnery *et al.,* 2010).

Cyanobium, Synechocystis and *Synechococcus* are some examples of underexplored unicellular free-living genera of cyanobacteria. Given the importance of marine cyanobacteria as potential producers of bioactive compounds and the extensive coastal area of Portugal, studies with the goal of isolating new strains from these regions and their characterization, from an ecotoxicological and pharmacological point of view were performed, in order to evaluate their potential impacts on ecosystems and public health. Since then, several strains, including some of these genera have been maintained in the LEGE (Laboratory of Ecotoxicology, Genomics and Evolution) cyanobacteria culture collection at CIIMAR (Interdisciplinary Centre of Marine and Environmental Research). Recently, a study performed by Costa *et al.,* (2014) revealed, through cytotoxicity assays of some unicellular free-living genera extracts against human cancer cell lines, that several strains had the potential for the isolation of secondary bioactive compounds. This happened for the compound hierridin B, which was isolated from the Cyanobium strain LEGE 06113, and exhibited selective cytotoxicity towards the colon adenocarcinoma cell line HT29 (Leão *et al.,* 2013).

Tan (2007), performed a revision work about 128 compounds isolated from marine cyanobacteria and determined that in more than 35% of them, cytotoxicity against cancer cell lines was detected. Shown in Table 2 are some other marine cyanobacterial compounds with potential anticancer properties.

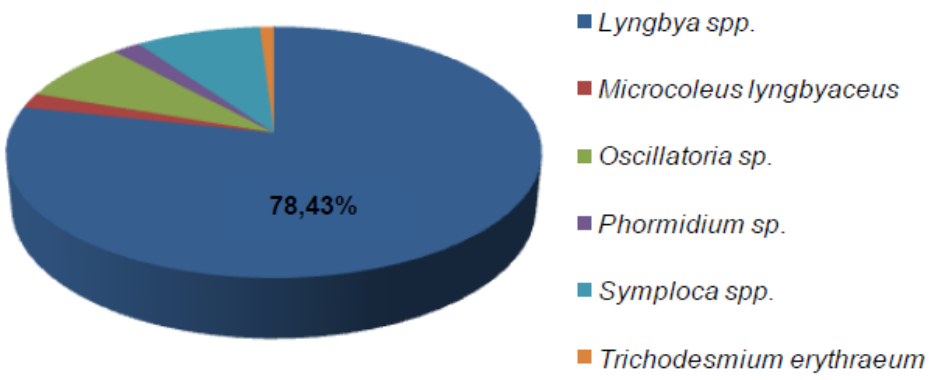

Figure 3 – Marine cyanobacteria from the order Oscillatoriales indicating the major species that produce secondary bioactive compounds (Gerwick *et al.,* 2008).

.

The fact that cyanobacterial compounds have revealed a large variety of structures and activities, has led to the creation of synthetic analogues with improved pharmacological and pharmacokinetic properties. Curacin A and Dolastatin 10 are some examples of molecules that have been in pre clinical or clinical trials as potential anticancer drugs (Gerwick *et al.,* 2001). From Dolastatin 10, the analogues TZT-1027, ILX-651 were synthesized (Mita *et al.,* 2006; Watanabe *et al.,* 2006). TZT-1027 (or soblitodin), designed to have increased antitumor activity and reduced side effects, revealed to be superior to former existing anticancer drugs and underwent phase I testing for the treatment of solid tumors (Watanabe *et al.,* 2006), while the antitumor agent ILX-651 (or tasidotin), after its successful run in phase I trials, underwent into phase II trials (Mita *et al.,* 2006). Brentuximab vedotin is the most recent anticancer agent from the marine environment. It was synthesized from monomethyl auristatin E, a dolastatin 10 analogue, and is an extremely effective and well tolerated agent in the treatment of Hodgkin lymphoma and systemic anaplastic large-cell lymphoma (de Claro *et al*., 2012).

Table 2 – Marine cyanobacterial compounds with potential anticancer properties. Adapted from Costa *et al.,* 2012.

Compound	Source	Class of compound	Anticancer activity	Reference
Ankaraholide A	*Geitlerinema*	Glycosilated swinholide	Cytotoxicity against NCI-H460 and MDA-MB-435 cell lines	(Andrianasolo *et al.,* 2005)
Apratoxins	*Lyngbya*	Cyclic depsipeptide	Cytotoxicity against a panel of cancer cell lines	(Luesch *et al.,* 2001,2002)

Aurilides	*Lyngbya majuscula*	Cyclic depsipeptide	Cytotoxicity against NCI-460 and neuro-2a mouse neuroblastoma cells	(Han *et al.,* 2006)
Belamide A	*Symploca sp.*	Linear tetrapeptide	Cytotoxicity against HCT-116 colon cancer line	(Simmons *et al.,* 2006)
Bisebromoamide	*Lyngbya sp*.	Peptide	Cytotoxicity against a panel of cancer cell lines	(Teruya *et al.,* 2009a)
Biselyngbyaside	*Lyngbya sp*.	Glicomacrolide	Cytotoxicity against a panel of cancer cell lines	(Teruya *et al.,* 2009b)
Calothrixins	*Calothrix*	Pentacyclic indolophenan-thridine	Bioactive against human HeLa cancer cells and apoptotic against human Jurkat cancer cells	(Chen *et al.,* 2003)
Caylobolide A	*Lyngbya majuscula*	Macrolactone	Cytotoxicity against a panel of cancer cell lines	(Macmilliam *et al.,* 2003)
Coibamide A	*Leptolyngbya sp.*	Cyclic depsipeptide	Cytotoxicity against NCI-H460 and mouse neuro-2a cells	(Medina *et al.,* 2008)
Cryptophycin 1	*Nostoc spp.*	Cyclic depsipeptide	Cytotoxic activity in in vitro human tumor cell models	(Wagner *et al.,* 1999)
Dolastatin 10	*Symploca sp.*	Linear pentapeptide	Cytotoxicity against four small-cell lung cancer (SCLS) lines	(Kalemkerian *et al.,* 1999)
Ethyl tumonoate A	*Oscillatoria margaritifera*	Peptide	Toxicity against H-460 human lung tumor cells	(Engene *et al.,* 2011)
Hoiamides	Assemblage of *Lyngbya majuscula and Phormidium gracile*	Cyclic depsipeptide	Cytotoxicity against H460 human lung tumor cells	(Choi *et al*., 2010)
Homodolastatin 16	*Lyngbya majuscula*	Cyclic depsipeptide	Activity against esophageal and cervical cancer cell lines	(Davies-Coleman *et al.,* 2003)
Isomalyngamide	*Lyngbya majuscula*	Fatty acid amides	Activity against tumor cell migration through the β1 integrin-mediated antimetastatic	(Chang *et al.,* 2011)

			pathway	
Jamaicamides	*Lyngbya majuscula*	Polyketide-Peptides	Cytotoxicity against H460 human lung cancer and mouse neuro-2a cells	(Edwards *et al.,* 2004)
Kalkitoxin	*Lyngbya majuscula*	Lipopeptide	Cytotoxicity against human colon cell line HCT-116	(White *et al.,* 2004)
Lagunamides	*Lyngbya majuscula*	Cyclic depsipeptide	Cytotoxicity against a panel of cancer cell lines	(Tripathi *et al.,* 2012)
Largazole	*Symploca sp.*	Cyclic depsipeptide	Anti-proliferative activity	(Zeng *et al.,* 2010)
Lyngbyabellin A	*Lyngbya majuscula*	Cyclic depsipeptide	Cytotoxicity against KB nasopharyngeal carcinoma and LoVo colon adenocarcinoma cells	(Luesch *et al.,* 2000)
Lyngbyaloside	*Lyngbya sp*.	Glicomacrolide	Cytotoxicity against KB and LoVo cells	(Luesch *et al.,* 2002)
Majusculamide C	*Lyngbya majuscula*	Cyclic depsipeptide	Induction of filamentous F-actin loss against a10 cells	(Pettit *et al.,* 2008)
Malevamide D	*Symploca hydnoides*	Peptide ester	Toxicity against AS49, HT29, MEL28 and P388 cell lines	(Horgen *et al.,* 2002)
Malyngamides	*Lyngbya*	Fatty acid amines	Cytotoxicity against NCI-H460 and neuro-2a cancer lines	(Gross *et al.,* 2010)
Malyngolide dimmer	*Lyngbya majuscula*	Cyclodepside	Toxicity against H460 human lung cancer cell line	(Gutierrez *et al.,* 2010)
Obyanamide	*Lyngbya confervoides*	Cyclic depsipeptide	Cytotoxic against KB and LoVo cancer cell lines	(Williams *et al.,* 2002a)
Palauamide	*Lyngbya sp.*	Cyclic depsipeptide	Cytotoxic against KB oral epidermoid cancer	(Zou *et al.,* 2005)
Palmyramide A	*Lyngbya majuscula*	Cyclic depsipeptide	Blocking of sodium channels in neuro-2a cells and cytotoxicity against H460 human lung cancer cells	(Taniguchi *et al.,* 2010)
Pitipeptolides	*Lyngbya majuscula*	Cyclic depsipeptide	Cytotoxicity against HT29 colon adenocarcinoma and	(Montaser *et al.,* 2011a)

			MCF7 breast cancer cell lines	
Pitiprolamide	*Lyngbya majuscula*	Cyclic depsipeptide	Cytotoxicity against HCT116 colon and MCF7 breast cancer cell lines	(Montaser *et al.,* 2011b)
Somocystinamide A	*Lyngbya majuscula*	Lipopeptide	Stimulates apoptosis in a number of tumor cell lines	(Wrasidlo *et al.,* 2008)
Symplostatin 1	*Symploca hydnoides*	Linear pentapeptide	Cytotoxicity against NCI-H460 and neuroblastoma cells	(Mooberry *et al.,* 2003)
Tasiamide	*Symploca sp.*	Cyclic peptide	Cytotoxicity against KB and LoVo cells	(Williams *et al.,* 2002b)
Tasipeptins	*Symploca sp.*	Cyclic depsipeptide	Cytotoxicity against KB cells	(Williams *et al.,*2003a)
Ulongapeptin	*Lyngbya sp.*	Cyclic depsipeptide	Cytotoxicity against KB cells	(Williams *et al.,*2003b)
Veraguamides	*Symploca cf. hydnoides*	Cyclic depsipeptide	Cytotoxicity against H460 human lung cancer cell line	(Mevers *et al.,* 2011)
Wewakazole	*Lyngbya sordida*	Cyclic dodecapeptide	Cytotoxicity against H460 human lung cancer cell line	(Malloy *et al.,* 2011)
Wewakpeptins	*Lyngbya semiplena*	Depsipeptides	Cytotoxicity against NCI-H460 human lung tumor and neuro-2a mouse neuroblastoma cell lines	(Han et al., 2005)

1.3 Methodology used to detect and isolate new compounds

Improvements in several approaches and strategies linking natural products with modern biology and screening platforms have been performed. The quality and amount of materials being studied in biological assays has been largely enhanced by automated extraction protocols joined with prefractionation strategies (Teruya *et al.,* 2009b; Thornburg *et al.,* 2011). The prefractionation of the extracts to lower complex mixtures or to single compounds enhances the success rates, due to the concentration of low abundance activities and speeds the identification process of the active compound. A fusion approach is usually performed, where extracts or fractions are tested for bioactive

agents, and if a significant activity is detected, then bioassay-guided techniques are used alongside with HPLC to fractionate and purify compounds while ^{1}H-NMR and LC-MS are used to analyze the chemical constituents (Gerwick and Moore, 2012).

1.3.1 Nuclear Magnetic Resonance Spectroscopy

Nuclear magnetic resonance spectroscopy is an extremely important and vastly used method for structure elucidation of new metabolites.

Several kinds of atomic nuclei act as if they were spinning around an axis. As they are positively charged, these spinning nuclei behave like small bar magnets and interact with an external magnetic field. This happens for both the proton (^{1}H) and the ^{13}C nucleus. When a proton is submitted to an external magnetic field, its angular momentum (or spin), will align itself by one of two ways: with the external magnetic field (parallel to) or against it (antiparallel to) (McMurry, 2007). Electromagnetic radiation can induce the proton to flip from one energy stage to another, leading the nucleus into a resonance stage. Resonance is the absorption of a certain frequency that will lead the nucleus of an atom to inverse its angular moment. However, once a magnetic field is applied, the electrons surrounding the nucleus create small and local magnetic fields that will be opposite to the external field. This shows that the effective field to which the nucleus is subjected is smaller than the applied one, because of the moving electrons generating a shield around it. This is called shielding, and, to achieve the particular value in which absorption occurs, a shielded proton requires a higher magnetic force than one without shielding (McMurry, 2007). This means that this phenomenon can increase NMR absorption values. A delta scale (δ) and a reference are used to improve the measure and to define the peak's position. The tetrametil-silano (TMS) absorption signal represents 0,0 ppm and the distance between the NMR signal of a certain proton and the one emitted by the TMS is called the proton's chemical shift (McMurry, 2007). Each nucleus present in a different environment has a distinctive shield, and, this way, the NMR analysis provides a spectrum representing the chemical shifts of each compound tested allowing its detailed characterization.

In the early stages of this work, to evaluate the separation procedure, the different NMR spectra were obtained for each fraction. When the compounds were pure, 1D and 2D NMR were used to differentiate the compounds obtained and as a first step towards structure elucidation.

1.3.2 Liquid Chromatography - Mass Spectrometry

LC-MS, like NMR is a widely used method for aiding in structural elucidation. In order to get identification of the bioactive compound, liquid chromatography can be followed by mass spectrometry (Harada *et al.,* 2004). Mass spectrometry is a method used for measuring the mass (molecular weight) and can provide information about its structure by breaking the molecule into smaller fragments while measuring their masses (McMurray, 2007). A mass spectrometer is composed by three parts: an ionization source, a mass analyzer and the detector. They operate by converting the molecules to a charged state with the ionization source, with consequent analysis of ions or fragment ions produced during this process according to their mass to charge ratio (*m/z*) by the mass analyzer. The detector observes and counts the separated ions and records them as peaks at different *m/z* (McMurray, 2007). The data of the mass spectroscopy is given as a bar graph with masses on the *x* axis and relative abundance of ions of a certain mass on the *y* axis (McMurray, 2007).

Different technologies are applicable for both ionization and ion analysis. Electrospray Ionization (ESI), the most widely used ion source for biological molecules was used in this work.

2. Objectives

Results from a screening on the anticancer potential of marine cyanobacteria strains isolated from the Portuguese coast performed in LEGE at CIIMAR, revealed several strains that had cytotoxicity against human cancer cell lines (Costa *et al.,* 2014). Following these results, *Synechocystis salina* LEGE 06099 was chosen as one of the strains used in this work as it appeared to be one of the most interesting strains for the isolation of bioactive compounds. The Unidentified Chroococcales strain LEGE 10410 was also chosen for this work, mainly due to the fact that it represents a largely untapped genus, even though for this strain no previous studies on its bioactive properties had been performed.

The main objectives of this work were to isolate new compounds, from the selected cyanobacteria strains based on a bioassay-guided fractionation with cancer cell lines, to characterize its structure and to estimate its anticancer potency (*in vitro*).

For this purpose, wet chemistry extraction techniques and High Performance Liquid Chromatography (HPLC) were used to isolate the compounds, Nuclear Magnetic Resonance (NMR) and Liquid Chromatography – Mass Spectrometry ($LC\text{-}MS^n$) were used for deriving structural information and the 3-(4.5-dimethylthiazol-2-yl)-2.5-diphenyl tetrazolium bromide (MTT) assay was used to estimate the anticancer potency. Complementary bioactive potential was also investigated by enzymatic and antimicrobial assays.

3. Materials and Methods

3.1 Cyanobacterial strains

Synechocystis salina LEGE 06099 was isolated from the Portuguese coast (Moledo do Minho) and a monocyanobacterial culture of this strain is maintained in the LEGE Culture Collection (Brito *et al*., 2012). Large-scale cultures of this strain were carried out for biomass production and subsequent chemical investigations. *S. salina* cells were grown in Z8 medium (Kotai, 1972), supplemented with 20 g L^{-1} NaCl. Cultures were maintained at 25 ºC, with a light intensity of approximately 30 µmol photons m^{-2} s^{-1} and with a light/dark cycle of 14:10h. Exponential growing cells were harvested by centrifugation, frozen at -20 ºC and freeze-dried. The lyophilized biomass was stored at -20 ºC. The Unidentified Chroococcales strain LEGE 10410 was also isolated from the Portuguese Coast (Vila Nova de Mil Fontes) and like the previous strain is maintained in the LEGE culture collection. Large-scale cultures of this strain were performed for biomass production and subsequent chemical investigations. Unidentified Chroococcales LEGE 10410 cells were grown in MN medium (Ripka, 1988) under the light and temperature conditions described above, then harvested, processed and stored also as *S. salina* cells.

3.2 DNA extraction, PCR, cloning and sequencing of LEGE 10410

The LEGE 10410 strain was characterized by molecular analysis of the 16S rRNA gene. Total genomic DNA was extracted from frozen samples using the Purelink™ Genomic DNA Mini Kit (Invitrogen, Carlsbad, CA, USA) following the protocol described for Gram-negative bacteria. The primers: CYA359F and 781R (Neilan et al., 1997) were used for amplifying the 16S rRNA gene. The PCR conditions were as follows: initial denaturation at 94ºC for 4 minutes, followed by 35 cycles of denaturation at 94ºC for 30 seconds, annealing at 52ºC for 30 seconds and extension at 72 ºC for 80 seconds and a final extension step at 72ºC for 5 minutes. All PCR reactions were prepared in a volume of 20.0 µL containing 1×PCR buffer, 2.5 mM $MgCl_2$, 250.0 mM of each deoxynucleotide triphosphate, 10.0 pmol of each of the primers, 0.5 U of *Taq* DNA polymerase (Bioline, Luckenwalde, Germany) and 10 ng of template DNA. PCR products were separated by

electrophoresis on a 1.5% (w:v) agarose gel. The gels were stained with ethidium bromide and photographed under UV transillumination.

Amplicons of the expected size (~400 bp) were purified using Cut&Spin, DNA Gel Extraction Columns (Grisp, Portugal), according to the manufacturer's instructions. Purified PCR products were then cloned into pGEM®-T Easy vector (Promega, Madison, WI, USA), and transformed into OneShot® TOP10 chemically competent *Escherichia coli* cells (Invitrogen, Carlsbad, CA, USA) using standard procedures (Sambrook and Russell, 2001) and following the manufacturer's instructions. Plasmid DNA was isolated using the GenElute™ Plasmid Miniprep Kit (Sigma-Aldrich, St. Louis, MO, USA) and sequenced (Macrogen, Inc, Seoul, Korea) using M13 primers. The 16S rRNA sequences were inspected for quality and aligned with Geneious 7.1.7 (Biomatters). After alignment, the sequences obtained were inserted in the BLASTn (Basic Local Alignment and Search Tool for nucleotide) database, which allowed inferring determining the genus of the strain.

3.3 Extraction and bioassay-guided fractionation of *S. salina* LEGE 06099 biomass

Cyanobacterial crude extracts were performed with the lyophilized material previously obtained by employing an apparatus assembled as shown in Figure 4. A mixture of dichloromethane:methanol (2:1) was added to and immersed the biomass of *S. salina* LEGE 06099 (15.3 g, d.w.). This mixture was allowed to remain for one hour at room temperature, while stirring homogenizing the biomass with a spatula. At the end of this hour the vacuum was turned on as the solvent contents were poured into the Büchner funnel and the resulting liquid phase was collected in a round bottom (RB) flask. Before starting a new step in the extraction, the biomass that had been poured was retained in the cheese cloth and recovered for a new extraction. This process was repeated one more time under these conditions and then four times at approximately 40ºC with the use of a hotplate, for 20 minutes each, with constant stirring. Following extraction, the RB flask was removed from the assembly and the solvents were removed in a rotary evaporator. The content of the RB flask was then resuspended and transferred to a pre-weighed glass vial which was dried *in vacuum* to yield 2.6 g of crude extract.

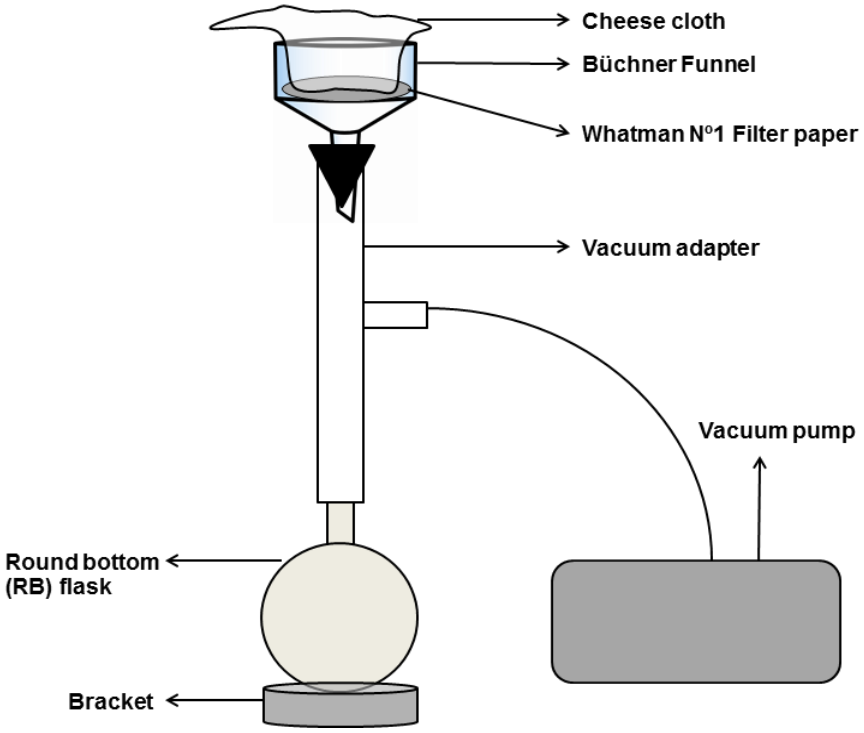

Figure 4 – System assemblage for organic extraction.

The crude extract was then subjected to normal phase (silica gel 60, 0.0015-0.040 mm, Merck, KgaA, Damstadt, Germany) vacuum liquid chromatography (VLC) (Figure 2). A gradient of solvents from 9:1 hexanes:EtOAc to 100% EtOAc to 100% MeOH was used in this VLC (Table 3), so as to obtain fractions with increased polarity.

Table 3 – Gradient used for the VLC fractionation.

Fraction	EtOAc (%)	Hexane (%)	MeOH (%)	Volume
A	10	90	-	> 250 mL
B	20	80	-	250 mL
C	30	70	-	250 mL
D	40	60	-	250 mL
E	60	40	-	250 mL
F	80	20	-	250 mL
G	100	-	-	250 mL
H	75	-	25	250 mL
Hx	75	-	25	250 mL
I	-	-	100	250 mL

The crude extract was dissolved in the same percentage of solvents used for fraction A with the help of ultrasounds and loaded onto Whatman No1 filter paper placed

on top of the silica column and the solvent mixtures were added stepwise, according to Table 3, without allowing the silica surface to become dry and resulting in ten fractions (A – I) that were collected separately in RB flasks. The fractions were dried under reduced pressure, resuspended, transferred to pre-weighed vials and weighed before being inspected by ^{1}H NMR (400 MHz, BrukerAvance III) and submitted to biological assays.

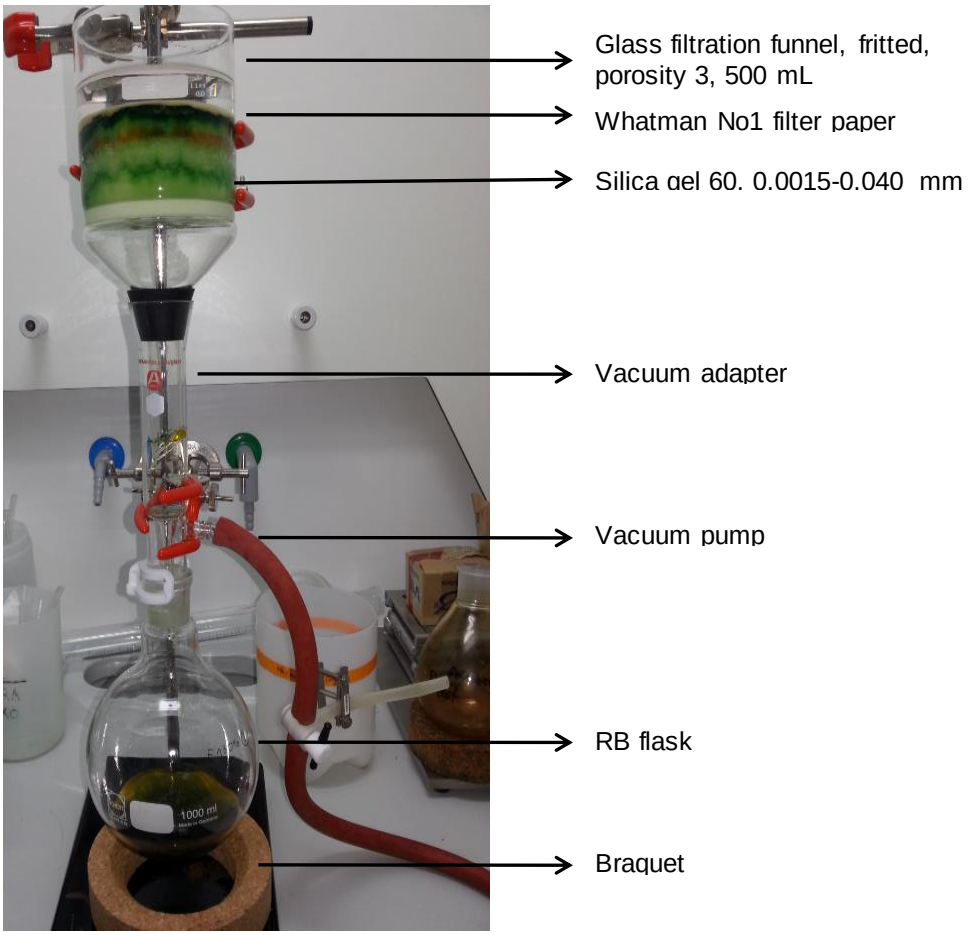

Figure 5 – Apparatus for the vacuum liquid chromatography (VLC).

Fraction F (196.2 mg), eluting with 80% EtOAc, was selected for further fractionation on the basis of its MTT cytotoxicity assay and because it had the highest mass. This was performed by a normal phase column chromatography (silica gel 60, 0.040-0.063 mm, Merck, KgaA, Damstadt, Germany).

A gradient of solvents from 30% EtOAc to 100% EtOAc to 25% MeOH was used for this fractionation (Table 4).

Table 4 – Gradient used for the normal phase gravity column chromatography of fraction F.

Collection tubes	(%) EtOAc	(%) Hexane	(%) MeOH	Volume
1 – 3	30	70	-	200 mL
4 – 27	40	60	-	200 mL
	40	60	-	200 mL
	40	60	-	200 mL
28 – 33	80	20	-	80 mL
34 – 38	100	-	-	80 mL
39 – 44	75	-	25	80 mL

Fraction F was dissolved in 30% EtOAc (Hexane) and loaded onto the silica column, which was assembled as shown in Figure 6. This chromatography was performed by gravity and 44 fractions were collected.

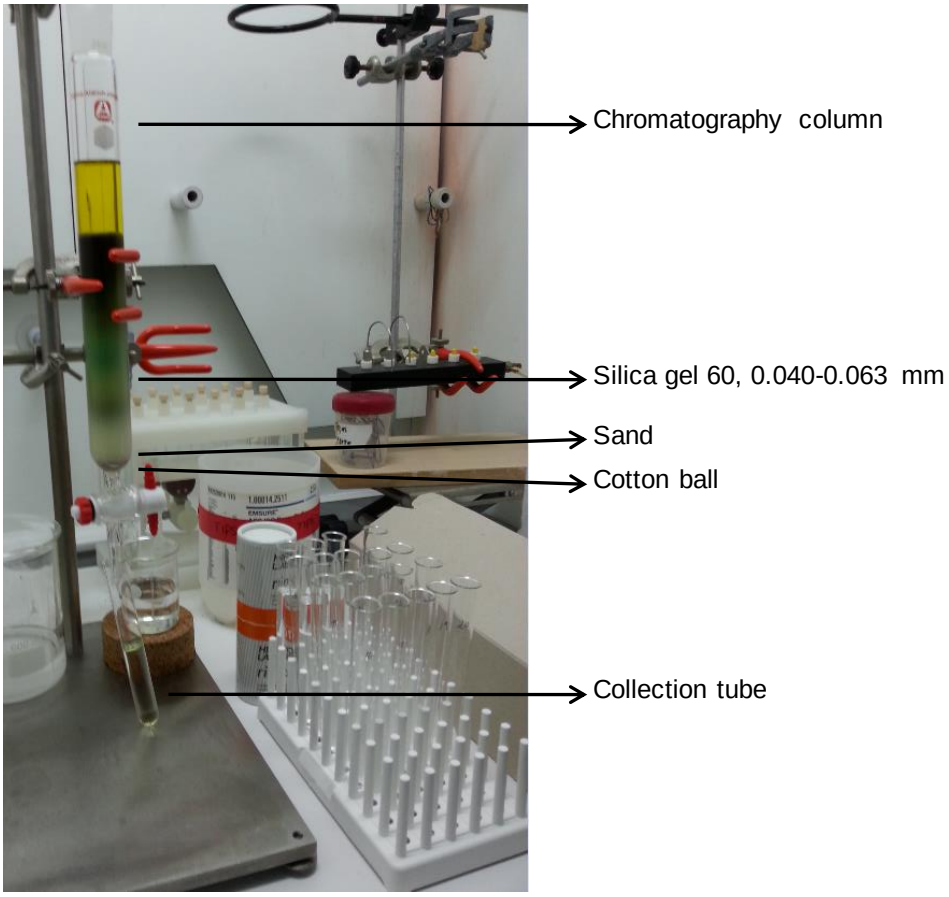

Figure 6 – System assemblage for the normal phase column chromatography of fraction F.

The fractions were inspected by thin-layer chromatography (TLC) and pooled in RB flasks according to their TLC profile (Table 5). The TLC was performed in a container with a 10 mL solution of 50% EtOAc and 50% Hexane. Each of the collection tubes were

spotted onto the TLC plate which was visualized under UV light and with PMA (Phosphomolybdic acid) stain.

Table 5 – Fraction pooling after TLC.

Collection Tubes	Fraction
1 – 2	F-1
3 – 4	F-2
5 – 6	F-3
7 – 11	F-4
12 – 13	F-5
14 – 15	F-6
16	F-7
17 – 23	F-8
24 – 28	F-9
29 – 32	F-10
33 – 41	F-11
42 – 44	F-12

The pooled fractions in RB flasks were dried on rotary evaporator, resuspended and transferred to pre-weighed glass vials. After solvent removal *in vacuum* each of the twelve sub-fractions (F-1 to F-12) was weighed, inspected by ^{1}H NMR (400 MHz, BrukerAvance III) and submitted to a cytotoxicity assay.

3.4 Semi-preparative HPLC conditions

After analyzing the ^{1}H NMR and the cytotoxicity assays, several fractions were selected for further purification by semi-preparative HPLC on the basis of its MTT cytotoxicity assay. A 1525 Binary HPLC pump and a 996 PDA detector (Waters, Milford, MA, USA) were used in all semi-preparative separations. Each fraction had to undergo a process of optimization whereby different gradients were tested until the best possible separation was achieved. The conditions for the optimized separation of the components of each sub fraction are described below. The peaks shown in the chromatograms were collected in RB flasks from multiple injections and the solvents removed *in vacuo* before being resuspended and transferred to pre-weighed vials. The HPLC fractions were

weighed and then inspected by ^{1}H NMR (400 MHz, BrukerAvance III) and submitted to a cytotoxicity assay.

3.4.1. Sub-fraction F-5

The separation of sub-fraction F-5 was carried out with a Synergi Fusion-RP column (10 μm, 250 x 10 mm, Phenomenex, Torrance, CA, USA) by employing the gradient program described in Table 6.

Table 6 – Mobile phase gradient used for the semi-preparative HPLC on sub-fraction F-5.

Time	Flow (mL/min)	MeCN (%)	H_2O (%)
0	3	87	13
40	3	87	13
45	3	100	0
52	3	100	0
55	3	87	13
60	3	87	13

3.4.2. Sub-fraction F-6

The chromatographic system used for the semi-preparative RP-HPLC of the sub-fraction F-6 was the same that was used for sub-fraction F-5. The gradient program used for the separation of this sub-fraction is shown in Table 7.

Table 7 – Mobile phase gradient used for the semi-preparative HPLC on sub-fraction F-6.

Time	Flow (mL/min)	MeCN (%)	H_2O (%)
0	3	85	15
25	3	100	0
60	3	100	0
70	3	85	15
75	3	85	15

After the HPLC, the collected samples were subjected to ^{1}H NMR and a cytotoxicity assay. Fractions F-6.2 and F-6.3 were found to require a new round of purification using analytical-scale HPLC.

3.4.3. Sub-fraction F-6.2

The chromatographic system used for the analytical-scale RP-HPLC purification of sub fraction F-6.2 was fitted with a Synergi Fusion-RP column (4 μm, 250 x 4.60 mm, Phenomenex, Torrance, CA, USA). The gradient program used for the separation of this fraction is shown in Table 8.

Table 8 – Mobile phase gradient used for the analytical-scale HPLC on sub-fraction F-6.2.

Time	Flow (mL/min)	MeCN (%)	H_2O (%)
0	1	70	30
43	1	70	30
45	1	99	1
60	1	99	1

3.4.4 Sub-fraction F-6.3

The chromatographic system used for the analytical-scale RP-HPLC of the sub fraction F-6.3 was the same used for the sub fraction F-6.2. For this separation an isocratic program of 73% MeCN (aq) was employed.

3.4.5 Sub-fraction F-7

The chromatographic system used for the semi-preparative RP-HPLC of the sub fraction F-7 was the same used for the sub fraction F-6. The gradient program used was also the same.

3.5 Extraction and fractionation of Uncultured Chroococcales strain LEGE 10410

Cyanobacterial crude extracts were performed with the lyophilized material obtained by employing an apparatus, identical to the one described for *S. salina* LEGE 06099. The mixture of dichloromethane:methanol (2:1) was added to and immersed the biomass of Uncultured Chroococcales strain LEGE 10410 (14.2 g, d.w.). The first two steps were carried out for 1 hour at room temperature. It was visible that few pigments were being extracted, an indication of poor solvent penetration in the cells due to the exopolyssacharide matrix, so, for the next step in the extraction, along with heat (approximately 40º C), ultrasounds were also used. Three steps of 20 minutes each were performed under these conditions. Still, very low pigment extraction was visible, so sonication was used 20 times for 30 seconds with a 30 second interval between each use. Despite these conditions, it was still difficult to extract mass from this cyanobacterial strain. For that reason the biomass was left with a solution of dichloromethane:methanol (2:1) over the 48 hours with constant stirring. After the weekend, two more steps (similar to the previously done with the use of the sonicator) were performed. As no more pigments were being extracted, the extraction was concluded. The RB flask was removed from the assembly and the solvents were removed under reduced pressure. The contents of the RB flask were then resuspended and transferred to a pre-weighed glass vial, which was dried *in vacuo* to yield 0.6 g of crude extract.

The VLC for this strain had the same conditions used for the VLC of *S. salina* LEGE 06099, except it wasn't required the collection of the fraction Hx.

The fractions obtained were then inspected by ^{1}H NMR (400 MHz, BrukerAvance III) and submitted to cytotoxic and enzymatic assays.

3.6 LC-HR-ESI-MS analysis

For the mass spectrometry analysis, samples were taken to Centro de Materiais da Universidade do Porto (CEMUP) for analysis. It was used an HPLC Accela with Accela PDA detector, Accela Autosampler and Accela 600 Pump (Thermo Fischer Scientific, Bremen, Germany) to perform the chromatographic separation. The utilized instrument was a LTQ Orbitrap XL mass spectrometer (Thermo Fischer Scientific, Bremen, Germany) controlled by LTQ Tune Plus 2.5.5 and Xcalibur 2.1.0.

The capillary voltage of the electrospray ionization (ESI) was set to 2800 V. The capillary temperature was 300ºC. The sheath gas and auxiliary gas flow rate (nitrogen) were set to 40 and 10 (arbitrary unit as provided by the software settings). The capillary voltage was -48 V and the tube lens voltage -247.79V. The volume of each injection was 20μL at approximately 50 μg mL^{-1} and the gradient program used for all samples were as indicated in Table 9.

Table 9 - Mobile phase gradient used for the chromatographic separation of all tested samples.

Time (min)	H_2O (%)	MeCN (%)	Flow (µL/mL)
0	13	87	500
25	13	87	500
30	0	100	500
35	0	100	500
36	13	87	500
40	13	87	500

3.7 NMR analysis

For the nuclear magnetic resonance (NMR), samples were prepared in the laboratory in specific NMR tubes (Norell Standard Series™ 5mm NMR tubes, Sigma-Aldrich) with $CDCl_3$ or DMSO-d_6 and taken to CEMUP for analysis at 400 MHz (BrukerAvance III) or 600 MHz (BrukerAvance III equipped with a CryoProbe™ Prodigy).

3.8 Cell lines and cytoxicity assays

All the cell lines included in this study are of human origin. Cytotoxic assays were performed with the cell lines T47D (breast carcinoma cells), RKO (colon carcinoma cells) and MG63 (osteosarcoma cells). Cell lines were selected according to previous studies (Costa *et al.,* 2014). Tumor cells were cultured in DMEM Glutamax medium (Dulbecco's modified Eagle Medium DMEM GlutaMAX™ – Gibco-Invitrogen), supplemented with 10% (v/v) fetal bovine serum (Gibco-Invitrogen), 5 mL fungizone (2.5 µg mL^{-1}) (Gibco-Invitrogen) and 5 mL of penicillin-streptomycin (Pen-Strep 100 IU mL^{-1} and 10 mg mL^{-1},

respectively) (Gibco-Invitrogen). Cells were incubated in a humidified atmosphere with 5% of CO_2, at 37ºC.

The cellular viability was evaluated by the reduction of the 3- (4.5 dimethylthiazole-2-yl)-2.5-diphenyltetrazolium bromide (MTT) (Alley *et al*., 1988) a yellow tretazole soluble in water, to purple formazan crystals that are insoluble in water. The reduction of MTT to formazan is directly proportional to the mitochondrial activity and consequently cell viability.

Cells were seeded in 96-well culture plates at a concentration of 3.3×10^4 cells cm^{-2}. After 24 hours of adhesion, cells were exposed to 100 μL fresh medium supplemented with the compounds to a final concentration of 3 and 30 μg mL^{-1} for a period of both 24 and 48 hours. After incubation cells were exposed to 10 μL of 0.5 mg mL^{-1} MTT. Following exposure, the purple-colored formazan salts were dissolved in 100 μL DMSO and the absorbance measured at 550 nm in a microplate reader (Synergy HT, Biotek, USA). All tests were run in triplicate and averaged. A similar procedure was undertaken for determining the IC_{50} value of the compounds in the T47D, RKO and MG63 cell lines. In this case, however, cells were incubated for 48 hours and the final concentrations of the compounds ranged from 0.003 to 50 μg mL^{-1}. Dose-response data was used to calculate the IC_{50} with the software GraphPad Prism v6.0 (GraphPad Software, La Jolla, CA, USA).

3.9 Enzymatic assays

3.9.1 HDAC assay

The HDAC-Glo™ I/II assay activity assay and screening system (Promega) was used to evaluate the relative activity of histone deacetylase (HDAC) class I and II enzymes. The assay was performed as indicated in the manufacturer's protocol. Briefly, the HDAC-Glo™ I/II Reagent was prepared by adding buffer and developer enzyme to lyophilized luciferase reaction components. Diluted HeLa nuclear extract and the inhibitor trichostatin A were prepared by adding buffer to stock solutions respectively. Then, the Reagent was added to the HeLa nuclear extract (HDAC enzyme source) with or without inhibitor. The tests were performed in 96-well white-walled plates with a final volume of 200 μL and the extracts were tested at 3 μg mL^{-1}. The plates were incubated at room temperature for 30 minutes, after which the luminescent signal was measured in a microplate reader (Synergy HT, Biotek, USA).

3.9.2 Proteasome assay

The Proteasome-Glo™ Chymotrypsin-Like Cell-Based Assay (Promega) was used in addition to the Trypsin-Like and Caspase-Like Assays to evaluate the three major proteolytic activities. The assays were performed as indicated in the manufacturer's protocol. Briefly, the Proteasome-Glo™ Substrate was prepared by adding buffer and substrate Suc-LLVY-Glo™ for the Chymotrypsin-Like Assay, Z-LRR-Glo™ substrate for the Trypsin-Like Assay and Z-nLPnLD-Glo™ substrate for the Caspase-Like Assay. The Proteasome-Glo™ Reagent was prepared by adding the Proteasome-Glo™ Substrate to the Luciferin Detection Reagent and it was left to incubate for 60 minutes. The 20S proteasome enzyme and the inhibitor epoxomicin were also prepared by adding buffer to stock solutions. The tests were performed in 96-well white-walled plates with a final volume of 100 μL and the extracts were tested at 3 μg mL^{-1}. The plates were incubated at room temperature for 30 minutes, after which the luminescent signal was measured in a microplate reader (Synergy HT, Biotek, USA).

3.10 Antimicrobial screening susceptibility assay

For the antimicrobial screening susceptibility assay two Gram-positive bacterial strains (*Staphylococcus aureus* ATCC 25923 and *Bacillus subtilis* ATCC 6633) and two Gram-negative bacterial strains (*Escherichia coli* ATCC 25922 and *Pseudomonas aeruginosa* ATCC 27853) were used as well as a species of yeast (*Candida albicans*). These bacteria were grown in Mueller-Hinton agar (MH – BioKar diagnostics, France) from stock cultures. MH plates were initially incubated at 37ºC so as to obtain fresh cultures for each *in vitro* bioassay. The disc diffusion method on MH was used. Briefly, bacterial pure colonies were picked from overnight cultures in MH and suspended in 5 mL of buffered peptone water (Oxoid, England). MH plates were seeded with that inoculum. Blank discs (6 mm in diameter, Oxoid, England) were placed in the inoculated plates and then, impregnated with 15 μL of a 1 mg mL^{-1} solution (in DMSO) of each test compound (DMSO was used as a negative control). Plates were incubated overnight at 37ºC and antimicrobial activity was recorded when a halo around the disc was visible.

4. Results and Discussion

4.1 Extraction and bioassay-guided fractionation of *S. salina* biomass.

From 15.3 g, d.w. of *S. salina* biomass, a 17.0% yield (2.6 g) of crude extract was obtained (extraction code E13010). This crude extract was then submitted to a normal phase liquid chromatography resulting in ten fractions (A – I). The MTT assay was used to evaluate the effects of the different fractions obtained on the inhibition of cellular proliferation of human cancer cell lines, as this is a fast colorimetric method frequently used to measure cell proliferation and cytotoxicity (Berridge & Tan, 1993). The MTT is accumulated by the cells by endocytosis and the reduction of the tetrazole ring in this salt results in the formation of purple formazan crystals, which accumulate in endosomal and/or lysosomal compartments, being later transported out of the cell by exocytosis. Due to the fact that this a fundamental mechanism of living cells, this assay has been frequently used to determine cellular viability.

To perform the MTT assay, three cancer cell lines were used, RKO, MG63 and T47D. Fractions for which a decrease in cellular viability was in the range of 90-80% were selected for follow-up studies.

The results regarding cell viability of the RKO, MG63 and T47D cell lines exposed to E13010 crude extract and E13010 VLC fractions, with a concentration of 100 μg mL^{-1} and 10 μg mL^{-1} in 96 well plates, revealed that fraction F, G and H inhibited cell viability at the end of both test times (24 and 48 hours) for the highest concentration. The lowest concentration tested showed no cellular inhibition (Figure 7).

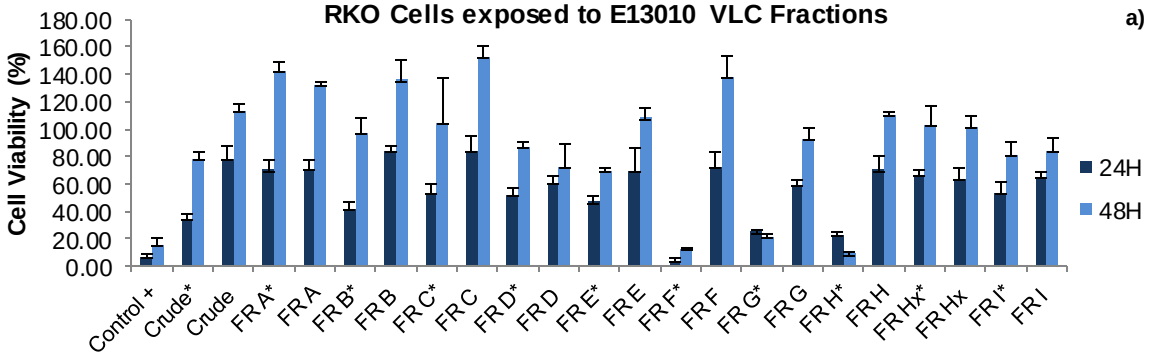

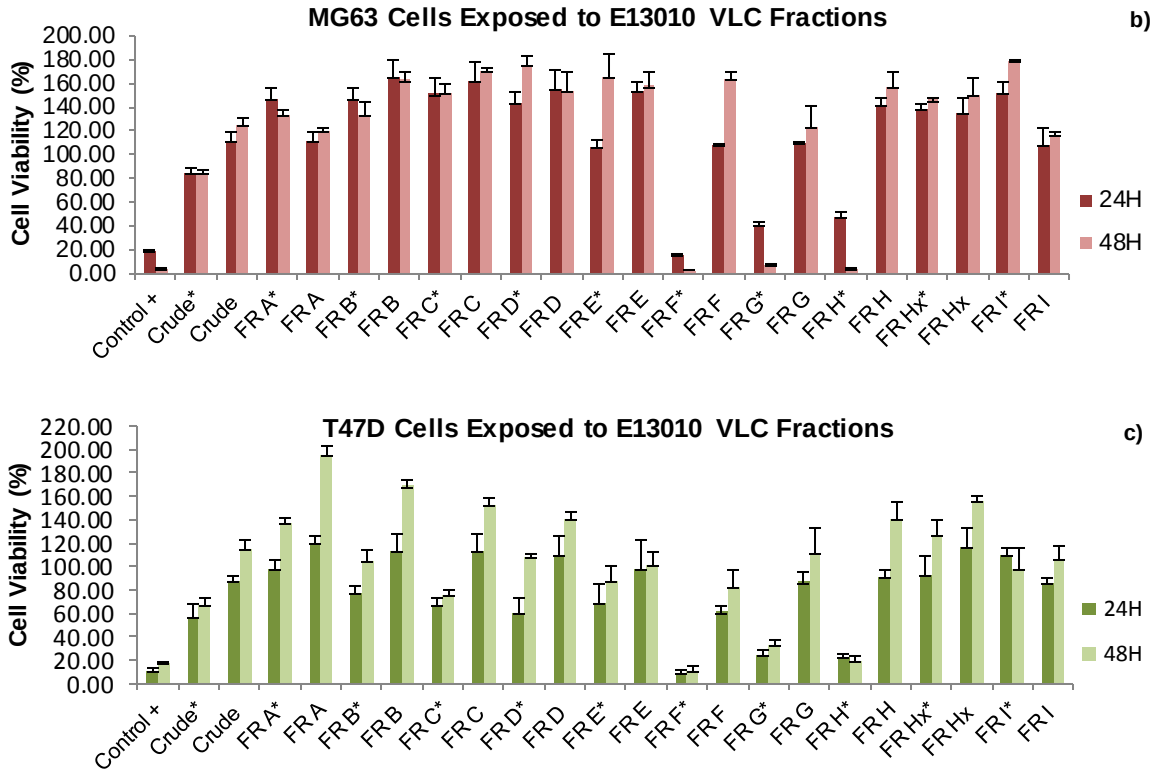

Figure 7 – Cell viability (% of negative control) from E13010 crude extract and VLC fractions (A – I) with the concentration of 100 μg mL^{-1}(*) and 10 μg mL^{-1} on the RKO (a), MG63 (b) and T47D (c) cancer cell lines, with two exposure times, 24H and 48H at 3.3 x 10^4 cells per well. Negative control corresponded to 1% DMSO and positive control to 20% DMSO.

For the enzymatic and antimicrobial susceptibility assays, no activity was detected for these fractions.

From these results, fraction F was selected for further purification as it was the bioactive fraction with higher mass (196.2 mg), thus increasing the possibility of isolating compounds with enough mass for the chemical investigations. This fraction was then subjected to a normal phase column chromatography and the resulting sub-fractions were tested for cytotoxicity at a concentration of 30 and 3 μg mL^{-1} on the MTT assay (see Appendix I, Figure 1). The results obtained from the assay revealed that bioactivity of fraction F was located in the resulting fractions E13010 F-5 (96.0 mg) and F-6 (40.3 mg). Following the bioactivity and analyzing the ^{1}H NMR of these fractions, they were selected for further purification by semi-preparative HPLC.

Semi-preparative HPLC of sub-fraction F-5 followed the gradient program described in Table 5 and the resulting chromatogram is shown is Figure 8. From this HPLC, ten sub-fractions were collected (E13010 F-5.1 to F-5.10) corresponding to single peaks or clusters of peaks, which were then subjected to the MTT assay.

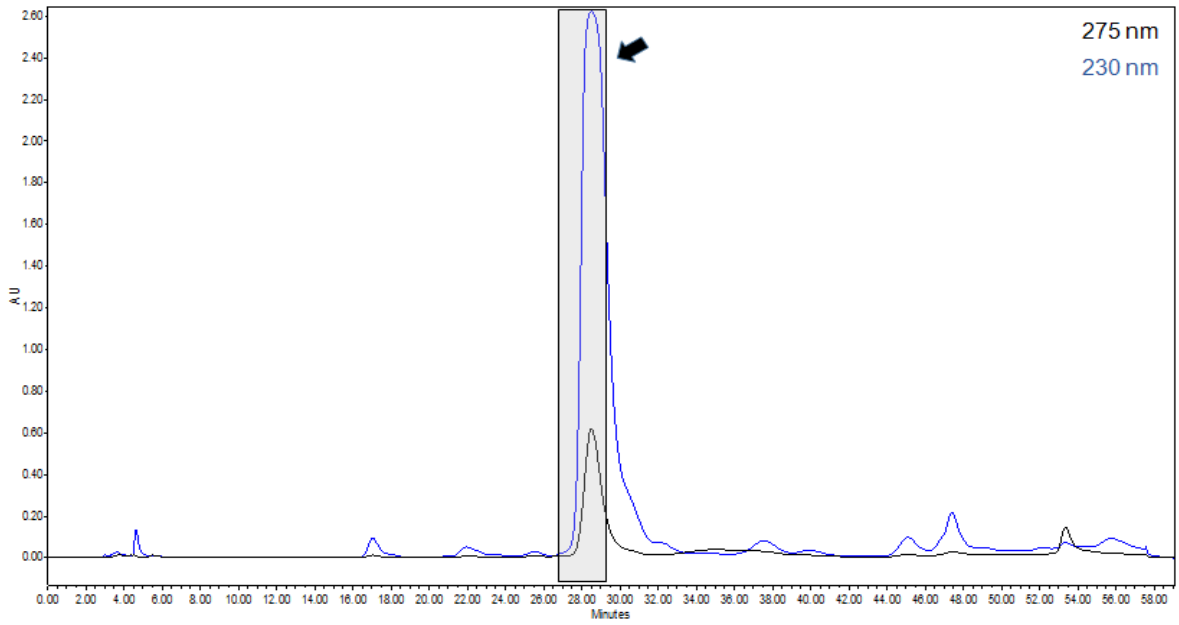

Figure 8 – Chromatogram of E13010 F-5 showing highlighted sub-fraction F-5.4. Conditions of the injection were as followed: 100 μL at a concentration of ~19 mg mL^{-1}.

Sub-fraction E13010 F-5.4 corresponds to the peak highlighted in Figure 8. Through the MTT assay, this sub-fraction revealed to highly decrease cellular viability for all the three cancer cell lines tested, thus showing that the bioactivity of fraction F-5 was located in this sub-fraction (see Appendix I, Figure 2). For the gradient program and conditions used, the retention time of this peak was of approximately 26.5 minutes. The visible peak was not collected entirely due to visible overlapping of different peaks around minutes 29 and 31. After all 96 mg of fraction F-5 had been subjected to semi-preparative HPLC, 30.4 mg of sub-fraction F-5.4 were collected. Analysis of the ^{1}H NMR of this sub-fraction revealed a pure compound that was selected for NMR-based characterization.

Semi-preparative HPLC of sub-fraction F-6 followed the gradient program described in Table 6 and twelve sub-fractions (F-6.1 to F-6.12) were collected from single peaks or clusters of peaks. The MTT assay revealed that sub-fractions E13010 F-6.2, F-6.3 and F-6.4 (respectively 1, 2 and 3 in Figure 9) decreased cellular viability for all three cancer cell lines (see Appendix I, Figure 3). After all 40.3 mg of fraction F-6 had been subjected to semi-preparative HPLC, 0.9 mg, 1.2 mg and 12.8 mg of sub-fractions F-6.2, F-6.3 and F-6.4 respectively, were collected. Analysis of the ^{1}H NMR of sub-fractions F-6.2 and F.6.3 revealed the need to perform another round of purification using analytical-scale HPLC. Sub-fraction F-6.4 (RT of approximately 20.5 minutes) revealed a pure compound and was selected for NMR-based characterization.

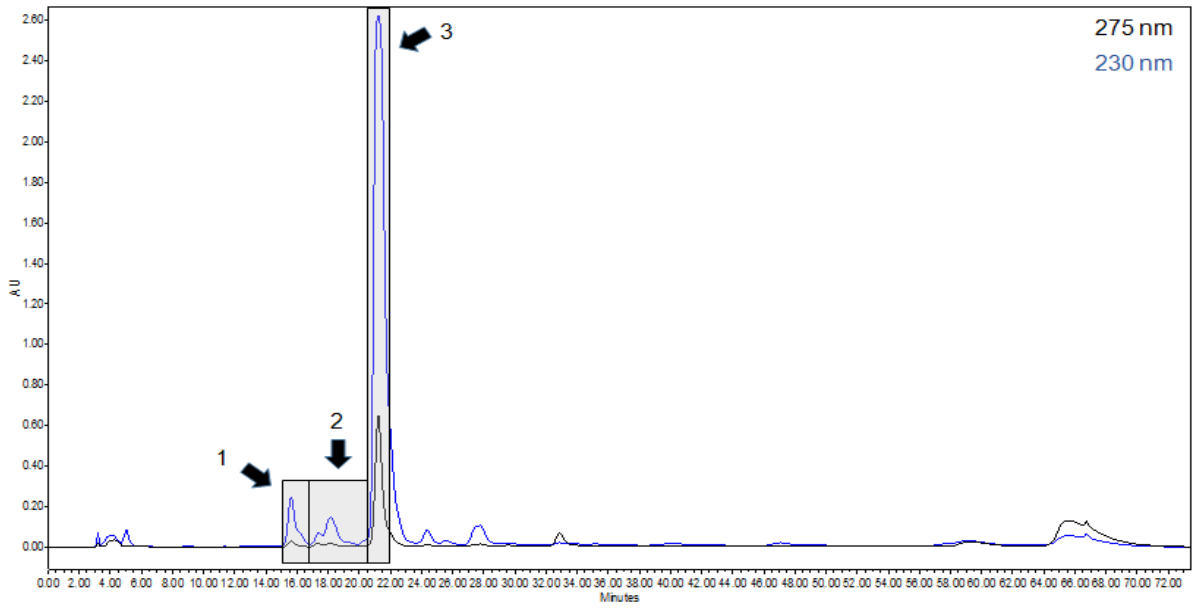

Figure 9 – Chromatogram of E13010 F-6 showing highlighted sub-fraction F-6.2 (1); F-6.3 (2) and F-6.4 (3). Conditions of the injection were as followed: 200 μL at a concentration of ~8 mg mL^{-1}.

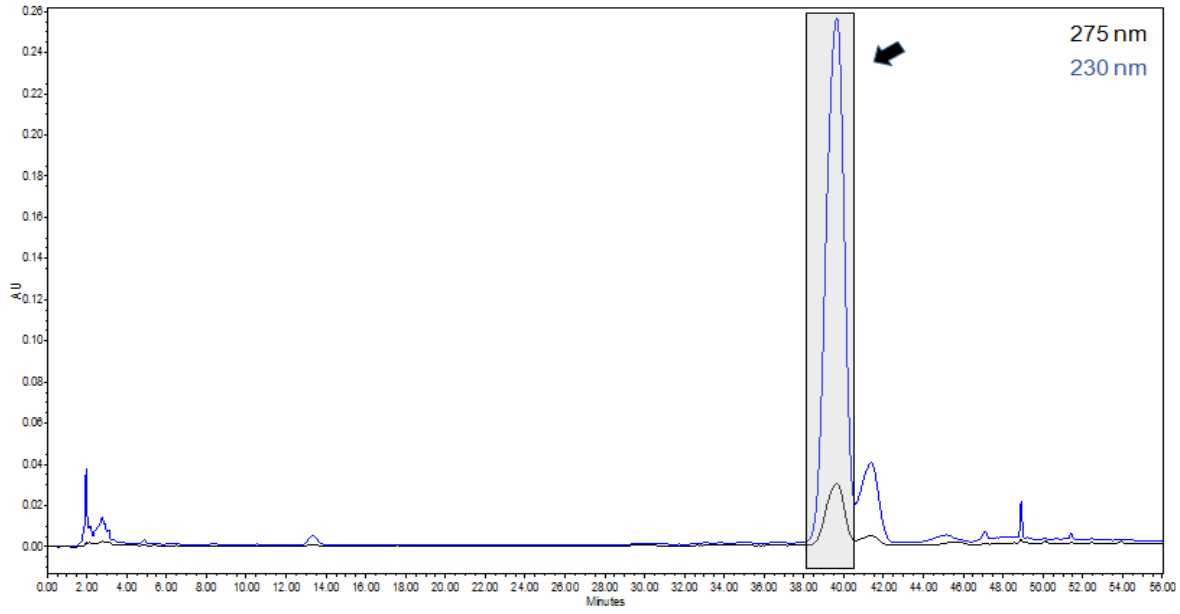

Figure 10 – Chromatogram of E13010 F-6.2 showing highlighted sub-fraction F-6.2.1. Conditions of the injection were as followed: 40 μL at a concentration of ~1 mg mL^{-1}.

Analytical-scale HPLC of sub-fraction F-6.2 followed the conditions described in Table 8 and the chromatogram obtained is showed in Figure 10. Sub-fraction F-6.2.1, corresponding to the peak highlighted in Figure 10 with a retention time of approximately 38 minutes was the major peak, yielding 0.5 mg. In the MTT assay of this sub-fraction, all

three cancer cell lines had their cellular viability decreased (see Appendix I, Figure 4). Analysis of the ^{1}H NMR of this sub-fraction revealed a pure compound that was selected for NMR-based characterization.

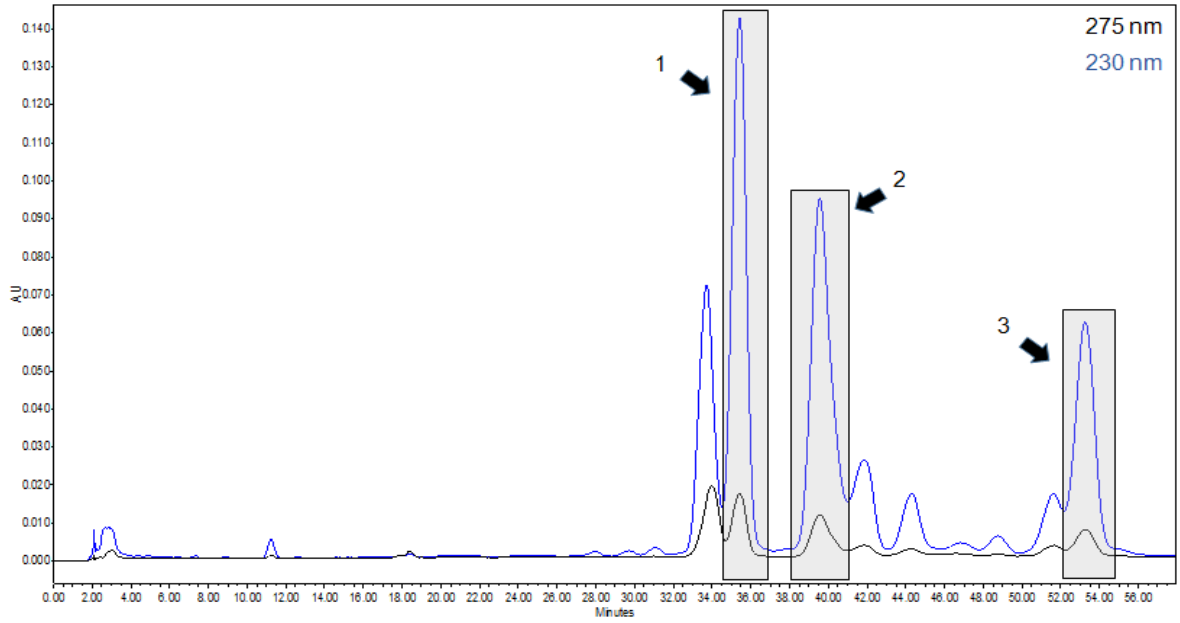

Figure 11 – Chromatogram of E13010 F-6.3 showing highlighted sub-fractions F-6.3.2 (1), F-6.3.3 (2) and F-6.3.8 (3). Conditions of the injection were as followed: 40 μL at a concentration of ~1 mg mL^{-1}.

Sub-fraction E13010 F-6.3 was submitted to analytical-scale HPLC, which followed the conditions described in the section 3.4.4. The chromatogram of this sub-fraction is shown in Figure 11. Through this chromatogram, 8 sub-fractions (F-6.3.1 to F-6.3.8) were collected and subjected to the MTT assay. Sub-fractions F-6.3.2 (highlighted as 1) and F-6.3.3 (highlighted as 2) showed a decrease in cellular viability for all three cancer lines tested (see Appendix I, Figure 4). F-6.3.8 (highlighted as 3) didn't show significant results in the MTT assay, but due to its ^{1}H NMR spectrum it was selected for further characterization. For these reasons, sub-fractions F-6.3.2 (0.2 mg; RT=34.5 minutes), F-6.3.3 (0.2 mg; RT=38 minutes) and F-6.3.8 (0.3 mg; RT=52.25 minutes) were selected for further characterization.

Even though through the cytotoxicity assay, fraction F-7 (4.1 mg) didn't reveal bioactivity, it was still submitted to a semi-preparative HPLC because it was the immediate fraction following the fractions containing bioactivity, and could still have some of the previous compounds in low quantities. The conditions of the HPLC were as described in section 3.4.5 and the resulting chromatogram is shown in Figure 12. This chromatogram was very similar to the one of fraction F-6.4 which was tested with the same gradient

program. The peak shown highlighted in Figure 5 was collected as sub-fraction F-7.4 (0.9 mg; RT=20 minutes) and tested in the MTT assay. In the cytotoxicity assay this sub-fraction didn't reveal appreciable activity (see Appendix I, Figure 4) but the ^{1}H NMR spectrum revealed a pure compound and so it was selected for NMR-based characterization.

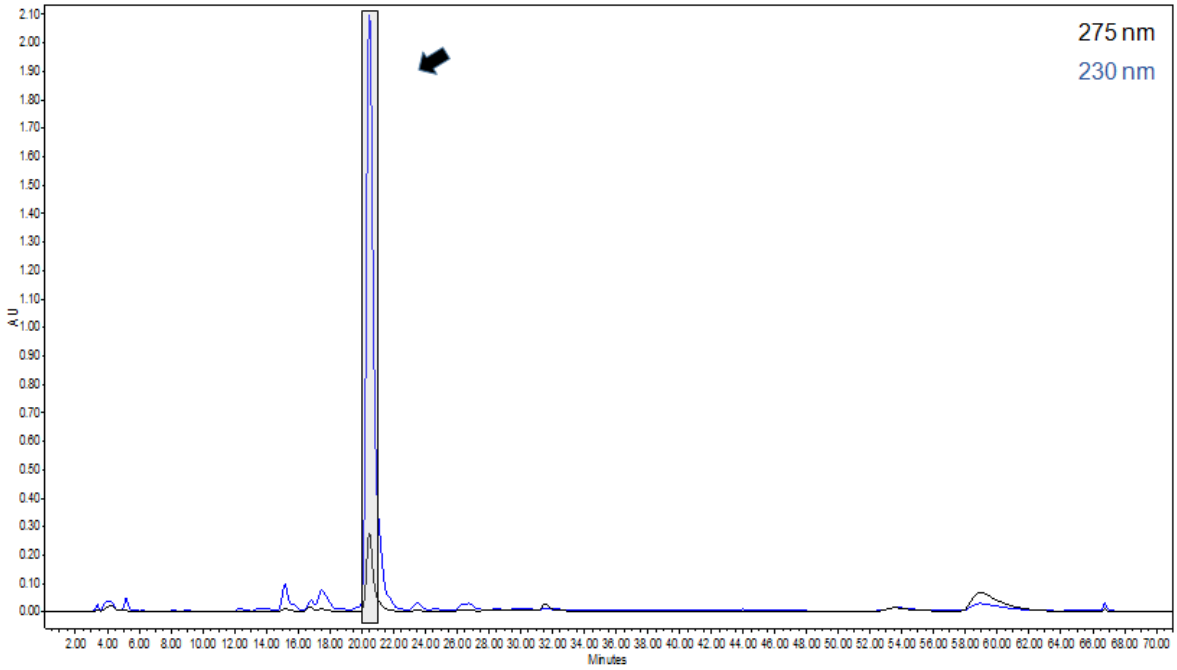

. **Figure 12** – Chromatogram of E13010 F-7 showing highlighted sub-fraction F-7.4. Conditions of the injection were as followed: 200 μL at a concentration of ~4 mg mL^{-1}.

Concluding the isolation process of all these fractions/compounds, they were selected for Nuclear Magnetic Resonance and Liquid Chromatography – Mass Spectrometry analysis. Table 10 summarizes all the isolated fractions of interest.

Table 10 – Compendium of all interesting isolated fractions for further chemical analysis and their respective obtained mass.

Isolated Fractions	Obtained Mass (mg)
F-5.4	30.4
F-6.4	12.8
F-6.2.1	0.5
F-6.3.2	0.2
F-6.3.3	0.2
F-6.3.8	0.3
F-7.4	0.9

4.2 LC-HR-ESI-MS and NMR of the Fractions obtained.

All fractions compiled in Table 9 were subjected to Mass Spectrometry analysis at CEMUP with the objective of deriving structural information of the present compounds.

In Figure 13A are shown the liquid chromatography results for each fraction and for a pool of all fractions, evidencing differences and similarities between fractions. Figure 13B shows the mass spectrum for each main peak present in the different fractions. Analysis of the NMR data obtained for each fraction/compound is also described in this section.

4.2.1 Compound F-5.4

E13010 F-5.4, a pale yellow amorphous solid UV MeOH [absorption maxima at λ = 205 nm (logε = 3.33), λ = 229 nm (logε = 3.37), λ = 245 nm (logε = 3.38), λ = 257 nm (logε = 3.36)]; the HR-ESI-MS established an $[M - H]^-$ *m/z* 659.3838, calculated 659.3845 for $C_{36}H_{61}Cl_2O_6$. In the conditions tested, this fraction presented a retention time of 10.33 minutes. Comparing the LC-MS of F-5.4 and F-6.4 their retention times were very similar, 10.33 and 10.26 minutes respectively. The mass spectrum for both was similar, and so were the NMR data, thus these two compounds are presumed to be equal. For this compound it was possible to obtain 1D ^{1}H and ^{13}C NMR spectra (Figure 14) and 2D HSQC, HMBC, COSY and NOESY NMR spectra (see Appendix II, Figure 1 and 2). Heteronuclear single quantum coherence (HSQC) provides one bond ^{1}H-^{13}C spectra while Heteronuclear multiple bond correlation (HMBC) provides an *N*-bond (*n* = 2 or 3) ^{1}H-^{13}C shift correlation spectra (Breton and Reynolds, 2013). Correlation spectroscopy (COSY) provides homonuclear ^{1}H-^{1}H correlation spectra and the Nuclear Overhauser effect spectroscopy (NOESY) identifies pairs of protons that are spatially close (Breton and Reynolds, 2013).

A)

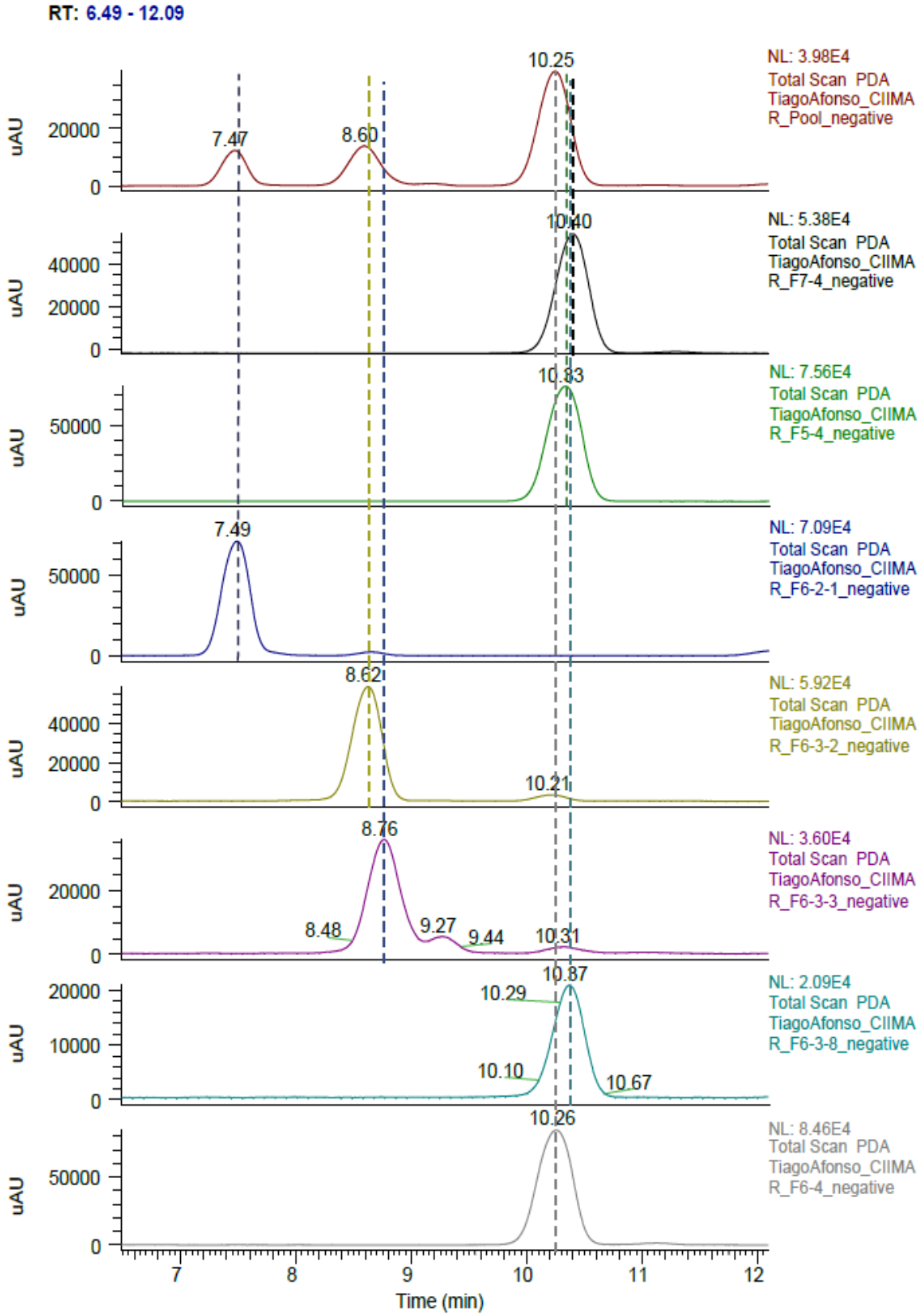
RT: 6.49 - 12.09
uAU
Time (min)
NL: 3.98E4
Total Scan PDA
TiagoAfonso_CIIMA
R_Pool_negative
NL: 5.38E4
Total Scan PDA
TiagoAfonso_CIIMA
R_F7-4_negative
NL: 7.56E4
Total Scan PDA
TiagoAfonso_CIIMA
R_F5-4_negative
NL: 7.09E4
Total Scan PDA
TiagoAfonso_CIIMA
R_F6-2-1_negative
NL: 5.92E4
Total Scan PDA
TiagoAfonso_CIIMA
R_F6-3-2_negative
NL: 3.60E4
Total Scan PDA
TiagoAfonso_CIIMA
R_F6-3-3_negative
NL: 2.09E4
Total Scan PDA
TiagoAfonso_CIIMA
R_F6-3-8_negative
NL: 8.46E4
Total Scan PDA
TiagoAfonso_CIIMA
R_F6-4_negative
7.47
8.60
10.25
10.40
10.33
7.49
8.62
10.21
8.48
8.76
9.27
9.44
10.31
10.29
10.37
10.10
10.67
10.26

B)

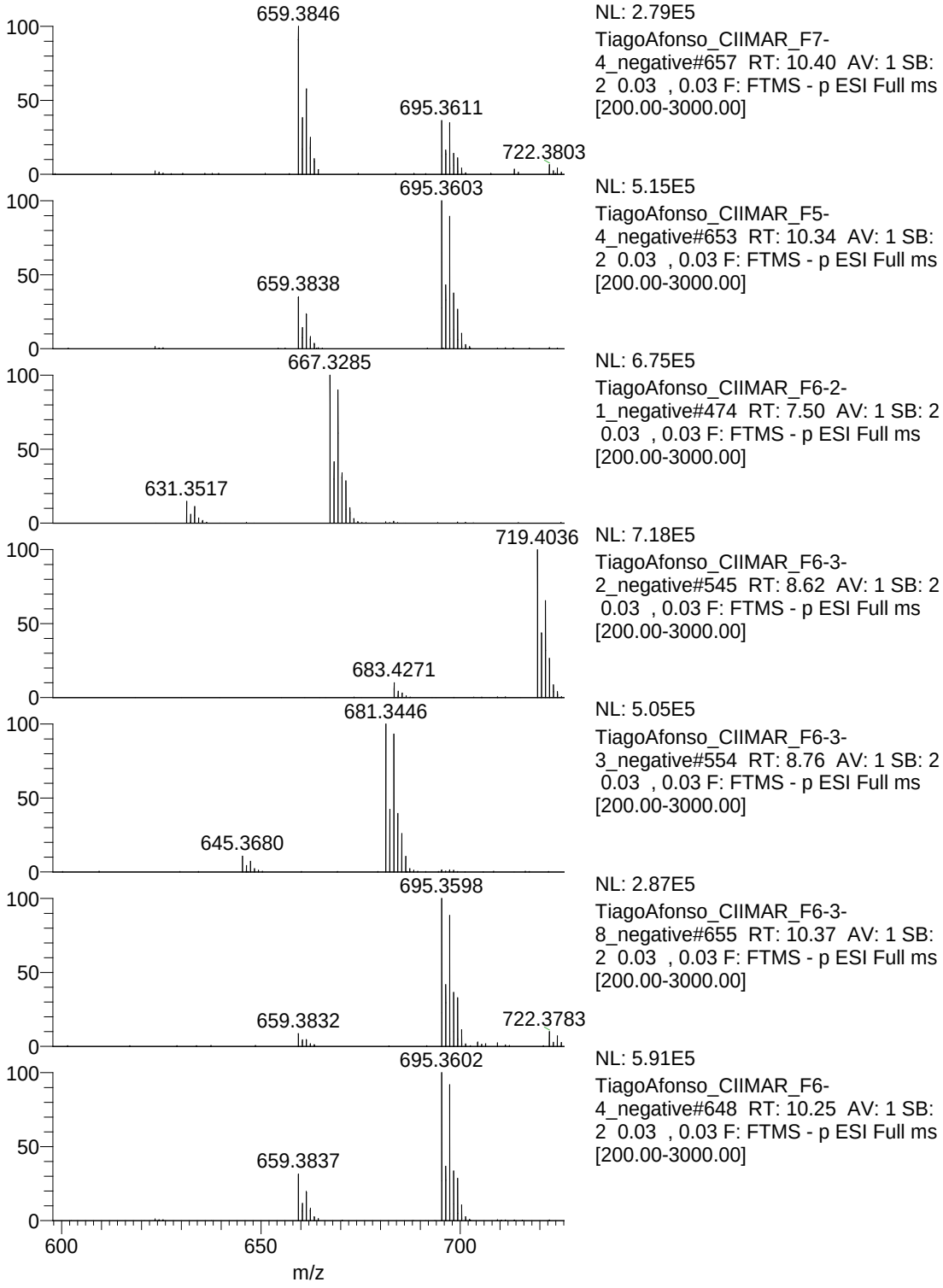

Figure 13 – LC-MS analysis of all fractions obtained. Panel A) – Liquid Chromatography of all individual fractions and a pool of all fractions. Panel B) – Mass spectrum for each of the main chromatographic peaks of each fraction.

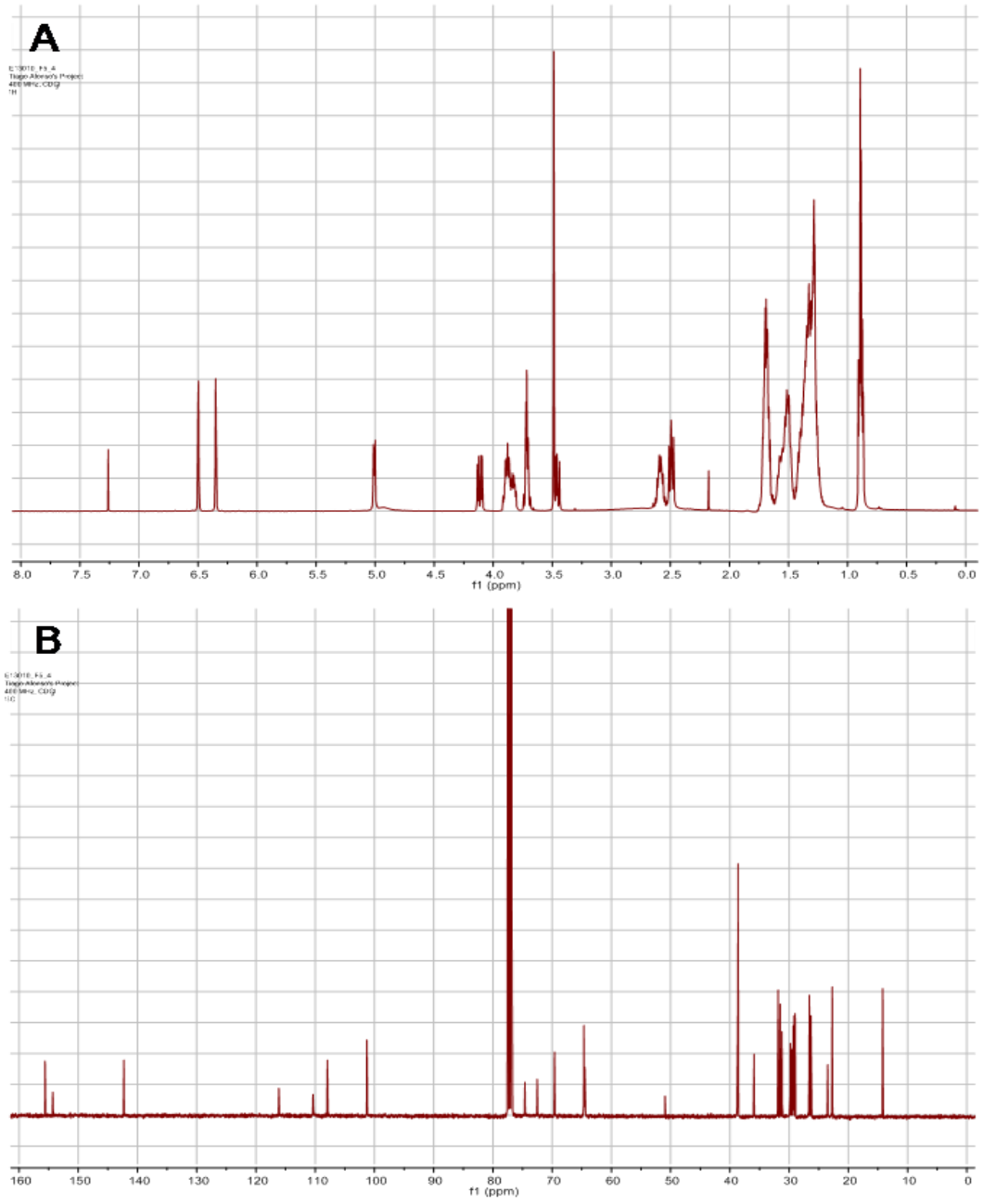

Figure 14 – ^{1}H-NMR (A) and ^{13}C-NMR (B) spectra of compound F-5.4/F-6.4 in $CDCl_3$ (recorded at 400 MHz).

Structural elucidation of this compound is underway, but the first step has already been made by identifying some correlations obtained from HSQC and HMBC spectra for single and multiple bond correlations, respectively (Table 11), suggesting the presence of an aromatic ring from several ^{13}C resonances between δ155.61-107.27 and ^{1}H resonances of δ6.50-6.35.

Table 11 – NMR spectroscopy data for F-5.4 in $CDCl_3$ at 600 MHz.

Number[a]	δ_C	δ_H (mult., *J* in Hz)	HMBC
1	155.61		
2	154.31		
3	142.28		
4	116.14		
5	110.36	6.35 (d, 1.1)	C-2, C-3, C-4, C-6, C-16, C-30
6	107.94	6.50 (d, 1.0)	C-1, C-3, C-4, C-5, C-16, C-30
7	101.27	5.01 (d, 6.1)	C-1, C-8, C-10, C-13
8	74.60	3.71 (m)	C-7, C-10, C-13
9	72.53	3.72 (m)	C-8, C-10
10	69.58	3.83 (m)	C-8, C-9, C-14
11	64.64		
12a	64.56	3.46 (d, 3.9)	C-7, C-8, C-10
12b		3.88 (m)	C-14, C-28
13	64.48	4.11 (dd, 4.3, 11.9)	
14	38.70		
15	38.63	1.69 (m)	
16	35.91	2.49 (m)	C-3, C-5, C-6, C-19, C-21
17	31.85	1.29 (m)	C-30, C34
18	31.52		
19	31.20	1.57 (m)	
20	29.80		
21	29.51	1.51 (m)	
22	29.31	1.34 (m)	
23	29.20		
24	29.17		
25	28.99		
26	26.61	1.51 (m)	
27	26.57		
28	26.56	1.40 (m)	
29	26.32	1.69 (m)	C-27
30	23.48	2.59 (m)	C-1, C-2, C-4, C-20
31a	22.73	1.30 (m)	
31b		0.89(t, 7.0)	
32	22.68		
33	14.20	0.89 (t, 7.0)	C-17/19, C-32
34	14.16	0.89(t, 7.0)	

[a] Numbering is for reference purposes, only.

4.2.2 Compound F-6.2.1

E13010 F-6.2.1, a colorless amorphous solid UV MeOH [absorption maxima at λ = 205 nm (logε = 3.81), λ = 229 nm (logε = 3.86), λ = 245 nm (logε = 3.87), λ = 257 nm (logε = 3.85)]; the HR-ESI-MS established an $[M - H]^-$ *m/z* 631.3517, calculated 631.3532

for $C_{34}H_{57}Cl_2O_6$. In the conditions tested, this fraction presented a retention time of 7.49 minutes (Figure 13A).

In comparison with compound F-5.4, compound F-6.2.1 appears to have lost an ethylene equivalent (C_2H_4), which corresponds to the *m/z* 28.032 difference. For this compound it was possible to obtain 1D ^{1}H and ^{13}C NMR spectra (Figure 15) and 2D HSQC, HMBC and COSY NMR spectra (see Appendix II, Figure 3 and 4).

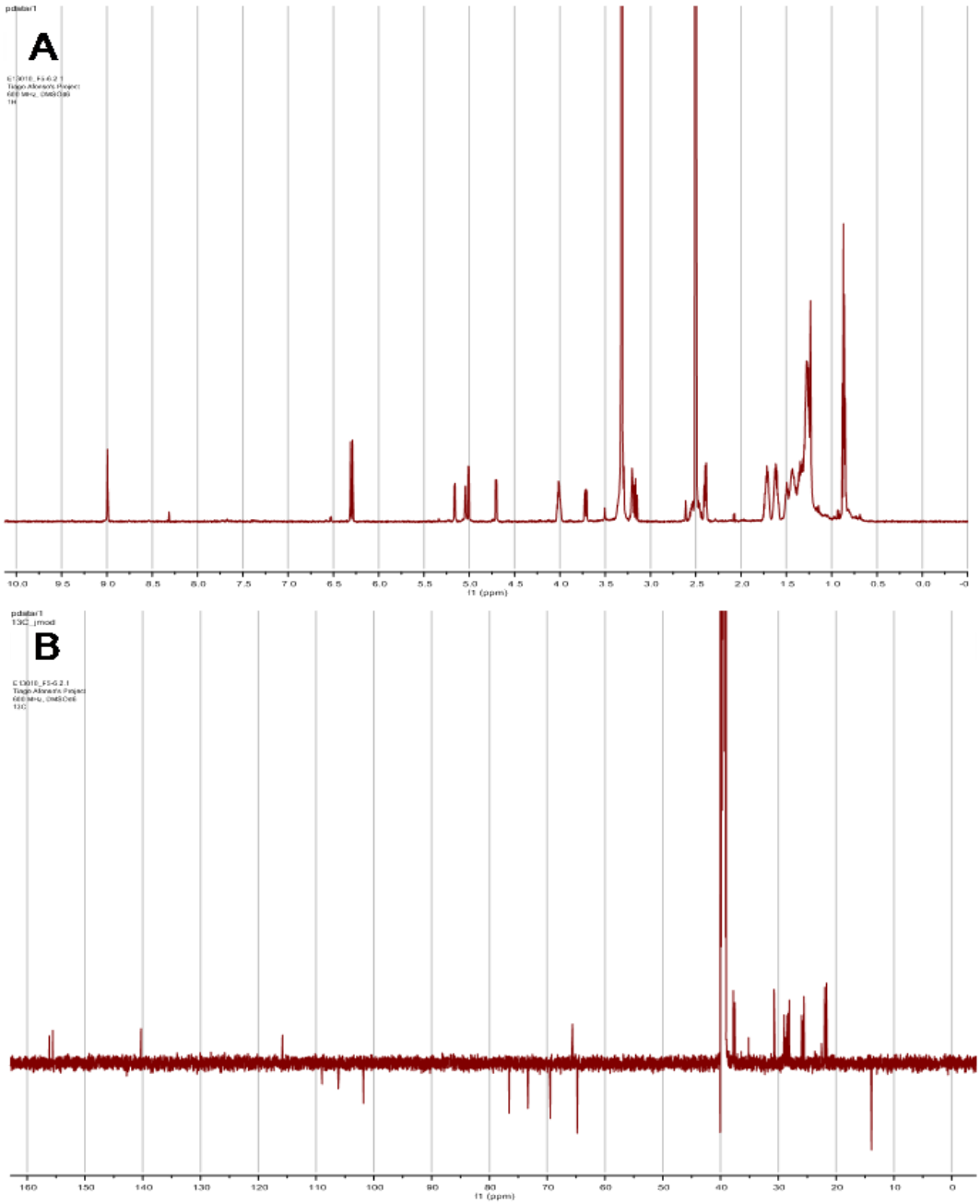

Figure 15 – ^{1}H-NMR (A) and ^{13}C-NMR (B) spectra of compound F-6.2.1 in DMSO-d_6 (recorded at 600 MHz).

Structural elucidation of this compound is underway, but, like for compound F-5.4, the first step has already been made by identifying some correlations obtained from HSQC and HMBC spectra for single and multiple bond correlations, respectively (Table 12). Like to the previous compound, these data suggest the presence of an aromatic ring from several ^{13}C resonances between δ156.18-106.15 and ^{1}H resonances of δ6.31-6.29.

Table 12 – NMR spectroscopy data for F-6.2.1 in DMSO-d_6 at 400 MHz.

Number[a]	δ_C	δ_H (mult., *J* in Hz)	HMBC
		8.99 (s)	C-2, C-4
1	156.18		
2	155.56		
3	140.30		
4	115.81		
5	108.96	6.29 (d, 1.3)	C-2, C-4, C-6, C-18
6	106.15	6.31 (d, 1.3)	C-1, C-4, C-5, C-18
7	101.80	4.70 (d, 7,2)	C-1
8	76.59	3.20 (m)	
9	73.32	3.20 (m)	
10a	69.44	3.34 (m)	C-9
10b		3.51 (s)	
11a	65.63	3.71 (dd, 5.3, 11.3)	C-10
11b		3.16 (m)	
12	64.88	4.01 (m)	
13	64.79	4.01 (m)	
14a	37.88	1.72 (m)	
14b		1.62 (m)	
15	37.80		
16	37.78		
17	37.54	1.62 (m)	
18	35.15	2.40 (m)	C-3, C-5, C-6, C-22/26, C-20
19	30.73	1.23 (m)	
20	30.66	1.49 (m)	C-18, C-24
21	29.02		
22	28.75	1.40 (m)	
23	28.52		
24	28.46		
25	28.32		
26	28.11		
27	25.96		
28	25.84		
29	25.56		
30a	22.54	2.54 (m)	C-2, C-4, C-22/26
30b		2.46 (m)	C-1, C-4, C-22/26
31	21.88		
32	21.67		
33a	13.87	0.86 (t, 7.0)	C-20, C-31
33b		0.87 (t, 7.4)	C-26, C-32

[a] Numbering is for reference purposes, only.

4.2.3. Compound F-7.4

E13010 F-7.4, a colorless amorphous solid UV MeOH [absorption maxima at λ = 205 nm (logε = 3.43), λ = 229 nm (logε = 3.47), λ = 245 nm (logε = 3.48), λ = 257 nm (logε = 3.46)]; the HR-ESI-MS established an $[M - H]^-$ *m/z* 659.3838, calculated 659.3845 for $C_{36}H_{61}Cl_2O_6$, same as F-5.4 and F-6.4, but further tests were necessary to confirm the hypothesis that it is the same compound. From Figure 13A, the retention time of this compound was of 10.40 minutes, again, very similar to F-5.4 (10.33 minutes). For this compound it was possible to obtain 1D ^{1}H and ^{13}C NMR spectra (Figure 16) and 2D HSQC, HMBC and COSY NMR spectra (see Appendix II, Figure 5 and 6).

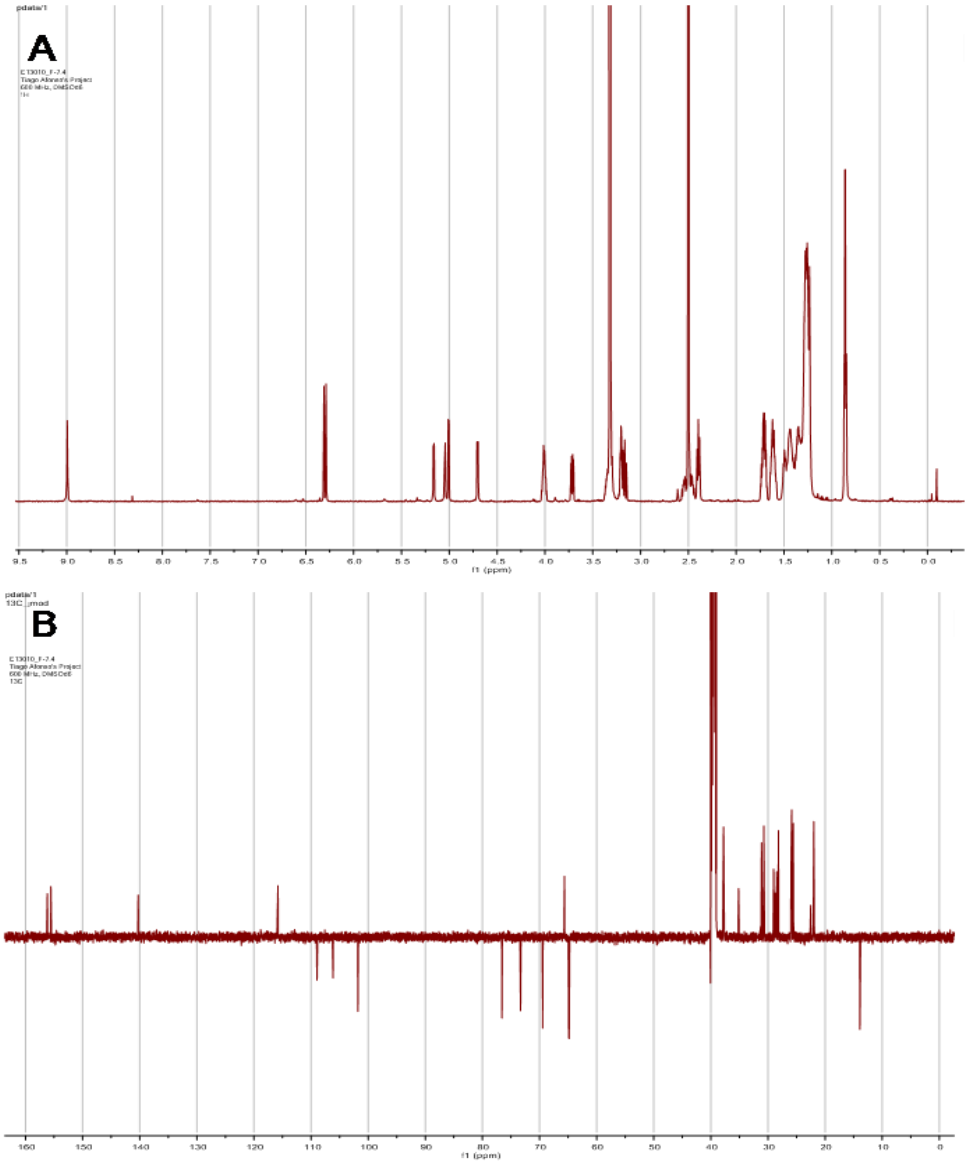

Figure 16 – ^{1}H-NMR (A) and ^{13}C-NMR (B) spectra of compound F-7.4 in DMSO-d_6 (recorded at 600 MHz).

Structural elucidation of this compound is underway and like for the previous compounds, correlations obtained from HSQC and HMBC spectra for single and multiple bond correlations, respectively, were established (Table 13). Comparing these data to the one obtained from the previous compound, compound F-7.3 shows a peak at δ_C31.13 which doesn't appear in compound F-6.2.1, while everything else seems similar including the aromatic ring. These are clearly a family of related compounds, based on the similar NMR data, and, given the similar HR-MS data for some of the isolated metabolites, some should either be constitutional or stereoisomers.

Table 13 – NMR spectroscopy data for F-7.4 in DMSO-d_6 at 400 MHz.

Number[a]	δ_C	δ_H (mult., *J* in Hz)	HMBC
		8.99 (s)	C-2, C-4
1	156.17		
2	155.56		
3	140.29		
4	115.80		
5	108.96	6.29 (d, 1.1)	C-2, C-4, C-6, C-18
6	106.15	6.31 (d, 1.1)	C-1, C-2, C-5, C-18
7	101.79	4.70 (d, 7.2)	C-1
8	76.58	3.20 (m)	C-9
9	73.31	3.20 (m)	C-7, C-8
10	69.44	3.35 (m)	
11a	65.62	3.16 (m)	C-7
11b		3.72 (dd, 5.3,11.3)	C-7, C-8, C-10
12	64.88		
13	64.81	4.01 (m)	
14a	37.88	1.71 (m)	
14b		1.61 (m)	C-13
15	37.83		
16	37.79		
17	37.78		
18	35.15	2.40 (t, 7.5)	C-3, C-5, C-6, C-23/27, C-21
19	31.13		
20	30.73	1.24 (m)	
21	30.66	1.49 (m)	C-18, C-25
22	29.01		
23	28.74	1.40 (m)	
24	28.52		
25	28.46		
26	28.31	1.27 (m)	
27	28.16		
28	25.95		
29	25.85		
30a	25.56	1.44 (m)	
30b		1.35 (m)	
31a	22.53	2.53 (m)	C-2, C-4, C-23/27
31b		2.46 (m)	C-1, C-4, C-23/27
32	22.00		
33a	21.98	0.86 (t, 7.0)	
33b		1.27 (m)	C-19, C-34
34	13.91		
35	13.87	0.86 (t, 7.0)	C-20, C-32

[a] Numbering is for reference purposes, only.

4.2.4 Compounds F-6.3.2, F-6.3.3 and F-6.3.8

E13010 F-6.3.2, a colorless amorphous solid UV MeOH [absorption maxima at λ = 205 nm (logε = 4.26), λ = 229 nm (logε = 4.31), λ = 245 nm (logε = 4.32), λ = 257 nm (logε = 4.30)]; the HR-ESI-MS showed an $[M - H]^-$ *m/z* 683.4271, calculated 683.4289 for $C_{38}H_{64}ClO_8$. From Figure 12A, the retention time of this compound was of 8.62 minutes. For this compound, due to its low amount, it was only possible to obtain the ^1H NMR spectra (Figure 17A).

E13010 F-6.3.3, a colorless amorphous solid UV MeOH [absorption maxima at λ = 205 nm (logε = 4.62), λ = 229 nm (logε = 4.66), λ = 245 nm (logε = 4.67), λ = 257 nm (logε = 4.65)]; the HR-ESI-MS established an $[M - H]^-$ *m/z* 645.3680, calculated 645.3688 for $C_{35}H_{59}Cl_2O_6$. The retention time of this compound was of 8.76 minutes as shown in Figure 12A. For this compound it was also only possible to obtain the ^1H NMR spectra (Figure 17B). Comparing compound F-6.3.3 with the main compound (F-5.4), it appears to correspond to the loss a methylene (CH_2) due to the decrease of *m/z* 14.0158.

E13010 F-6.3.8, a colorless amorphous solid UV MeOH [absorption maxima at λ = 205 nm (logε = 4.18), λ = 229 nm (logε = 4.22), λ = 245 nm (logε = 4.23), λ = 257 nm (logε = 4.21)]; established the same $[M - H]^-$ as compound F-5.4 for the main peak obtained for the peak with a retention time of 10.37 minutes, indicating the great similarity between these compounds. However, this compound appears not to be completely pure due to the presence of peaks at 10.10, 10.29 and 10.67 minutes. In Figure 18 the ^1H NMR spectra of this compound is shown. Again, given the NMR data and HR-MS data (molecular formula), these are members of the same family of compounds, although their precise structure is, at the moment, unknown.

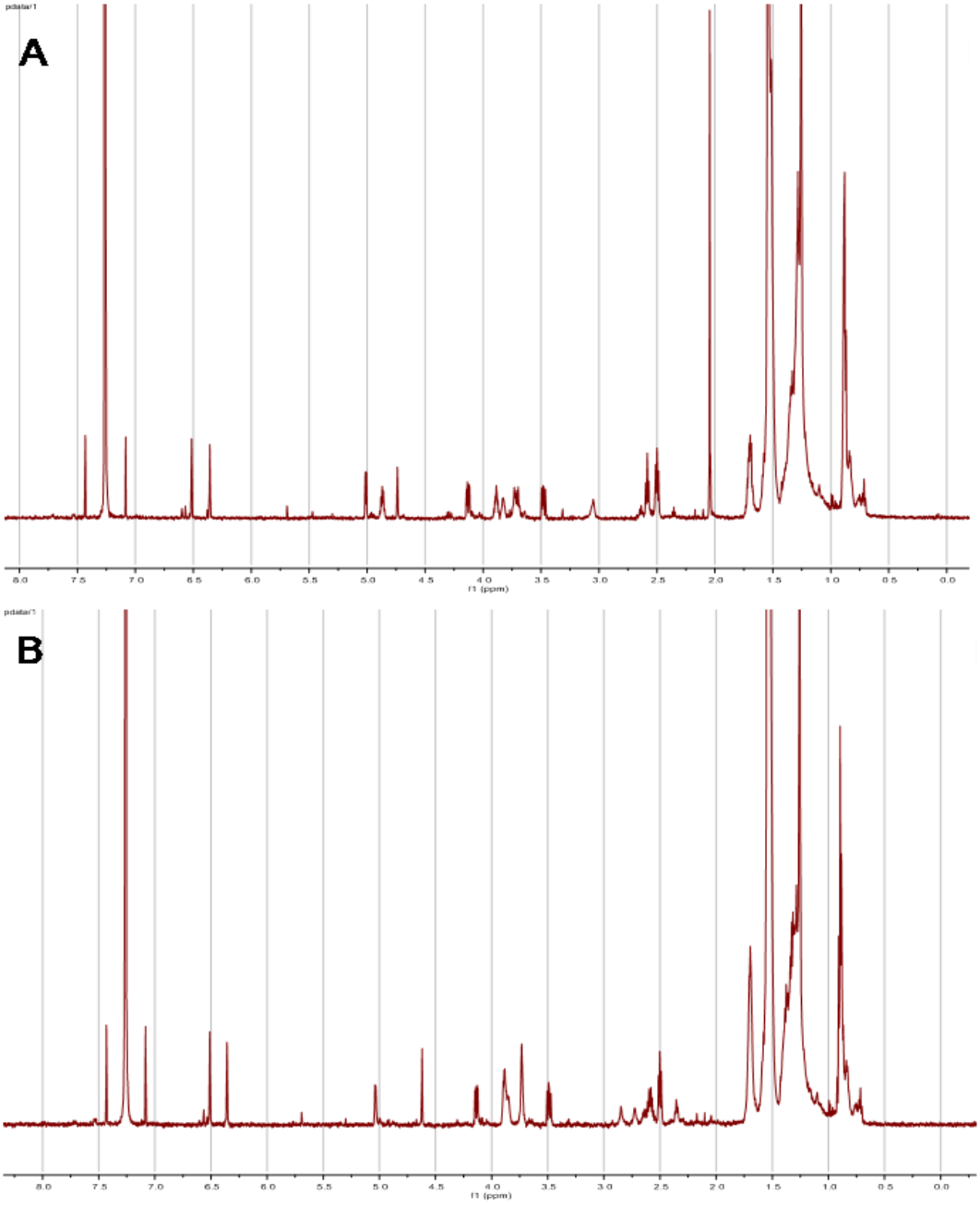

Figure 17 – ^{1}H-NMR spectra of compound F-6.3.2 (A) and F-6.3.3 (B) in $CDCl_3$ (recorded at 600 MHz).

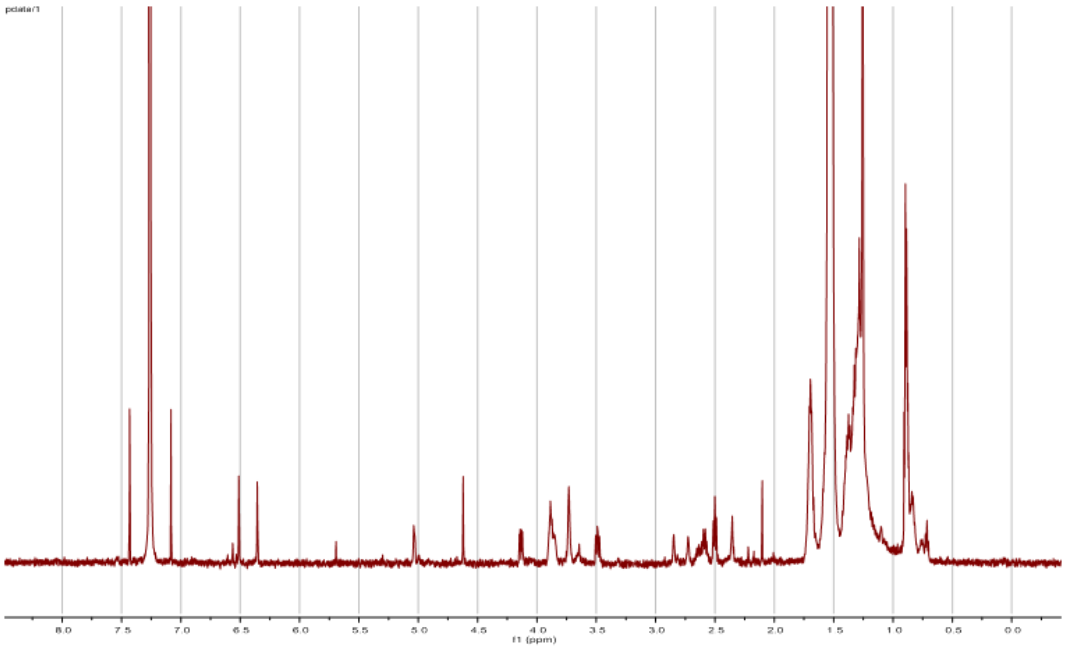

Figure 18 – ^{1}H-NMR spectra of compound F-6.3.8 in $CDCl_3$ (recorded at 600 MHz).

4.5 IC50 of the compounds

To calculate the IC_{50} of the compounds, a similar procedure as the one used to measure bioactivity in the cancer cell lines by the MTT assay was used. The IC_{50} was calculated for the three cancer cell lines tested (RKO, MG63 and T47D) and the concentration interval to its determination ranged from 0.003 to 50 μg mL^{-1}. Cells were incubated for 48 hours, after which the absorbance was measured at 550 nm in the microplate reader.

From the results obtained, the IC_{50} of F-5.4 (Figure 19) and F-6.2.1 (see Appendix I, Figure 6) for the three cancer cell lines was calculated (Table 14).

Table 14 – IC_{50} of compounds F-5.4 and F-6.2.1 in the MG63, RKO and T47D cancer cell lines.

	IC_{50} (μM)		
Cell line / Compound	**MG63**	**RKO**	**T47D**
F-5.4	30.5	41.3	22.7
F-6.2.1	38.9	40.0	21.5

From these values it can be said that the T47D cancer cell line showed the highest sensibility to these compounds whilst the RKO cell line was the least affected.

For the rest of the compounds, same concentrations as these were tested, but only for the highest concentration (50 μg mL^{-1}) inhibition of cell viability was observed, thus not allowing for the IC_{50} values to be calculated. To calculate the IC_{50} values for these compounds, concentrations between 50 and 30 μg mL^{-1} (first concentration with no observable effect tested) should have been tested, but due to the fact that almost all initial obtained mass of these compounds was used up, no mass was available to perform a new assay with the new concentrations.

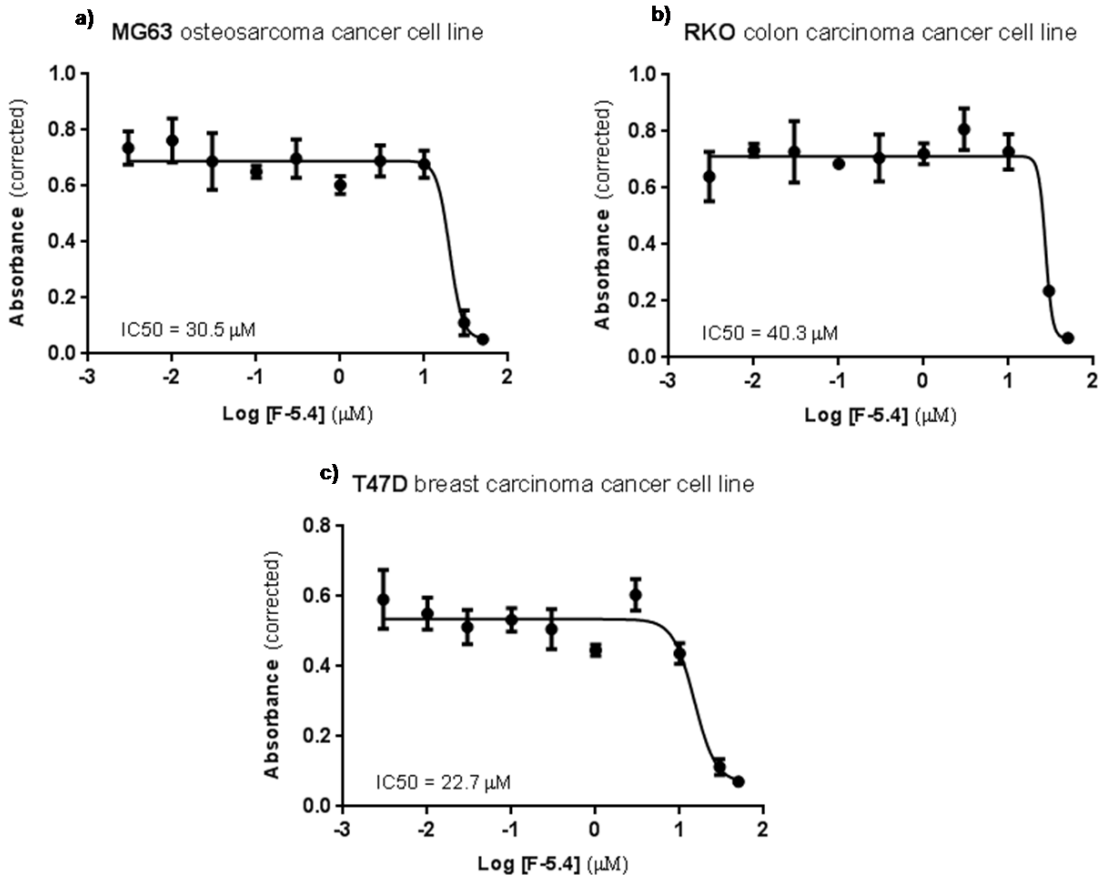

Figure 19 – Dose-response curves for compound E13010 F-5.4 in MG63 osteosarcoma cancer cell line (a), RKO colon carcinoma cancer cell line (b) and T47D breast carcinoma cancer cell line (c).

4.6 MarinLit search of the obtained compounds.

The data obtained in this work, along with informative databases of natural compounds that contain analytical information, such as MarinLit (Gerwick and Moore, 2012), allowed to promptly identifying if the compounds here obtained were already known or if they represent new chemical substances. The results of this search are shown in Table 15.

Table 15 – MarinLit search for each compounds mass.

Compound	$[M-H]^-$	Chemical Formula	Molecular Mass	MarinLit Hits
F-5.4	659.3838	$C_{36}H_{61}Cl_2O_6$	659.3845	0
F-6.4	659.3837			
F-7.4	659.3846			
F-6.3.8	659.3832			
F-6.2.1	631.3517	$C_{34}H_{57}Cl_2O_6$	631.3532	0
F-6.3.2	683.4271	$C_{38}H_{64}ClO_8$	683.4289	0
F-6.3.3	645.3680	$C_{35}H_{59}Cl_2O_6$	645.3688	0

With no hits obtained for the masses of either compounds in the database, the results revealed that these are in fact new compounds that haven't been previously described.

The compounds here described are halogenated metabolites, which is frequent in marine cyanobacteria (Cabrita *et al*., 2010). Halogenation is a common modification of secondary metabolites and is this transformation that confers biological activity to some of these compounds, including anticancer activity (Neumann *et al*., 2008). Chlorination, such as what happens for the compounds here described, is the predominant modification, followed by bromination, which reflects the high presence of chloride, and, to a less extent, bromide ions in seawater (Neumann *et al*., 2008; Cabrita *et al*., 2010). As a result, chlorine and bromine seem to be the major halogens used to raise biological activity of secondary metabolites (Cabrita *et al*., 2010).

For the majority of the bioactive secondary metabolites, a natural role is yet to be described. Some appear to have a protective role against predators, acting as feeding deterrants or toxins, or of competition with other organisms for resources such as light, space or nutrients (Nagle and Paul, 1999; Berry *et al*., 2008). These could be one of the reasons why this strain produces these newly discovered compounds.

Although the compounds here described showed low to moderate activity against cancer cell lines, it is still the beginning of unraveling the possible topics of research and applications that these bioactive compounds might have. Despite their only moderate bioactivity, further studies of the biological processes in which they cause inhibition; on their total structure characterization and comprehending their total synthesis could reveal a wide range of applications.

From total synthesis, new chemical architectures allow investigators to develop new analogs that may be more efficient as anticancer agents (Zhang *et al*., 2011). Structure-activity relationship studies might help with this objective in the future (Zhang *et al*., 2011).

The discovery of new compounds is also important in the area of biocatalysis. By encoding enzymes that catalyse a variety of reactions, nature produces an extremely wide range of biomolecules that display bioactivity, which may then be used in synthetic biology (Michels *et al*., 1998; Rich *et al*., 2002).

New natural compounds are also important to study cellular processes, being used as molecular tools or biological probes, such as epoxomicin, a potent proteasome inhibitor, which is a helpful tool for the discernment of proteasome biology (Sin *et al*., 1999). In fact, epoxomicin is now widely used as one of the main inhibitors of proteasome activity in standard proteasome cell based assays (Moravec *et al*., 2009). Many more similar examples exist.

For all these reasons and applications, several further studies on different molecular targets should be performed for the new compounds described in this work in order to elucidate their full potential.

4.7 Extraction and fractionation of Uncultured Chroococcales strain LEGE 10410

From 14.2 g (d.w.) of *S. salina* biomass, a 4.23% yield (0.6 g) of crude extract was obtained. To this extraction the code E14027 was designated. Following normal phase chromatography of the E14027 crude extract, nine fractions were obtained (A-I). All fractions were subjected to the MTT assay, enzymatic assays and to an antimicrobial susceptibility screening assay.

The results obtained from the MTT assay revealed no significant effects regarding the decrease in cell inhibition in either cancer cell lines tested at the concentration of both 30 and 3 $\mu g\ mL^{-1}$ (see Appendix I, Figure 5).

Regarding the HDAC enzymatic assay, there was no inhibition of histone deacetylase by either fraction at the tested concentration.

Results from the Proteasome enzymatic assay revealed that fraction F was the one that showed higher inhibition for the chymotrypsin-like (Figure 20) and caspase-like proteolytic activities (Figure 21). Other fractions also revealed some inhibitory effects such as fractions E, G and H for the caspase-like proteolytic activity (Figure 21). For the trypsin-like proteolytic activity, no fraction revealed inhibitory effects.

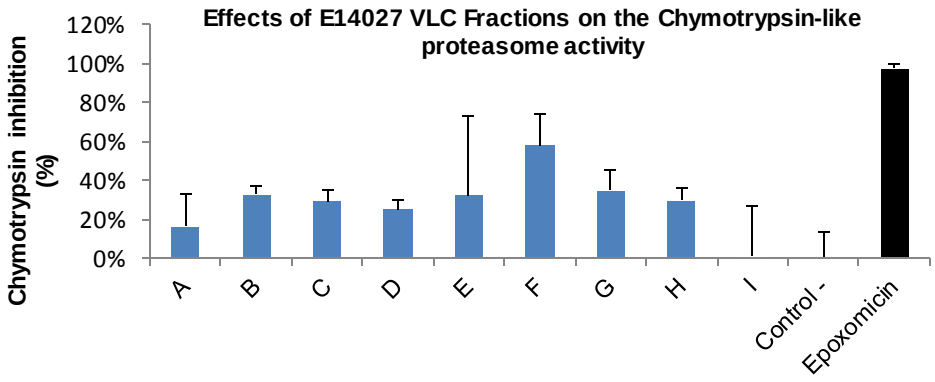

Figure 20 – Chymotrypsin-like proteasome activity when tested with E14010 VLC fractions (A-I). Fractions tested at a final concentration of 3 μg mL^{-1}. The proteasome inhibitor epoxomicin was used for the positive control.

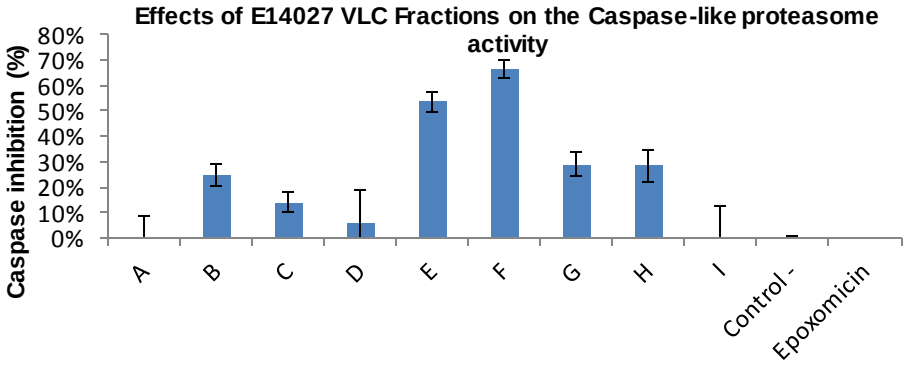

Figure 21 – Caspase-like proteasome activity when tested with E14010 VLC fractions (A-I). Fractions tested at a final concentration of 3μg mL^{-1}. The proteasome inhibitor epoxomicin was used for the positive control (the used concentration was not sufficient to cause inhibition).

From the antimicrobial susceptibility screening assay, fraction F revealed to be the most interesting, showing inhibition halos in *C. albicans* and in all tested bacteria except *S. aureus*. Fractions E, G and I also revealed inhibition halos in *C. albicans*, being this the most sensitive specie to the compounds tested in this assay (Figure 22).

Although some fractions revealed bioactivity in this assays, especially fraction F, the mass collected from the normal phase chromatography for each fraction was low. The mass of the most interesting fractions here tested were 8.5 mg for fraction E, 2.1 mg for fraction F and 0.6 mg for fraction G, thus rendering further studies impracticable before re-extraction of the strains biomass. Fraction I (187.0 mg), in a ratio between mass and bioactivity, showed more promise to lead to the possible isolation of bioactive compounds. This will constitute future work in our laboratory.

Figure 22 – Antibiogram of *C. albicans* exposed to E14027 VLC fractions (A-I). Each blank disk was impregnated with 15 μL of a 1 mg mL^{-1} solution (DMSO). DMSO was used as the negative control.

4.8 Molecular identification of Uncultured Chroococcales strain LEGE 10410

The portion of the DNA that codifies ribosomal RNA (rRNA) in the smallest portion of the ribosome (16S) has been broadly used in molecular identification, since it has an ubiquitous distribution among the prokaryotic group (Otsuka *et al.,* 1998; Wilson *et al.,* 2000). This portion, designated 16S rRNA, although being conserved in the prokaryotes, presents some variation, thus showing the ability to confer specificity to the groups of

which it belongs (Lyra *et al.,* 2001; Falcon *et al.,* 2002). This gene, besides distinguishing species of a certain genus, can also differentiate strains in a species (Sangolkar *et al*., 2006).

The pair of primers 359F/781R was used to amplify the 16S rRNA gene and, after sequencing the resulting amplicon (Figure 23) and searching it in the BLASTn database, the strain LEGE 10410 was identified as belonging to the genus *Chroococcidiopsis.* The determination of the genus was based on a combination of the maximum score (758) and the percent similarity (99%).

GGGGAATCTTCCGCAATGGGCGAAAGCCTGACGGAGCAATACCGCGTGAGGGAGGAAGGCTTTTGGGTTGTAAACCTCTTT
TATCAAGGAAGAAGAAAGTGACGGTACTTGAAGAATCAGCATCGGCTAACTCCGTGCCAGCAGCCGCGGTAATACGGAGGA
TGCAAGCGTTATCCGGAATCATTAGGCGTAAAGCGTCCGCAGGTGGTGGTTCAAGTCTGCTGTTAAAGACAGAAGCTCAAC
TTCTGAGCGGCAGTGGAAACTGGGCAACTAGAGTACGGTAGGGGTTGAGGGAATTCCCAGTGTAGCGGTGAAATGCGTAGA
TATTGGGAAGAACACCAGTGGCGAAGGCGCTCAACTGGGCCGTAACTGACACTCAGGGACGAAAGCTAGGGTAGCGAATGG
GATTAGATACCCCAGTAGTC

Figure 23 – Amplicon obtained from the 16S rRNA gene for the strain LEGE 10410.

5. Conclusion

In this work we discovered a family of different compounds obtained from the cyanobacterial strain *Synechocystis salina* LEGE 06099 with moderate anticancer activity. These results confirm what previous studies revealed, unicellular free-ling species have the ability to produce a variety of bioactive compounds with interesting bioactivity.

Although the compounds here described showed only low to moderate activity against cancer cell lines, it doesn't exclude the possibility that, by the reasons previously mentioned, these metabolites could have other interesting activities against different molecular targets. For this reason, more studies on different molecular targets should be performed for these new compounds in order to elucidate their full potential.

Also, as there are many more cyanobacterial strains currently being overlooked, the results here obtained reveal the necessity to continue with this line of work in order to potentially discover new interesting natural substances.

The next step will be to fully characterize the structures of the compounds here described, and try to discover the mode of action in which they cause growth inhibition on the cancer cell lines, as well as to continue to fractionate and possibly isolate new compounds from *Chroococcidiopsis sp.* LEGE 10410.

6. References

Alley, M.C., Scudiero, D.A., Monks, A., Hursey, M.L., Czerwinski, M.J., Fine, D.L., Abbott, B.J., Mayo, J.G., Shoemaker, R.H., Boyd, M.R., 1988. Feasibility of drug screening with panels of human tumor cell lines using a microculture tetrazolium assay. Cancer Research, 48, 589-601.

Berridge, V., Tan, A.S., 1993. Characterization of the cellular reduction of 3-(4,5-dimethylthiazol 2-yl)-2,5-diphenyltetrazolium bromide (MTT): subcellular localization, substrate dependence, and involvement of mitochondrial electron transport in MTT reduction. Archives of Biochemistry and Biophysics, 303, 474-82.

Berry, J.P., Gantar, M., Perez, M.H., Berry, G., Noriega, F.G., 2008. Cyanobacterial Toxins as Allelochemicals with Potential Applications as Algaecides, Herbicides and Insecticides. Marine Drugs, 6, 117-146.

Biondi, N., Tredici, M.R., Taton, A., Wilmotte, A., Hodgson, D.A., Losi, D., Marinelli, F., 2008. Cyanobacteria from benthic mats of Antarctic lakes as a source of new bioactivities. Journal of Applied Microbiology, 105, 105-115.

Bláha, L., Babica, P., Marsalek, B., 2009. Toxins produced in cyanobacterial water blooms - toxicity and risks. Interdisciplinary Toxicology 2, 36-41.

Blunt, J.W., Copp, B, R., Keyzers, R.A., Munro, M.H.G., Prinsep, M.R., 2013. Marine natural products. Natural Product Reports, 30, 237-323.

Breton, R.C., Reynolds, W.F., 2013. Using NMR to identify and characterize natural products. Natural Product Reports, 30, 501-524.

Brito, A., Ramos, V., Seabra, R., Santos, A., Santos, C.L., Lopo, M., Ferreira, S., Martins, A., Mota, R., Frazão, B., Martins, R., Vasconcelos, V., Tamagnini, P., 2012. Culture-dependent characterization of cyanobacterial diversity in the intertidal zones of the Portuguese Coast: A polyphasic study. Systematic and Applied Microbiology, 35, 110-119.

Butler, M.S., 2008. Natural products to drugs: natural products derived compounds in clinical trials. Natural Product Reports, 25, 475-516.

Cabrita, M.T., Vale, C., Rauter, A.P., 2010. Halogenated compounds from Marine Algae. Marine Drugs, 8, 2301-2317.

Castenholz, R.W., Boone, D.R., 2001. The Archae and the Deeply Branching and Phototrophic Bacteria. In: Manual of Systematic Bacteriology (Garrity, G. M. Edition). New York: Bergey's Springer.

Chang, T.T., More, S.V., Lu, I.H., Hsu, J.C., Chen, T.J., Jen, Y.C., Lu, C.K., Li, W.S., 2011. Isomalyngamide A, A-1 and their analogs suppress cancer cell migration *in vitro*. European Journal of Medicinal Chemistry, 46, 3810-3819.

Chen, X.X., Smith, G.D., Waring, P., 2003. Human cancer cell (Jurkat) killing by the cyanobacterial metabolite calothrixin A. Journal of Applied Phycology, 15, 269–277.

Choi, H., Pereira, A.R., Cao, Z., Shuman, C.F., Engene, N., Byrum, T., Matainaho, T., Murray, T.F., Mangoni, A., Gerwick, W.H., 2010. The hoiamides, structurally intriguing neurotoxic lipopeptides from Papua New Guinea marine cyanobacteria. Journal of Natural Products, 73, 1411-1421.

de Claro, R.A., McGinn, K., Kwitkowski, V., Bullock, J., Khandelwal, A., Habtemariam, B., Ouyang, Y., Saber, H., Lee, K., Koti, K., Rothmann, M., Shapiro, M., Borrego, F., Clouse, K., Chen, X.H., Brown, J., Akinsanya, L., Kane, R., Kaminskas, E., Farrel, A., Pazdur, R., 2012. U.S. Food and Drug Administration approval summary: Brentuximab vedotin for the treatment of relapsed Hodgkin Lymphoma or relapsed systemic anaplastic large-cell lymphoma. Clinical Cancer Research, 18 (21), 5845-5849.

Cohen, Y., Gurevitz, M., 2006. The Cyanobacteria – Ecology, Physiology and Molecular Genetics. In: Prokaryotes 4 (Dworkin, M., Falkow, S., Rosenberg, E., Schleifer, K-H., Stackebrandt, E., edition), 1074-1098. New York: Springer US.

Costa, M., Costa-Rodrigues, J., Fernandes, M.H., Barros, P., Vasconcelos, V., Martins, R., 2012. Marine Cyanobacteria compounds with Anticancer Properties: A Review on the Implication of Apoptosis, Marine Drugs, 10, 2181-2207.

Costa, M., Garcia, M., Costa-Rodrigues, J., Costa, M.S., Ribeiro, M.J., Fernandes, M.H., Barros, P., Barreiro, A., Vasconcelos, V., Martins, R., 2014. Exploring Bioactive Properties of Marine Cyanobacteria Isolated from the Portuguese Coast: High Potential as a Source of Anticancer Compounds. Marine Drugs, 12, 98-114.

Davies-Coleman, M.T., Dzeha, T.M., Gray, C.A., Hess, S., Pannell, L.K., Hendricks, D.T., Arendse, C.E., 2003. Isolation of homodolastatin 16, a new cyclic depsipeptide from a Kenyan collection of *Lyngbya majuscula*. Journal of Natural Products, 66, 712-715.

Dixit, R.B., Suseela, M.R., 2013. Cyanobacteria: potential candidates for drug discovery. Antonie Van Leeuwenhoek, 103, 947-961.

Edwards, D.J., Marquez, B.L., Nogle, L.M., McPhail, K., Goeger, D.E., Roberts, M.A., Gerwick, W.H., 2004. Structure and biosynthesis of the jamaicamides, new mixed polyketide-peptide neurotoxins from the marine cyanobacterium *Lyngbya majuscula*. Chemistry & Biology, 11, 817-833.

Engene, N., Choi, H., Esquenazi, E., Byrum, T., Villa, F.A., Cao, Z., Murray, T.F., Dorrestein, P.C., Gerwick, L., Gerwick, W.H., 2011. Phylogeny-Guided isolation of ethyl tumonoate A from the marine cyanobacterium cf. *Oscillatoria margaritifera*. Journal of Natural Products, 74, 1737-1743.

Engene, N., Rottacker, E.C., Kastovský, J., Byrum, T., Choi, H., Ellisman, M.H., Komárek, J., Gerwick, W.H., 2012. *Moorea producens* gen. nov., sp. nov. and *Moorea bouillonii* comb. nov. tropical marine cyanobacteria rich in bioactive secondary metabolites. International Journal of Systematic and Evolutionary Microbiology, 62, 1171-1178

Falcon, L. I., Cipriano, F., Chistoserdov, A. Y., Carpenter, E. J., 2002. Diversity of diazotrophic unicellular cyanobacteria in the tropical North Atlantic Ocean. Applied and Environmental Microbiology, 68 (11), 5760-4.

Ferreira, W.F.C., Sousa, J.C.F., 1998. Volume I. In: Microbiologia. Lisboa: Lidel.

Gerwick, W.H., Tan, L.T, Sitachitta, N., 2001. Nitrogen-containing metabolites from marine cyanobacteria. Alkaloids: Chemistry and Biology, 57, 75–184.

Gerwick, W.H., Coates, R.C., Engene, N., Gerwick, L., Grindberg, R.V., Jones, A.C., Sorrels, C.M., 2008. Giant marine cyanobacteria produce exciting potential pharmaceuticals. Microbe, 3 (6), 277–284.

Gerwick, W.H., Moore, B.S., 2012. Lessons from the Past and Charting the Future of Marine Natural Products Drug Discovery and Chemical Biology. Chemistry & Biology, 19, 85-98.

Gross, H., McPhail, K.L., Goeger, D.E., Valeriote, F.A., Gerwick, W.H., 2010. Two cytotoxic stereoisomers of malyngamide C, 8-epi-malyngamide C and 8-O-acetyl-8-epi-malyngamide C, from the marine cyanobacterium *Lyngbya majuscula*. Phytochemistry 71, 1729-1735.

Gutierrez, M., Tidgewell, K., Capson, T.L., Engene, N., Almanza, A., Schemies, J., Jung, M., Gerwick, W.H., 2010. Malyngolide dimer, a bioactive symmetric cyclodepside from the Panamanian marine cyanobacterium *Lyngbya majuscula*. Journal of Natural Products 73, 709-711.

Han, B., Goeger, D., Maier, C.S., Gerwick, W.H., 2005. The wewakpeptins, cyclic depsipeptides from a Papua New Guinea collection of the marine cyanobacterium *Lyngbya semiplena*. The Journal of Organic Chemistry, 70, 3133-3139.

Han, B., Gross, H., Goeger, D.E., Mooberry, S.L., Gerwick, W.H., 2006. Aurilides B and C, cancer cell toxins from a Papua New Guinea collection of the marine cyanobacterium *Lyngbya majuscula*. Journal of Natural Products, 69, 572–575.

Harada, K., Nakano, T., Fujii, K., Shirai, M., 2004. Comprehensive analysis system using liquid chromatography–mass spectrometry for the biosynthetic study of peptides produced by the cyanobacteria. Journal of Chromatography A, 1033, 107-113.

Hoiczyk, E., Hansel, A., 2000. Cyanobacterial Cell Walls: News from an Unusual Prokaryotic Envelope. Journal of Bacteriology, 182(5), 1191-1199.

Horgen, F.D., Kazmierski, E.B., Westenburg, H.E., Yoshida, W.Y., Scheuer, P.J., 2002. Malevamide D: Isolation and structure determination of an isodolastatin H analogue from the marine cyanobacterium *Symploca hydnoides*. Journal of Natural Products, 65, 487-491.

Kalemkerian, G.P., Ou, X.L., Adil, M.R., Rosati, R., Khoulani, M.M., Madan, S.K., Pettit, G.R., 1999. Activity of dolastatin 10 against small-cell lung cancer *in vitro* and *in vivo*: Induction of apoptosis and bcl-2 modification. Cancer Chemotherapy and Pharmacology, 43, 507-515.

Kotai, J., 1972. Instructions for preparation of modified nutrient solution Z8 for algae. Norwegian Institute for Water Research B-11769 (Blindern), Oslo, 5.

Leão, P.N., Costa, M., Ramos, V., Pereira, A.R., Fernandes, V.C., Domingues, F.V., Gerwick, W.H., Vasconcelos, V.M., Martins, R., 2013. Antitumor Activity of Hierridin B, a Cyanobacterial Secondary Metabolite Found in both Filamentous and Unicellular Marine Strains. PLoS ONE, 8 (7), 1-8.

Li, J.W., Vederas, J.C., 2009. Drug discovery and natural products: End of an era or an endless frontier? Science, 325, 161-165.

Lyra, C., Suomalainen, S., Gugger, M., Vezie, C., Sundman, P., Paulin, L., Sivonen, K., 2001. Molecular characterization of planktic cyanobacteria of *Anabaena, Aphanizomenon, Microcystis* and *Planktothrix* genera. International Journal of Systematic and Evolutionary Microbiology, 51(Pt 2), 513-26.

Luesch, H., Yoshida, W.Y., Moore, R.E., Paul, V.J., Mooberry, S.L., 2000. Isolation, structure determination, and biological activity of Lyngbyabellin A from the marine cyanobacterium *Lyngbya majuscula*. Journal of Natural Products, 63, 611-615.

Luesch, H., Yoshida, W.Y., Moore, R.E., Paul, V.J., Corbett, T.H. 2001. Total structure determination of apratoxin A, a potent novel cytotoxin from the marine cyanobacterium *Lyngbya majuscula*. Journal of the American Chemical Society. 123, 5418-5423.

Luesch, H., Yoshida, W.Y., Moore, R.E., Paul, V.J., 2002a. New apratoxins of marine cyanobacterial origin from Guam and Palau. Bioorganic & Medical Chemistry, 10, 1973-1978.

Luesch, H., Yoshida, W.Y., Harrigan, G.G., Doom, J.P., Moore, R.E., Paul, V.J., 2002b. Lyngbyaloside B, a new glycoside macrolide from a Palauan marine cyanobacterium, *Lyngbya* sp. Journal of Natural Products, 65, 1945-1948.

MacMillan, J.B., Molinski, T.F., 2002. Caylobolide A, a unique 36-membered macrolactone from a Bahamian *Lyngbya majuscula*. Organic Letters 4, 1535–1538.

Madigan, M.T., Martinko, J.M., Parker. J. 2003. Brock Biology of Microorganisms (10^{th} edition). Pearson Education Inc.

Malloy, K.L., Villa, F.A., Engene, N., Matainaho, T., Gerwick, L., Gerwick, W.H., 2011. Malyngamide 2, an oxidized lipopedtide with nitric oxide inhibiting activity from a Papua New Guinea marine cyanobacterium. Journal of Natural Products, 74, 95-98.

Martins, R.F., Pereira, P., Welker, M., Fastner, J., Vasconcelos, V.M., 2005. Toxicity of culturable cyanobacteria strains isolated from the Portuguese coast. Toxicon, 46, 454-464.

Martins, R.F., Ramos, M, F., Herfindal, L., Sousa, J.A., Skærven, K., Vasconcelos, V.M., 2008. Antimicrobial and Cytotoxic Assessment of Marine Cyanobacteria - *Synechocystis* and *Synechococcus*. Marine Drugs, 6 (1), 1-11.

Mayer, A.M.S., Glaser, K.B., Cuevas, C., Jacobs, R.S., Kem, W., Little, R.D., McIntosh, J.M., Newman, D.J., Potts, B.C., Shuster, D.E., 2010. The odyssey if marine pharmaceuticals: a current pipeline perspective. Trends in Pharmacological Sciences, 31, 255-265.

Mayer, A.M.S., Rodríguez, A.D., Berlinck, R.G.S., Fusetani, N., 2011. Marine Pharmacology in 2007-08: Marine compounds with antibacterial, anticoagulant, antifungal, anti-inflammatory, antimalarial, antiprotozoal, antituberculosis, and antiviral activities; affecting the immune and nervous system, and other miscellaneous mechanisms of action. Comparative Biochemistry and Physiology, 153 (C), 191-222.

McMurray, J., 2007. Organic chemistry (7th Edition). Thomson Learning Inc.

Medina, R.A., Goeger, D.E., Hills, P., Mooberry, S.L., Huang, N., Romero, L.I., Ortega-Barria, E., Gerwick, W.H., McPhail, K.L., 2008. Coibamide A, a potent antiproliferative cyclic depsipeptide from the Panamanian marine cyanobacterium *Leptolyngbya* sp. Journal of the American Chemical Society, 130, 6324–6325.

Mevers, E., Liu, W.T., Engene, N., Mohimani, H., Byrum, T., Pevzner, P.A., Dorrestein, P.C., Spadafora, C., Gerwick, W.H., 2011. Cytotoxic veraguamides, alkynyl bromide-containing cyclic depsipeptides from the marine cyanobacterium cf. *Oscillatoria margaritifera*. Journal of Natural Products, 74, 928-936.

Michels, P.C., Khmelnitsky, Y.L., Dordick, J.S., Clark, D.S., 1998. Combinatorial biocatalysis: a natural approach to drug discovery. Trends in Biotechnology, 16, 210-215.

Mishra, B.B., Tiwari, V.K., 2011. Natural products: an evolving role in future drug discovery. European Journal of Medicinal Chemistry, 46, 4769-4807.

Mita, A.C., Hammond, L.A., Bonate, P.L., Weiss, G., McCreery, H., Syed, S., Garrison, M., Chu, Q.S., DeBono, J.S., Jones, C.B., Weitman, S., Rowinsky, E.K., 2006. Phase I and pharmacokinetic study of tasidotin hydrochloride (ILX651), a third-generation dolastatin-15 analogue, administered weekly for 3 weeks every 28 days in patients with advanced solid tumors. Clinical Cancer Research, 12, 5207-5215.

Mooberry, S.L., Leal, R.M., Tinley, T.L., Luesch, H., Moore, R.E., Corbett, T.H., 2003. The molecular pharmacology of symplostatin 1: A new antimitotic dolastatin 10 analog. International Journal of Cancer, 104, 512-521.

Montaser, R., Paul, V.J., Luesch, H., 2011a. Pitipeptolides C–F, antimycobacterial cyclodepsipeptides from the marine cyanobacterium *Lyngbya majuscula* from Guam. Phytochemistry, 72, 2068-2074.

Montaser, R., Abboud, K.A., Paul, V.J., Luesch, H., 2011b. Pitiprolamide, a proline-rich dolastatin 16 analogue from the marine cyanobacterium Lyngbya majuscula from Guam. Journal of Natural Products, 74, 109-112.

Moravec, R.A., O'Brien, M.A., Daily, W.J., Scurria, M.A., Bernard, L., Riss, T.L., 2009. Cell-based bioluminescent assays for all three proteasome activities in a homogeneous format. Analytical Biochemistry, 387, 294-302.

Nagle, D.G., Paul V.J., 1999. Production of Secondary Metabolites by Filamentous Tropical Marine Cyanobacteria: Ecological Functions of the Compounds. Journal of Phycology, 35, 1412-1421.

Newman, D.J., Cragg, G.M., 2012. Natural Products as Sources of New Drugs over the 30 years from 1981 to 2010. Journal of Natural Products, 75, 311-335.

Neilan, B. A., Jacobs, D., Del Dot, T., Blackall, L. L., Hawkins, P. R., Cox, P. T., Goodman, A. E., 1997. rRNA sequences and evolutionary relationships among toxic and nontoxic cyanobacteria of the genus *Microcystis*. International Journal of Systematic Bacteriology, 47 (3), 693-697.

Neumann, C.S., Fujimori, D.G., Walsh, C.T., 2008. Halogenation Strategies In Natural Product Biosynthesis. Chemistry and Biology, 15, 99-109.

Nunnery, J.K., Mevers, E., Gerwick, W.H., 2010. Biologically active secondary metabolites from marine cyanobacteria. Current Opinion in Biotechnology, 21, 787-793.

Otsuka S, Suda S, Li R, Watanabe M, Oyaizu H, Matsumoto S, Watanabe MM., 1998. 16S rDNA sequences and phylogenetic analyses of *Microcystis* strains with and without phycoerythrin. FEMS Microbiology Letters, 164 (1), 119-124.

Pettit, G.R., Hogan, F., Xu, J.P., Tan, R., Nogawa, T., Cichacz, Z., Pettit, R.K., Du, J., Ye, Q.H., Cragg, G.M., Herald, C.L., Hoard, M.S., Goswami, A., Searcy, J., Tackett, L., Doubek, D.L., Williams, L., Hooper, J.N., Schmidt, J.M., Chapuis, J.C., Tackett, D.N., Craciunescu, F., 2008. Antineoplastic agents. 536. New sources of naturally occurring cancer cell growth inhibitors from marine organisms, terrestrial plants, and microorganisms (1a). Journal of Natural Products, 71, 438-444.

Rath, B., Priyadarshani, I., 2013. Antibacterial and Antifungal activity of marine cyanobacteria from Odisha Coast. International Journal of Current Trends in Research, 2 (1), 248-251.

Rippka, R., 1988. Isolation and purification of cyanobacteria. In: Methods in Enzymology, Edited by: Packer, L., and Glazer, A.N., 167, 3-27.

Rich, J.O., Michels, P.C., Khmelnitsky, Y.L., 2002. Combinatorial biocatalysis. Current Opinion in Chemical Biology, 6, 161-167.

Sangolkar, L.N., Maske, S.S., Chakrabarti, T., 2006. Methods for determining microcystins (peptide hepatotoxins) and microcystin-producing cyanobacteria. Water Research, 40(19), 3485- 3496.

Schlegel, I., Doan, N.T., Chazal, N., Smith, G.D., 1999. Antibiotic activity of new cyanobacterial isolates from Australia and Asia against green algae and cyanobacteria. Journal of Applied Phycology, 10, 471-479.

Shih, P.M., Wu, D., Latifi, A., Axena, S.D., Fewere, D.P., Tallad, E., Calteau, A., Cai, F., Marsac, N.T., Rippka, R., Herdman, M., Sivonen, K., Coursin, T., Laurent, T., Goodwin, L., Nolan, M., Davenport, K.W., Han, C.S., Rubin, E.M., Eisen, J.A., Woyke, T., Gugger, M., Kerfeld, C.A., 2013. Improving the coverage of the cyanobacterial phylum using diversity-driven genome sequencing. Proceedings of the National Academy of Sciences of the United States of America, 110 (3), 1053-1058.

Simmons, T.L., McPhail, K.L., Ortega-Barria, E., Mooberry, S.L., Gerwick, W.H., 2006. Belamide A, a new antimitotic tetrapeptide from a Panamanian marine cyanobacterium. Tetrahedron Letters, 47, 3387–3390.

Sin, N., Kim, K.B., Elofsson, M., Meng, L., Auth, H., Kwok, B.H.B., Crews, C.M., 1999. Total synthesis of the potent proteasome inhibitor epoxomicin: a useful tool for understanding proteasome biology. Bioorganic & Medicinal Chemistry Letters, 9, 2283-2289.

Tan, L.T., 2007. Bioactive natural products from marine cyanobacteria for drug discovery. Phytochemistry, 68, 954-979.

Taniguchi, M., Nunnery, J.K., Engene, N., Esquenazi, E., Byrum, T., Dorrestein, P.C., Gerwick, W.H., 2010. Palmyramide A, a cyclic depsipeptide from a Palmyra Atoll

collection of the marine cyanobacterium *Lyngbya majuscula*. Journal of Natural Products 73, 393-398.

Teruya, T., Sasaki, H., Fukazawa, H., Suenaga, K., 2009a. Bisebromoamide, a potent cytotoxic peptide from the marine cyanobacterium *Lyngbya* sp.: isolation, stereostructure, and biological activity. Organic Letters, 11, 5062–5065.

Teruya, T., Sasaki, H., Kitamura, K., Nakayama, T., Suenaga, K., 2009b. Biselyngbyaside, a macrolide glycoside from the marine cyanobacterium *Lyngbya* sp. Organic Letters, 11, 2421-2424.

Tidgewell, K., Clark, B.T., Gerwick, W.H., 2010. Comprehensive Natural Products Chemistry. 2nd Ed. Moore, B., Crews, P., editors. Oxford, UK: Pergamon Press, 141-188.

Thornburg, C.C., Thimmaiah, M., Shaala, L.A., Hau, A.M., Malmo, J.M., Ishmael, J.E., Youssef, D.T., McPhail, K.L., 2011. Cyclic depsipeptides, grassypeptolides D and E and Ibu-epidemethoxylyngbyastatin 3, from a Red Sea *Leptolyngbya cyanobacterium*. Journal of Natural Products, 74, 1677-1685

Tripathi, A., Puddick, J., Prinsep, M.R., Rottmann, M., Chan, K.P., Chen, D.Y., Tan, L.T., 2011. Lagunamide C, a cytotoxic cyclodepsipeptide from the marine cyanobacterium *Lyngbya majuscula*. Phytochemistry, 72, 2369-2375.

Uzair, B., Tabassum, S., Rasheed, M., Rehman, S.F., 2012. Exploring Marine Cyanobacteria for Lead Compounds of Pharmaceutical Importance. The Scientific World Journal 2012, 1-10.

Vasconcelos, V., 2006. Eutrophication, toxic cyanobacteria and cyanotoxins: when ecosystems cry for help. Limnetica, 25, 425-432.

Wagner, M.M., Paul, D.C., Shih, C., Jordan, M.A., Wilson, L., Williams, D.C. 1999. *In vitro* pharmacology of cryptophycin 52 (LY355703) in human tumor cell lines. Cancer Chemotherapy and Pharmacology 43, 115–125.

Watanabe, J., Minami, M., Kobayashi, M., 2006. Antitumor activity of TZT-1027 (Soblidotin). Anticancer Research, 26, 1973-1982.

Welker, M., Döhren, H.V., 2006. Cyanobacterial peptides – Nature´s own combinatorial biosynthesis. FEMS Microbiology Reviews, 30, 530-563.

White, J.D., Xu, Q., Lee, C.S., Valeriote, F.A., 2004 Total synthesis and biological evaluation of (+)-kalkitoxin, a cytotoxic metabolite of the cyanobacterium *Lyngbya majuscula*. Organic & Biomolecular Chemistry, 2, 2092-2102.

Whitton, B.A., Potts, M. 2002. The Ecology of cyanobacteria: their diversity in time and space. New York: Kluwer Academic Publishers.

Williams, P.G., Yoshida, W.Y., Moore, R.E., Paul, V.J., 2002a. Isolation and structure determination of obyanamide, a novel cytotoxic cyclic depsipeptide from the marine cyanobacterium *Lyngbya confervoides*. Journal of Natural Products, 65, 29-31.

Williams, P.G., Yoshida, W.Y., Moore, R.E., Paul, V.J., 2002b. Tasiamide, a cytotoxic peptide from the marine cyanobacterium *Symploca* sp. Journal of Natural Products, 65, 1336-1339.

Williams, P.G., Yoshida, W.Y., Moore, R.E., Paul, V.J., 2003a. Tasipeptins A and B: New cytotoxic depsipeptides from the marine cyanobacterium *Symploca* sp. Journal of Natural Products, 66, 620-624.

Williams, P.G., Yoshida, W.Y., Quon, M.K., Moore, R.E., Paul, V.J., 2003. Ulongapeptin, a cytotoxic cyclic depsipeptide from a Palauan marine cyanobacterium *Lyngbya* sp. Journal of Natural Products, 66, 651-654.

Wilson, K.M., Schembri, M.A., Baker, P.D., Saint, C.P., 2000. Molecular characterization of the toxic cyanobacterium *Cylindrospermopsis raciborskii* and design of a species-specific PCR. Applied and Environmental Microbiology, 66, 332-338.

Wrasidlo, W., Mielgo, A., Torres, V.A., Barbero, S., Stoletov, K., Suyama, T.L., Klemke, R.L., Gerwick, W.H., Carson, D.A., Stupack, D.G., 2008. The marine lipopeptide somocystinamide A triggers apoptosis via caspase 8. Proceedings of the National Academy of Sciences, 105, 2313-2318.

Zhang, W., Ding, N., Li, X., 2011. Synthesis and biological evaluation of analogues of the marine cyclic depsipeptide obyanamide. Journal of Peptide Science, 17, 533-539.

Zeng, X., Yin, B., Hu, Z., Liao, C., Liu, J., Li, S., Li, Z., Nicklaus, M.C., Zhou, G., Jiang, S., 2010. Total synthesis and biological evaluation of largazole and derivatives with promising selectivity for cancers cells. Organic Letters, 12, 1368-1371.

Zou, B., Long, K., Ma, D.W., 2005. Total synthesis and cytotoxicity studies of a cyclic depsipeptide with proposed structure of palau'amide. Organic Letters, *7*, 4237-4240.

7. Appendix

7.1 Appendix I – MTT viability assays (96 well plates; 3.3 x 10^4 cells per well; 4 hours exposure to MTT).

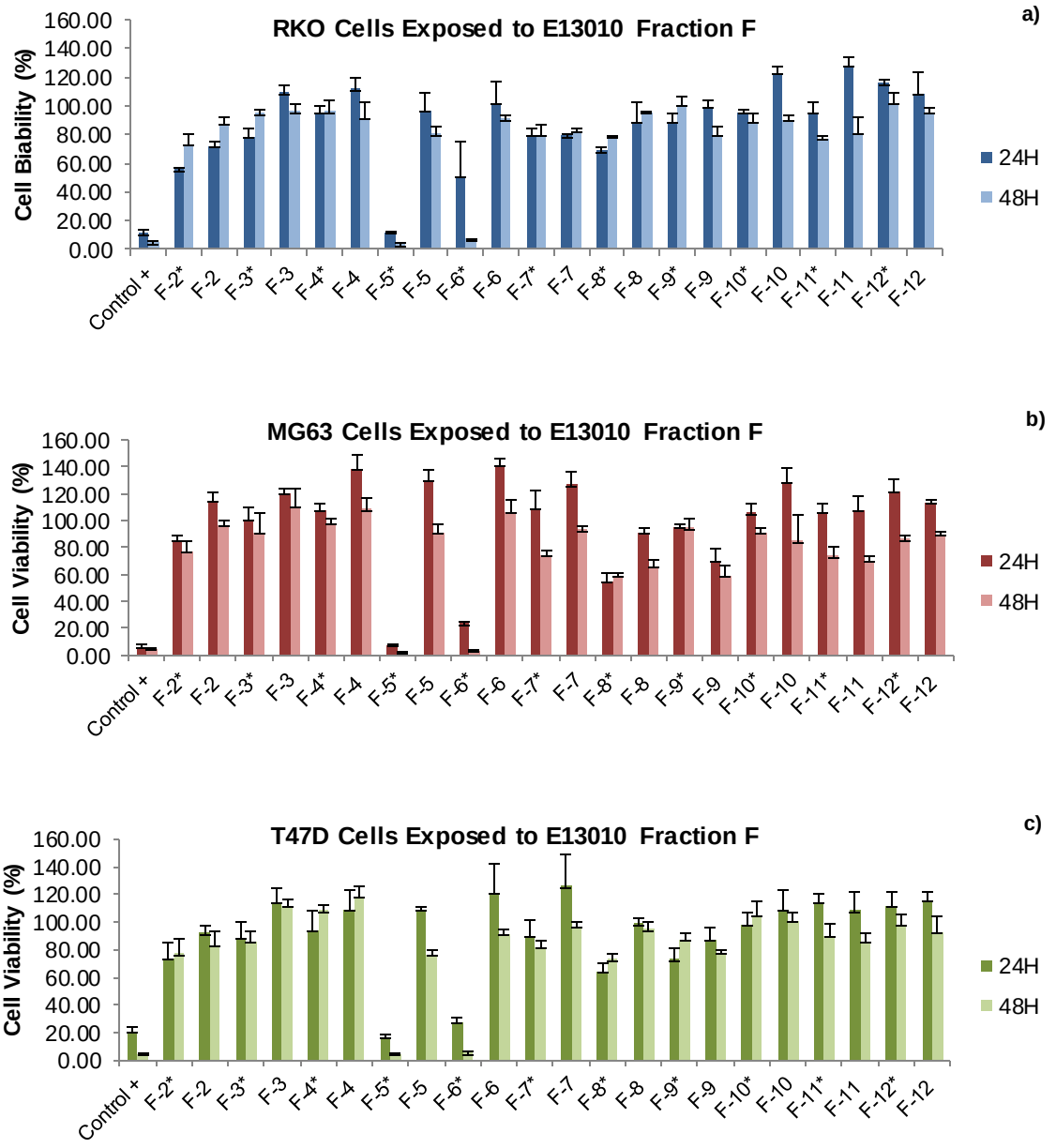

Figure 1 – Cell viability (% of negative control) from E13010 Fraction F sub-fractions (F-2 – F-12) with the concentration of 30 μg mL^{-1}(*) and 3 μg mL^{-1} on the RKO (a), MG63 (b) and T47D (c) cancer cell lines, with two exposure times, 24H and 48H at 3.3 x 10^4 cells per well. Negative control corresponded to 1% DMSO and positive control to 20% DMSO.

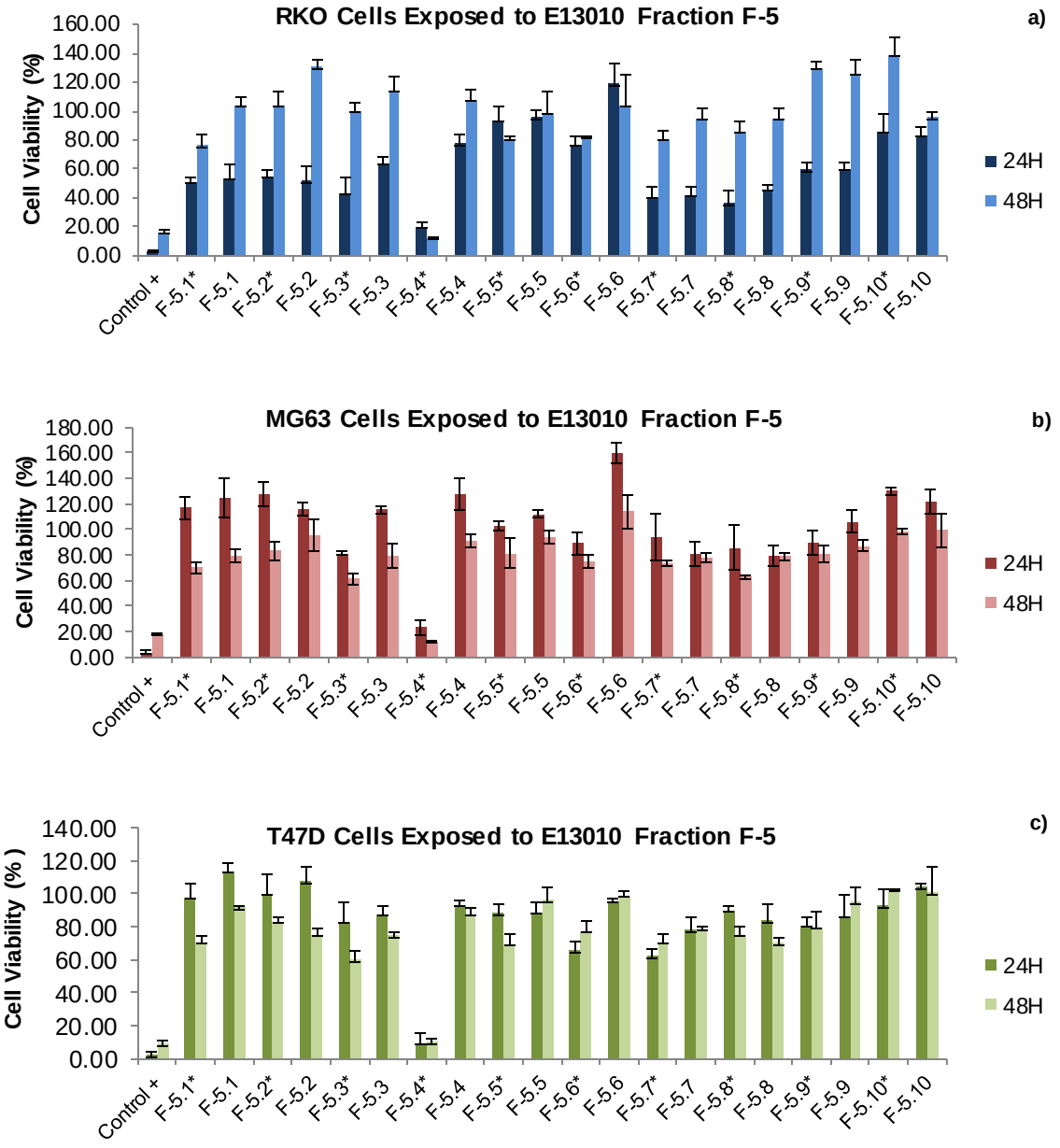

Figure 2 – Cell viability (% of negative control) from E13010 Fraction F-5 sub-fractions (F-5.1 – F-5.10) with the concentration of 30 μg mL^{-1}(*) and 3 μg mL^{-1} on the RKO (a), MG63 (b) and T47D (c) cancer cell lines, with two exposure times, 24H and 48H at 3.3 x 10^4 cells per well. Negative control corresponded to 1% DMSO and positive control to 20% DMSO.

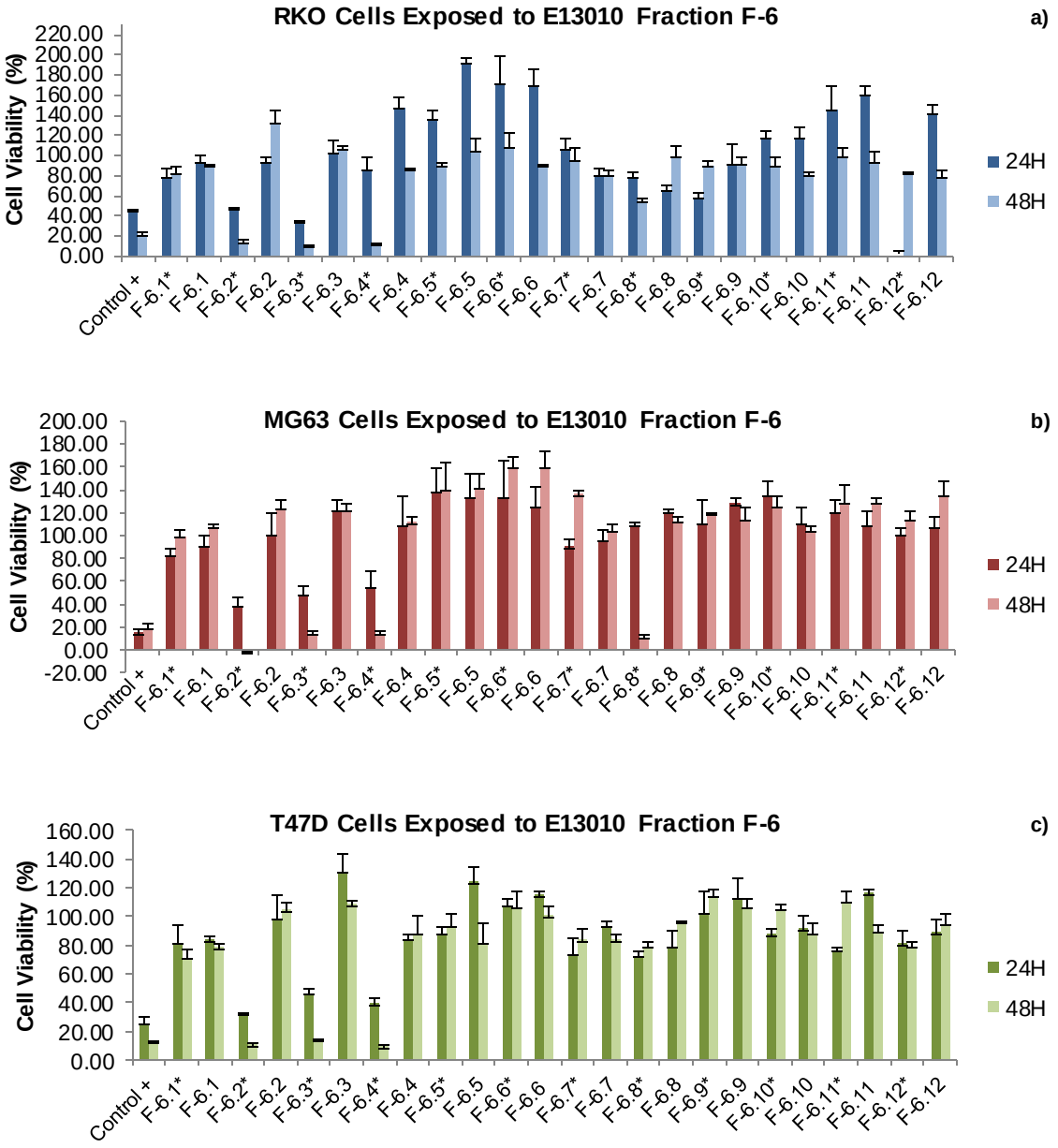

Figure 3 – Cell viability (% of negative control) from E13010 Fraction F-6 sub-fractions (F-6.1 – F-6.12) with the concentration of 30 μg mL^{-1}(*) and 3 μg mL^{-1} on the RKO (a), MG63 (b) and T47D (c) cancer cell lines, with two exposure times, 24H and 48H at 3.3 x 10^4 cells per well. Negative control corresponded to 1% DMSO and positive control to 20% DMSO.

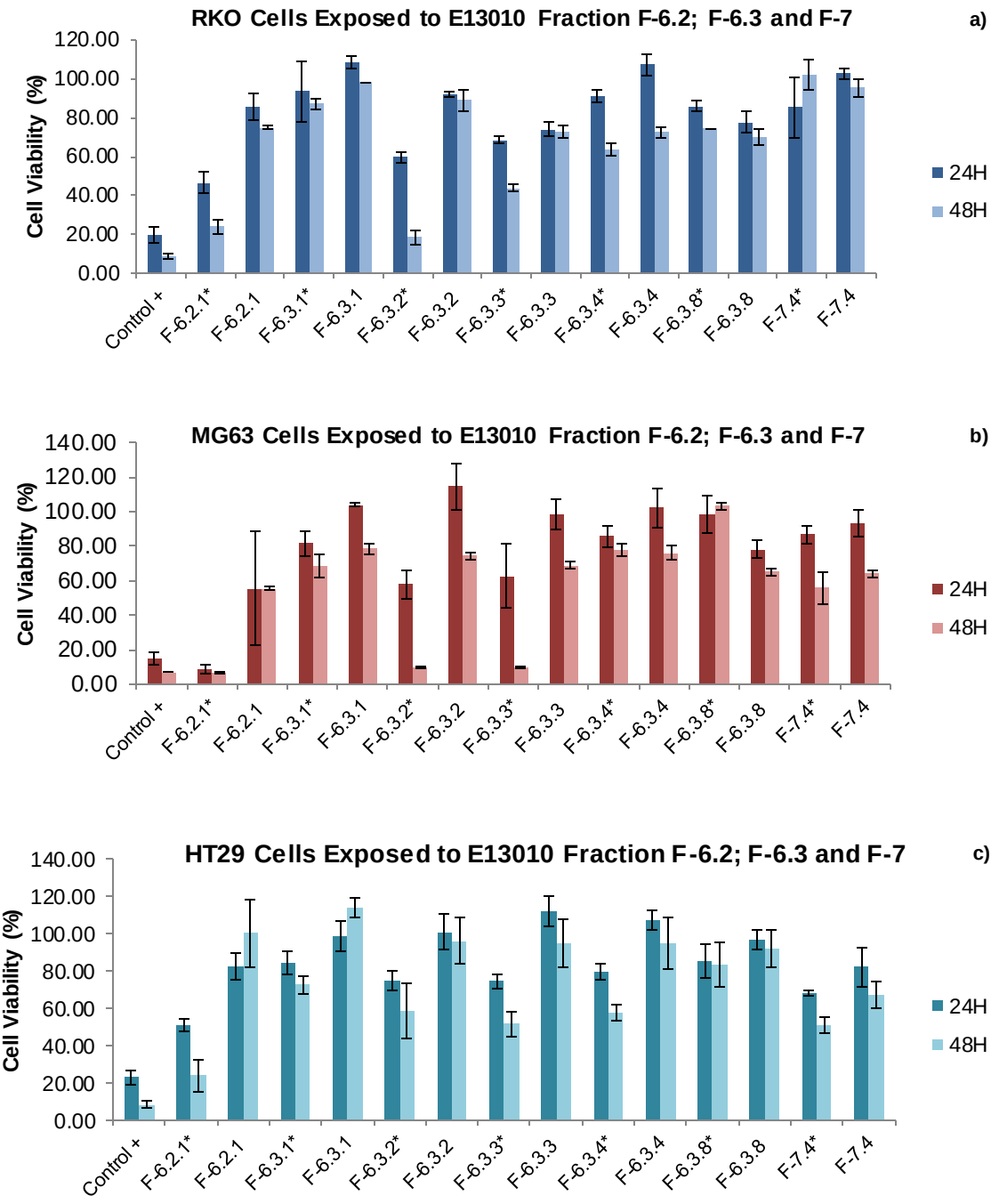

Figure 4 – Cell viability (% of negative control) from E13010 Fraction F-6.2; F-6.3 and F-7 sub-fractions with the concentration of 30 μg mL^{-1}(*) and 3 μg mL^{-1} on the RKO (a), MG63 (b) and HT29 (c) cancer cell lines, with two exposure times, 24H and 48H at 3.3 x 10^4 cells per well. Negative control corresponded to 1% DMSO and positive control to 20% DMSO.

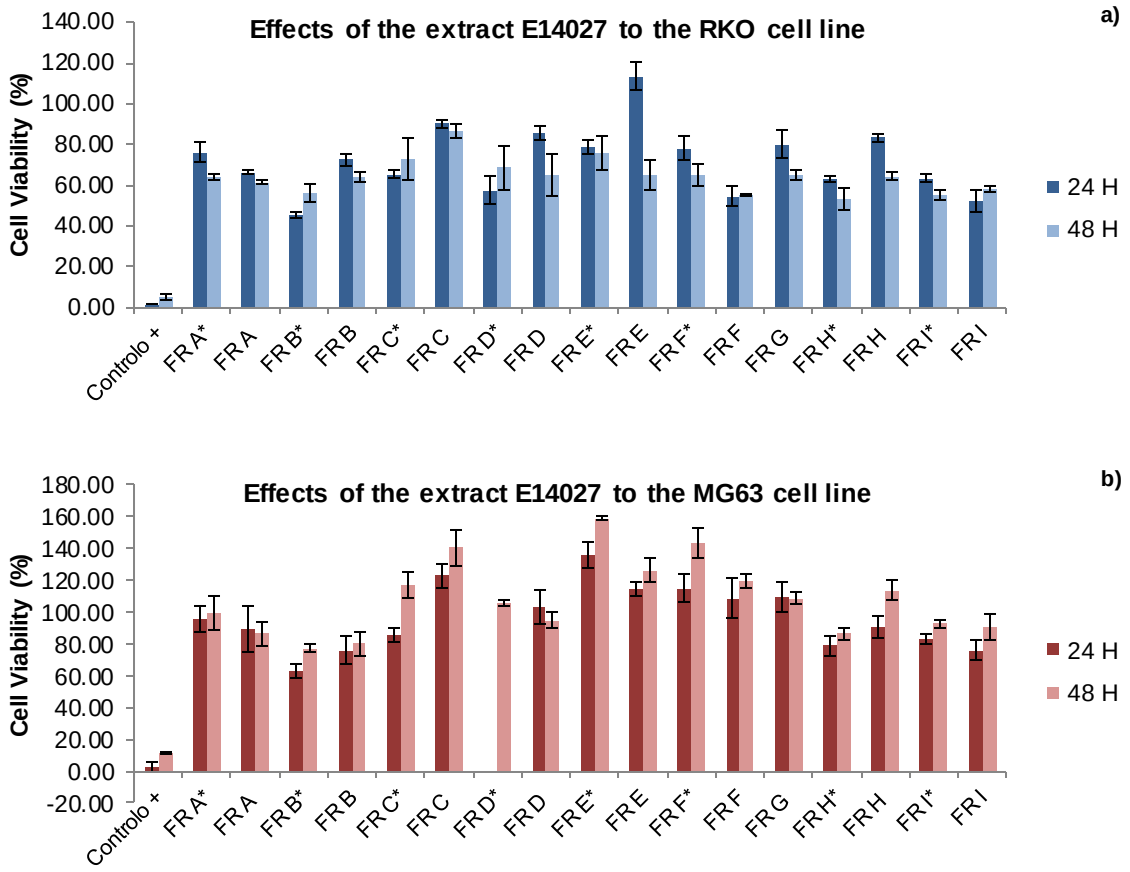

Figure 5 – Cell viability (% of negative control) from E14027 VLC Fractions (A-I) with the concentration of 30 μg mL^{-1}(*) and 3 μg mL^{-1} on the RKO (a) and MG63 (b) cancer cell lines, with two exposure times, 24H and 48H at 3.3 x 10^4 cells per well. Negative control corresponded to 1% DMSO and positive control to 20% DMSO (T47D cell line had growing problems*).

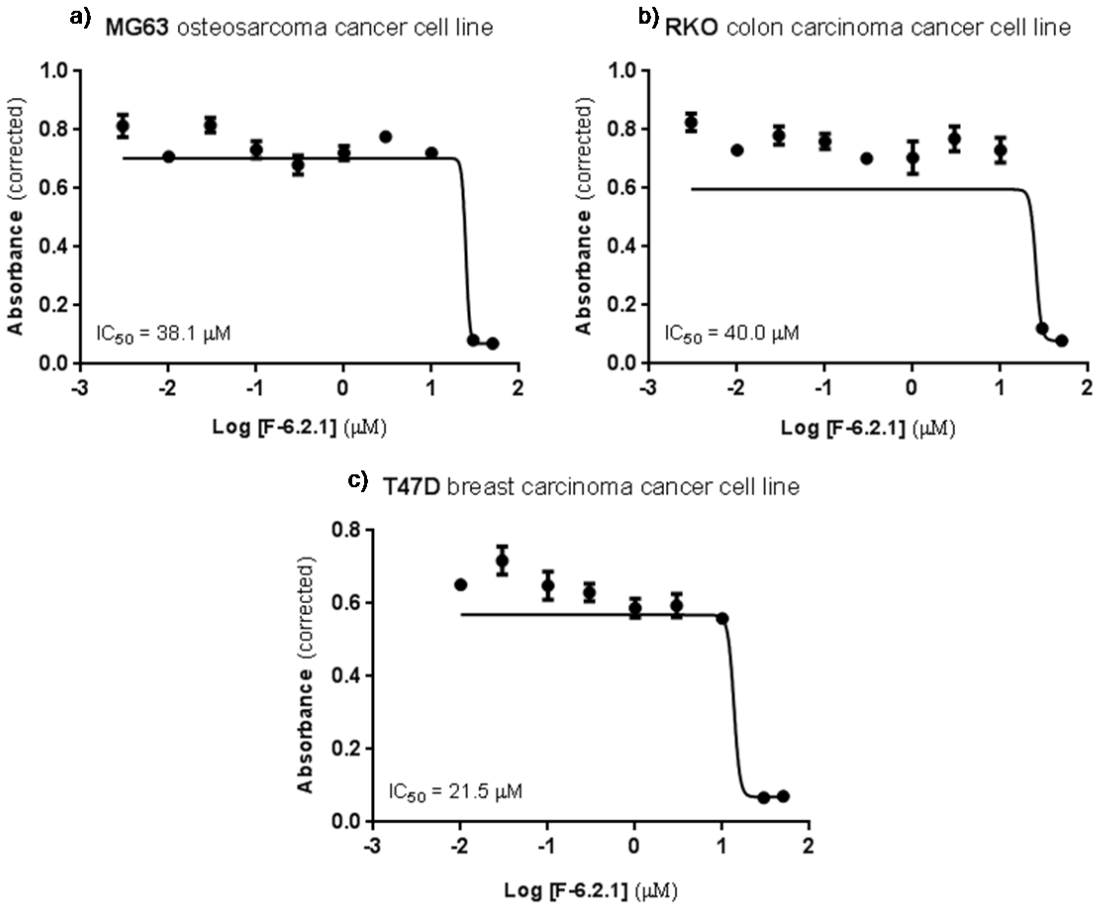

Figure 6 – Dose-response curves obtained for compound E13010 F-6.2.1 in MG63 osteosarcoma cancer cell line (a), RKO colon carcinoma cancer cell line (b) and T47D breast carcinoma cancer cell line (c).

7.2 **Appendix II –** 2D NMR data of compounds F-5.4, F-6.2.1 and F-7.4.

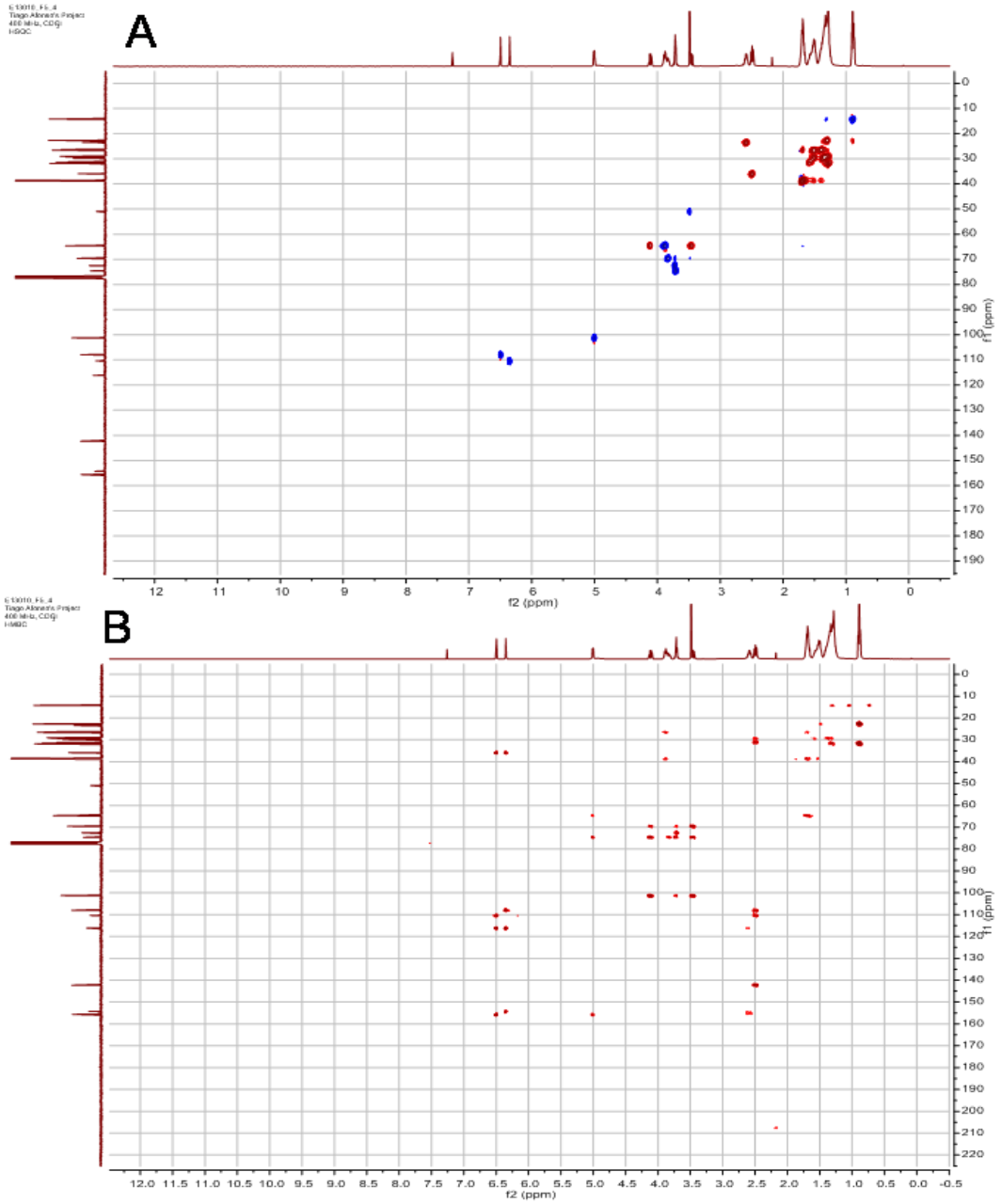

Figure 1 – HSQC (A) and HMBC (B) spectra of compound F-5.4/F-6.4 in $CDCl_3$ (recorded at 400 MHz).

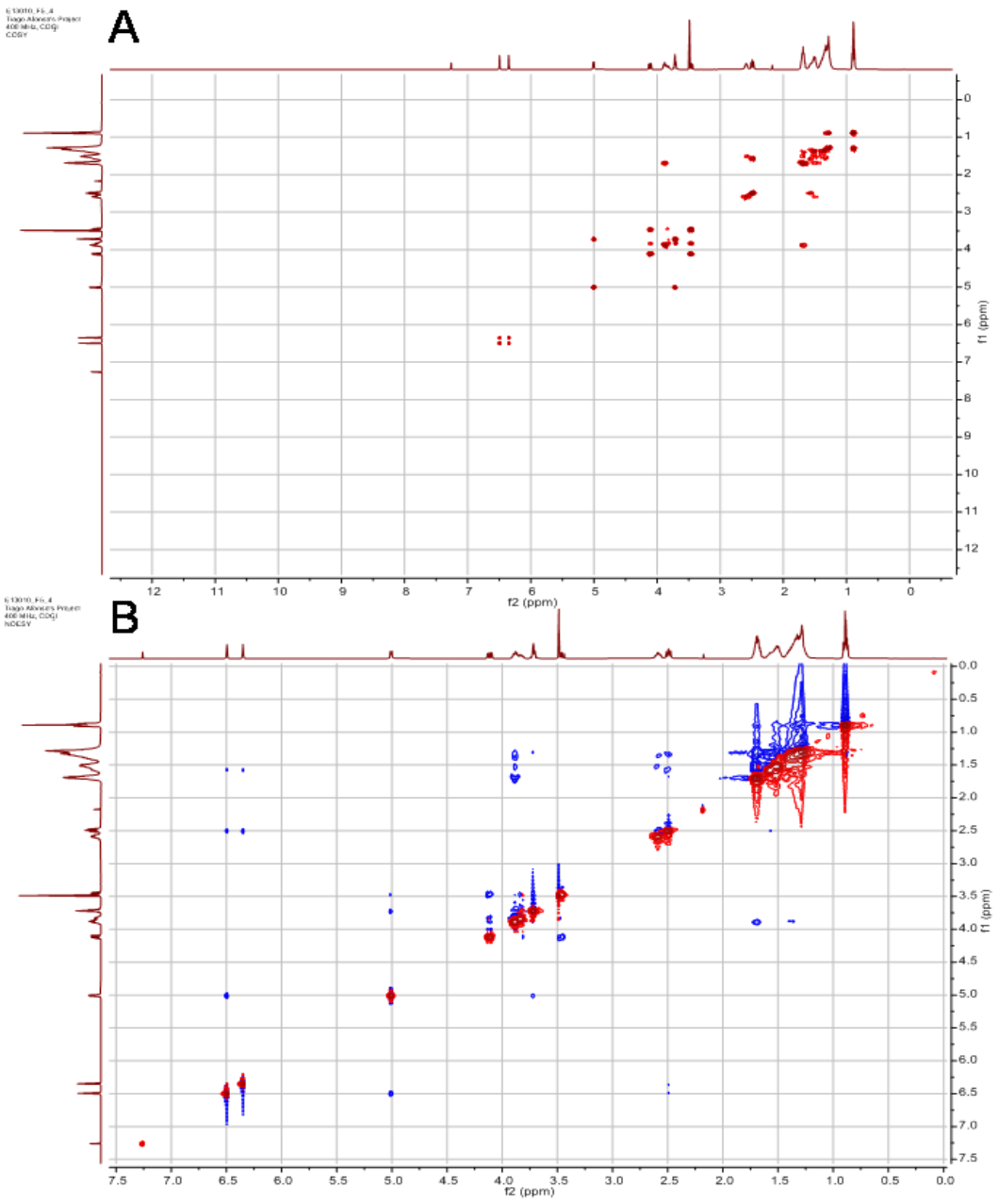

Figure 2 – COSY (A) and NOESY (B) spectra of compound F-5.4/F-6.4 in $CDCl_3$ (recorded at 400 MHz).

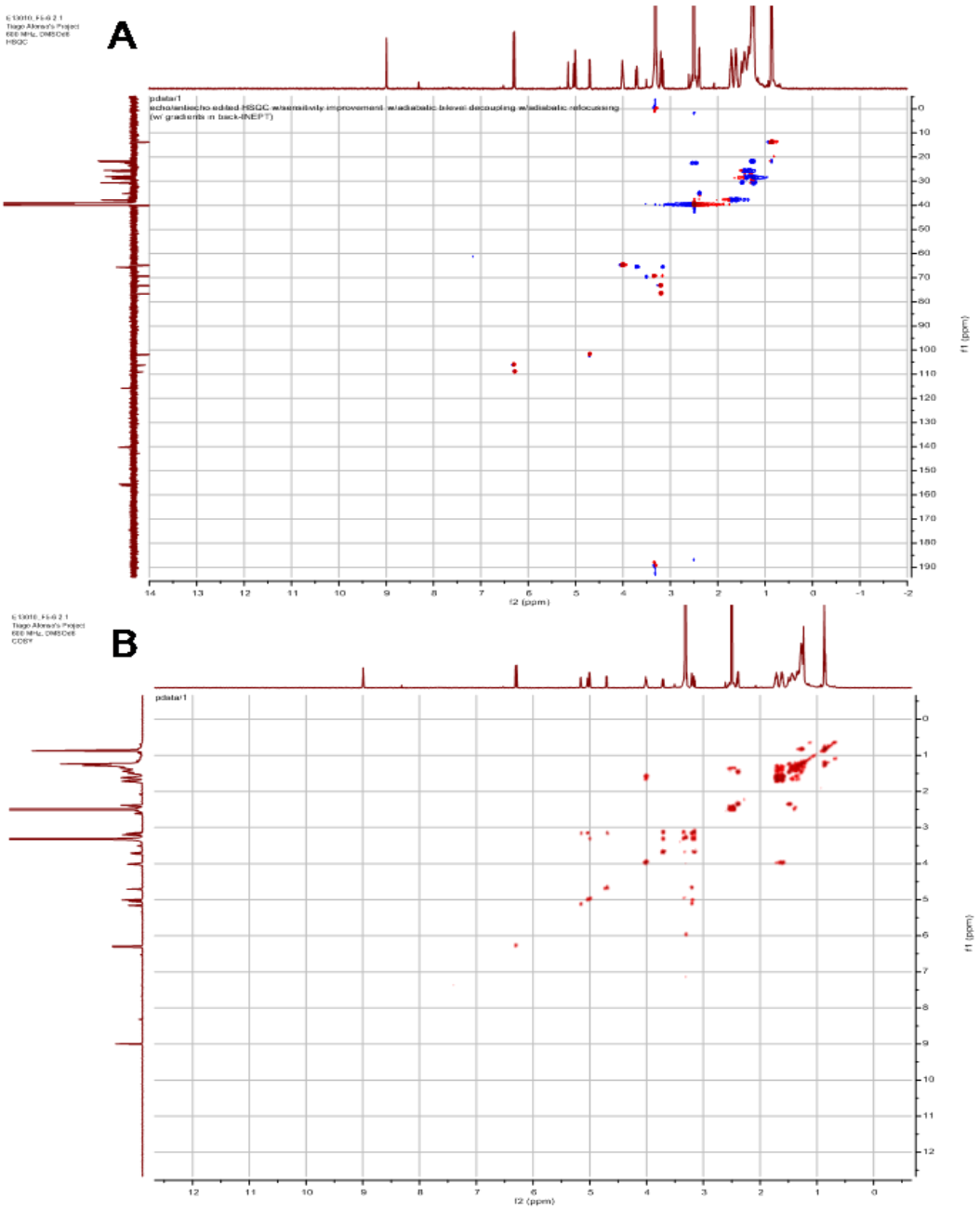

Figure 3 – HSQC (A) and HMBC (B) spectra of compound F-6.2.1 in DMSO-d_6 (recorded at 600 MHz).

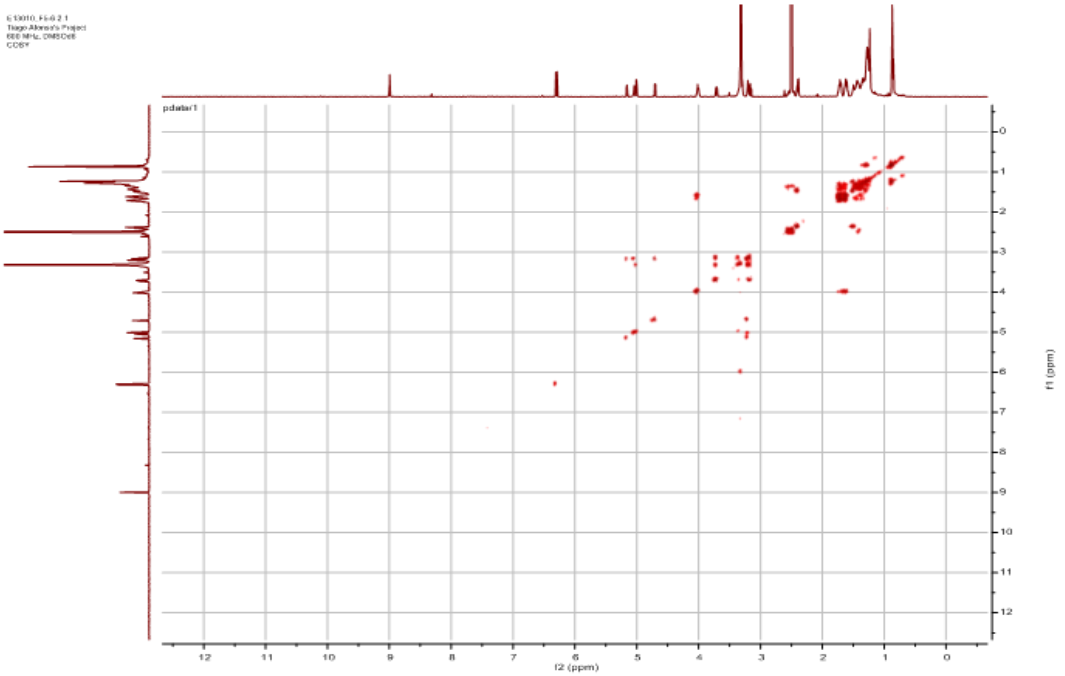

Figure 4 – COSY spectra of compound F-6.2.1 in DMSO-d_6 (recorded at 600 MHz).

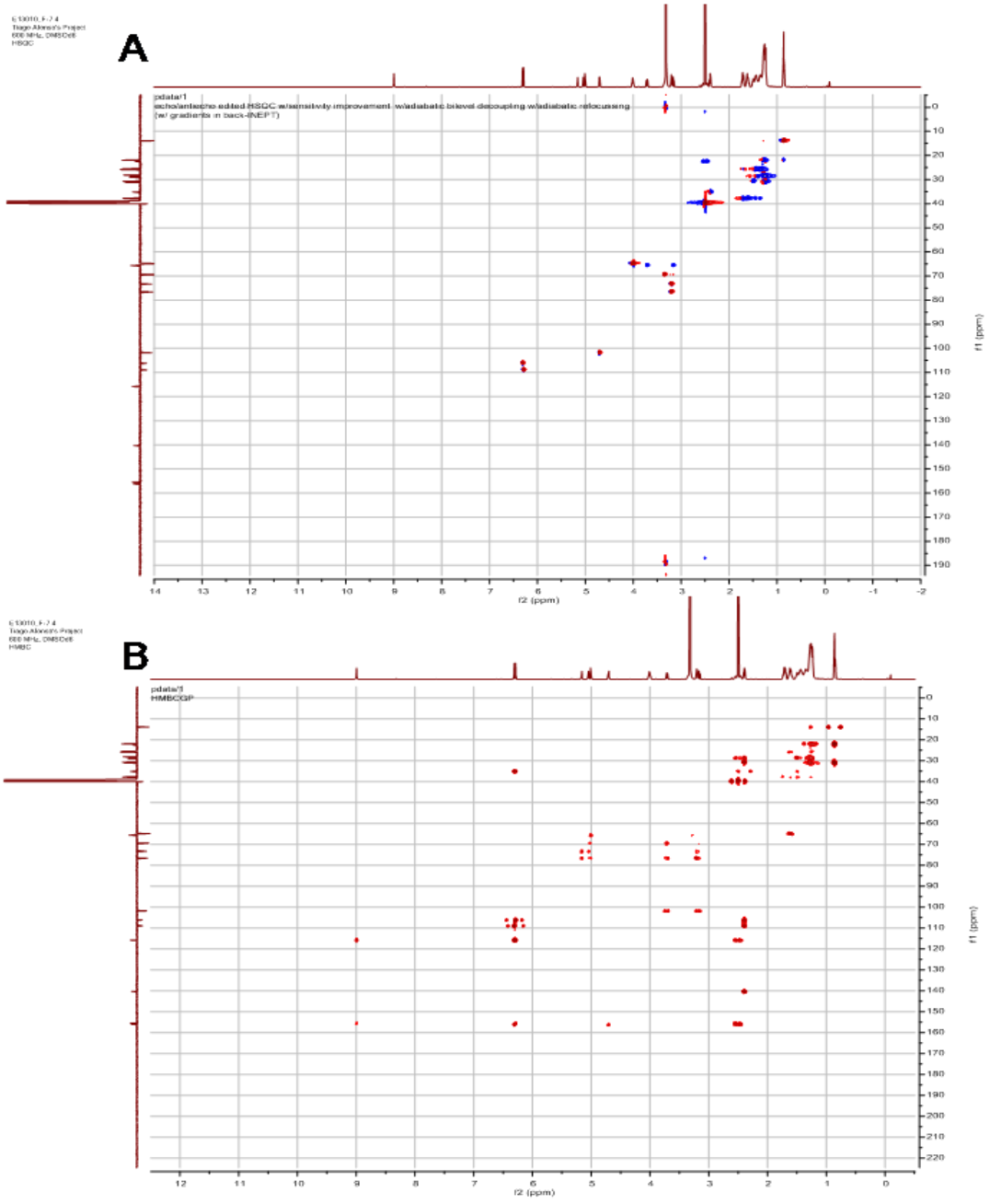

Figure 5 – HSQC (A) and HMBC (B) spectra of compound F-7.4 in DMSO-d_6 (recorded at 600 MHz).

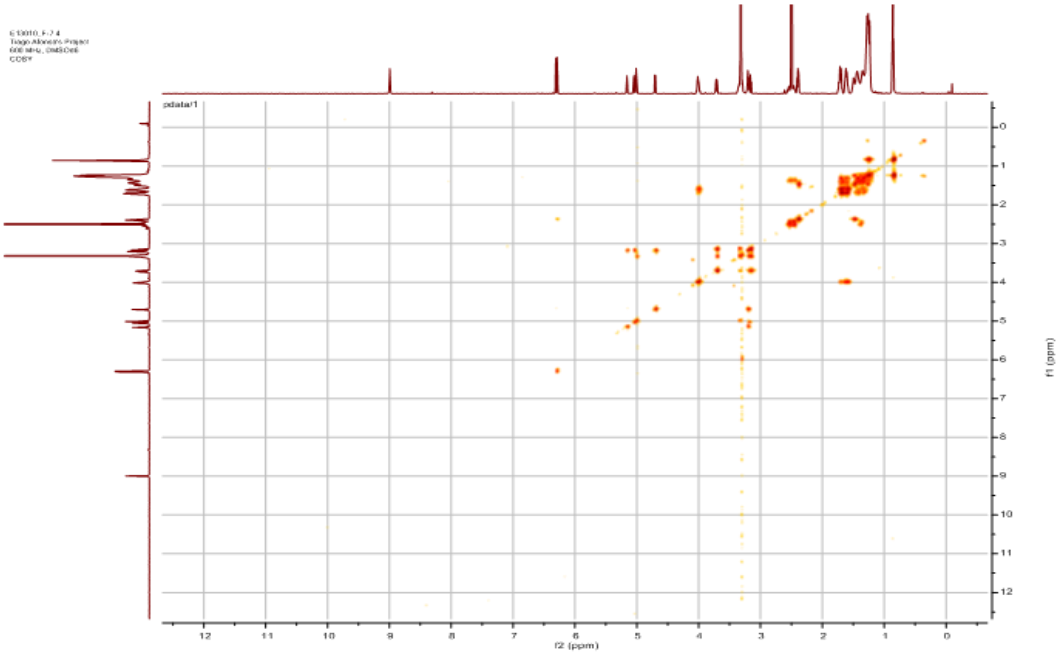

Figure 6 – COSY spectra of compound F-7.4 in DMSO-d_6 (recorded at 600 MHz).

7.3 **Appendix III –** UV-Vis data for each compound.

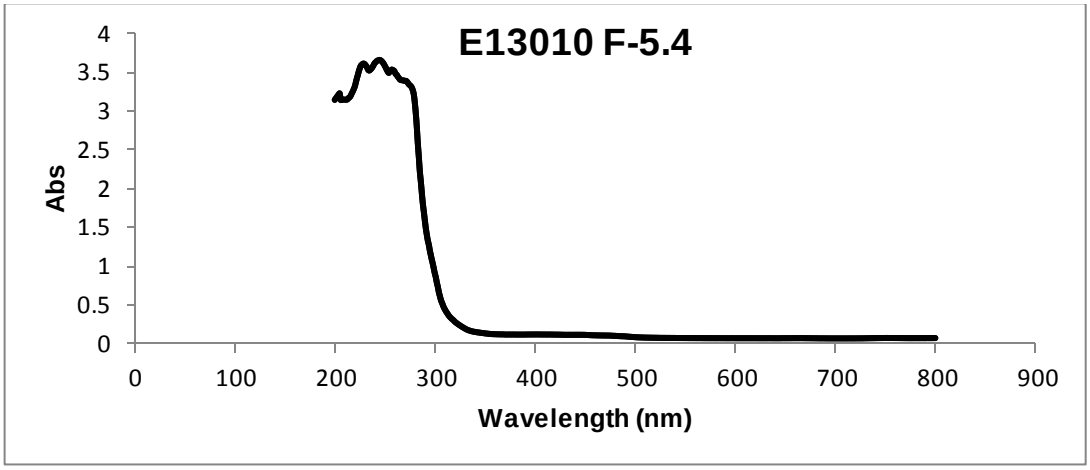

Figure 1 – UV-Vis spectra of compound F-5.4 in MeOH (Absorption maxima were registered at 205, 229, 245 and 257 nm).

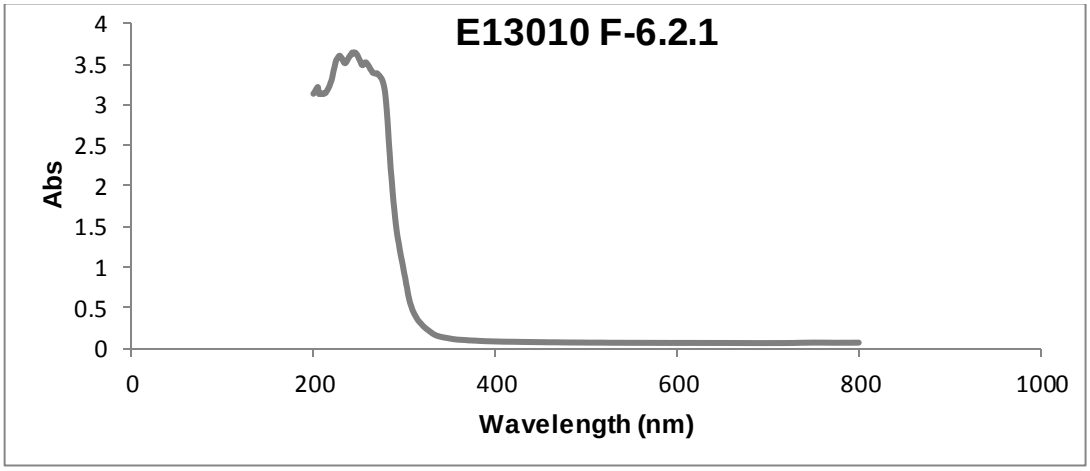

Figure 2 – UV-Vis spectra of compound F-6.2.1 in MeOH (Absorption maxima were registered at 205, 229, 245 and 257 nm).

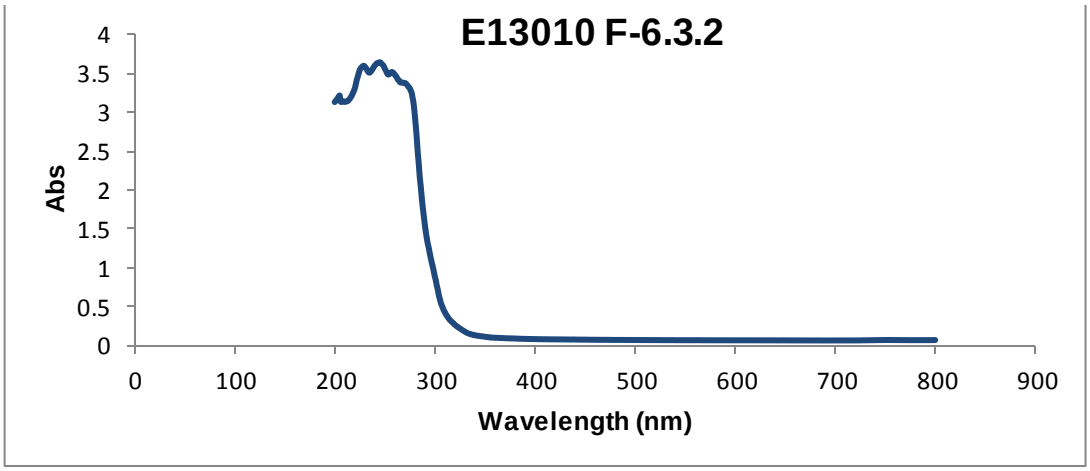

Figure 3 – UV-Vis spectra of compound F-6.3.2 in MeOH (Absorption maxima were registered at 205, 229, 245 and 257 nm).

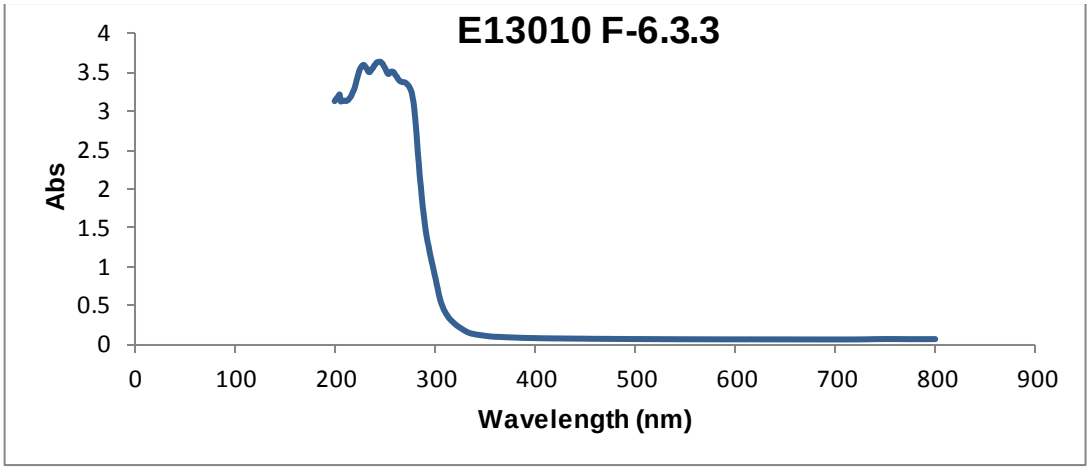

Figure 4 – UV-Vis spectra of compound F-6.3.3 in MeOH (Absorption maxima were registered at 205, 229, 245 and 257 nm).

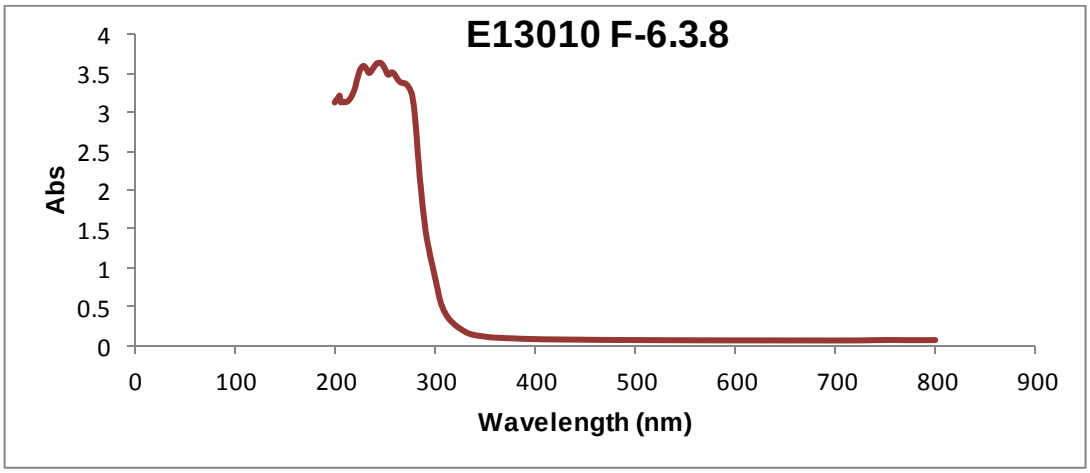

Figure 5 – UV-Vis spectra of compound F-6.3.8 in MeOH (Absorption maxima were registered at 205, 229, 245 and 257 nm).

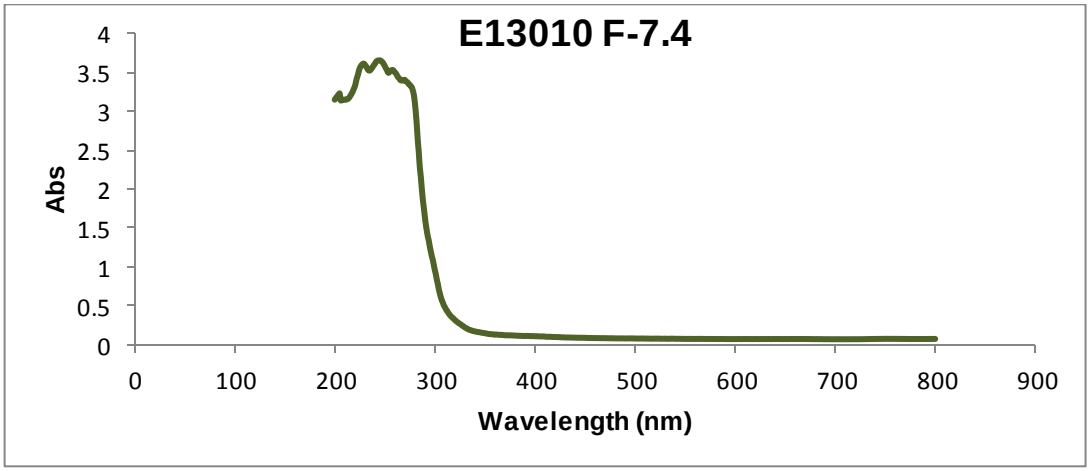

Figure 6 – UV-Vis spectra of compound F-7.4 in MeOH (Absorption maxima were registered at 205, 229, 245 and 257 nm).